A HOT WIRE ANEMOMETER STUDY OF THE EFFECT OF DISTURBANCES ON THE LAMINAR BOUNDARY LAYER ON A FLAT PLATE

by

FRANCIS HAMILTON BARNES, B.Sc. (Edinburgh)

Thesis presented for the

Degree of

DOCTOR OF PHILOSOPHY

of the University of Edinburgh

in the Faculty of Pure Science

University of Edinburgh

October, 1966.

TABLE OF CONTENTS

TABLE OF CONTENTS (Contd.)

TABLE OF CONTENTS (Contd.)

TABLE OF CONTENTS (Contd.)

TABLE OF CONTENTS (Contd.)

List of Diagrams

PREFACE

The research in this thesis was carried out in Heriot Watt University and in the University of Edinburgh under the joint supervision of Dr. M.A.S. Ross of the Department of Natural Philosophy, University of Edinburgh, and Professor W.H.J. Childs of the Department of Physics, Heriot Watt University.

SYMBOLS

The following symbols are used to describe the quantities indicated in this list unless otherwise stated in the text.

x	distance from leading edge of the flat plate.
y	distance from the surface of the flat plate.
z	distance from the centre line of the plate, perpendicular to x and y.
U_o	free stream velocity.
U	mean velocity at a point in the boundary layer.
u	x-component of fluctuation velocity.
v	y-component of fluctuation velocity.
w	z-component of fluctuation velocity.
u', v', w'	intensities or root mean square values of u,v,w.
C_r	wave velocity.
$\beta_r = 2\pi f$	where f = oscillation frequency.
$\alpha = {}^{2\pi}/\lambda$	wave number.
ν	kinematic viscosity.
∂	boundary layer thickness.
∂^*	boundary layer displacement thickness.

$\partial^* = 1.72\sqrt{\frac{\nu x}{U_o}}$ for Blasius distribution.

$\partial^* = 0.341\ \partial$ relation used by Tollmein & Schlichting.

$R = \frac{U_o \partial^*}{\nu}$ boundary-layer Reynold's Number.

H	rate of heat loss from a heated wire.
T_w	temperature of the wire when heated.

SYMBOLS (Contd.)

T_∞ air temperature and the temperature of wire when cold.

T_m $(T_w + T_\infty)/2$.

N Nusselt Number.

R_w resistance of the hot-wire at temperature T_w.

R_a 'cold' resistance of the wire at temperature T_∞.

i current through the hot-wire.

CHAPTER I

INTRODUCTION AND HISTORICAL REVIEW

1. Introduction

The stability of boundary layer flow has been of interest to fluid dynamicists for a number of years. Even in its simplest guise, the incompressible flow over a flat plate with zero pressure gradient, it is an extremely complex problem. Predictions of the initial behaviour of a small disturbance in the boundary layer on a flat plate have been successful. However, full theoretical or experimental knowledge has yet to be attained of the behaviour of a disturbance of finite size. It is hoped that this thesis illuminates at least some aspects of the transition to turbulence of the boundary layer on a flat plate. Experimental work was first carried out in an 18 inch open-circuit tunnel, and it was from this tunnel that the work on the generation of harmonics, a phenomenon associated with a disturbance of finite size, was derived. Work was then transferred to the 4 foot closed-circuit tunnel. The flow in the tunnel had first to be investigated, and in fact, the measurements of the free stream turbulence are of as much interest from the point of view of tunnel behaviour as they are in relation to natural transition of a boundary layer. Finally, an experimental study was made of the behaviour of small disturbances in the boundary layer.

2. Historical Review

(a) The boundary layer

During the 19th century theoretical interest in fluid dynamics centred on the development of the inviscid fluid theory. It was felt that inviscid theory might give solutions in good agreement with observation for the motion of bodies through air and water, as for these two fluids, the viscous forces were expected to be very small compared with the forces due to gravity and pressure. This was found not to be true, inviscid theory predicting, for instance, zero drag on a body in steady flow. The Navier-Stokes equations were formulated in 1830. However, the difficulty of obtaining solutions for exact cases resulted in their being, to a certain extent, ignored. Stokes (1851) had treated the problem of a pendulum in a viscous fluid by assuming a condition of no slip between bob and fluid. However, the results were valid only for slow motions, and it was even suggested that the condition of no slip might be valid only for slow motion.

The problem of fluid flow about a body was clarified, when Prandtl (1904) introduced the boundary layer theory. He postulated that the effects of viscosity were limited to a small region about the body, and that outside that region inviscid fluid theory was valid. Within the layer the velocity of the fluid increased rapidly from

zero relative velocity at the surface of the body and approached asymptotically the free stream velocity at the edge of the layer. For two-dimensional flow over a semi-infinite flat plate, at zero incidence and with zero pressure gradient in the flow direction, Prandtl's "boundary layer" assumption allows approximations to be made in the Navier-Stokes equations. This problem was first solved by Blasius (1908) in terms of an infinite power series. Improved calculations were made later by Goldstein (1930) and Howarth (1938).

The boundary layer theory for a flat plate was first verified experimentally by Burgers (1924) and van der Hegge Zijnen. Dryden (1936) reported results which were in much closer agreement with theory than those of Burgers, but the most complete and careful measurements are those due to Nikuradse (1942).

(b) Stability of the boundary layer

The classic work of Reynolds (1883) stimulated interest in the problem of stability of fluid flows. Reynolds investigated the properties of the flow of water in a cylindrical tube by introducing into the flow a thin thread of coloured liquid. For a ~~given~~ suitable flow velocity and tube, laminar conditions could be held down the length of the tube. Increase of the flow velocity above a certain critical value, however, resulted in an eddying motion in the tube. By using a variety of tubes, Reynolds was able

to define a critical non-dimensional number, which if exceeded meant that the flow in the tube would no longer be laminar. This number, now known as the critical Reynold's Number, was a function of the flow velocity, of a typical dimension of the flow (in this case the diameter of the tube), and of the kinematic viscosity of the fluid ($R = Ud/\nu$).

Two views developed on the cause of turbulence in fluid flow. The first view considered turbulence as being due to a definite instability in which small disturbances initially grew exponentially. The second view, on the other hand, considered the flow as being stable to infinitesimal disturbances, turbulence being caused by either finite sized disturbances or an adverse pressure gradient of sufficient magnitude.

The theory of disturbances of finite size dates back to Reynolds (1895). Later Synge (1936) was to consider the stability of a quadratic profile, and found it stable below a critical value for the square of the vorticity of the disturbance. Taylor (1936) investigated the stability of the laminar boundary layer, his theory being that finite size disturbances in the free stream impressed themselves on the laminar boundary layer, so causing it to become turbulent. Taylor pointed out that the boundary layer, on for instance a flat plate or sphere, thickens in the downstream direction and so grows more

unstable. Therefore, a given amount of disturbance in the free stream becomes capable of causing turbulence in the boundary layer only at a certain distance downstream. The disturbing effect of turbulence in the free stream on the boundary layer is then due to pressure gradients which accompany the variations of pressure in the turbulent flow. With this theory a necessary condition for turbulence was that there should be a separation, not necessarily permanent, of the boundary layer preceding turbulence.

The theory of infinitesimal disturbances was, in itself, approached in two ways, firstly by considerations of energy balance, and secondly by the solving of the linearised equations.

Positive definite integrals of the energy and vorticity of the disturbance were used extensively in the first method. The stability of the boundary layer being indicated by the growth or decay of the disturbance energy with time. However, this method only gives the necessary conditions for stability as all disturbances are allowed, even those not satisfying the Navier-Stokes equations. The inclusion of all types of disturbance necessitates a larger viscous decay to give stability than that required if only hydrodynamically possible disturbances are considered. The limit of stability determined was therefore very much less than that found in

experiment. Lorentz (1898), has discussed this method, and found a critical Reynolds Number of 288 for Couette Flow. Orr (1907), for the same problem, gave a value of 177. Experimentally, however, the critical number found by Couette (1890) was 1940. Noether (1921) and Prandtl (1935) have both written very interesting accounts of this work.

The second method involved solving the eigen-value problem associated with the linearised equations governing the disturbance. Rayleigh (1880), (1887), (1892), (1895) and (1913), in a series of papers, used this method to study the stability of a flow profile composed of a series of straight lines. He considered the inviscid case only, where the influence of viscosity on the mean flow, but not on the disturbance, is considered. Rayleigh showed the instability of a profile with an inflexion, and also found that simple shearing motion between two planes was stable, along with the flow between two parallel walls. Rayleigh (1914), (1915) in two later papers also considered the stability of a viscous fluid.

Prandtl (1921) and Tietjens (1925) applied Rayleigh's method of approximation to the stability of a boundary layer on a flat plate. Tietjens approximated the Blasius profile to a series of straight lines. With this method he was able to take account of the viscous layer at the wall but, as the curvature of the profile vanished throughout the boundary layer, he was unable to

consider the singularity at the critical layer. The critical layer occurs where the wave velocity of the disturbance is identical to the local velocity of the flow. Tietjens was unsuccessful in finding a critical Reynolds Number but he did, however, show that the flow was unstable, for $R = \infty$, when the profile contained an inflexion. Tollmein (1935) was later to confirm this result for a curved boundary layer profile.

Heisenberg (1924) was the first to study the stability of a flow with a continuously curved profile. He presented a criticism of Rayleigh's results and showed that plane Poiseuille Flow was unstable for sufficiently large Reynold's Number. Tollmein (1929) adopted Heisenberg's method to study the flow on a flat plate. He approximated the Blasius profile to a straight line and a parabola, and ensured that the curvature was finite at the critical layer. He was thus able to consider the effect of viscosity at the critical layer. Tollmein found a critical Reynolds Number for the flow and also defined those oscillations which would be unstable. Tollmein's results may be summed up on the Neutral Stability Diagram which is a plot of the non-dimensional frequency ($\beta_r \nu/U_o^2$) against Reynolds Number ($R = U_o \delta^*/\nu$) see Figure I.1. The area inside the curve denotes instability and that outside, stability. Schlichting (1933) calculated the curves of constant amplification for the unstable

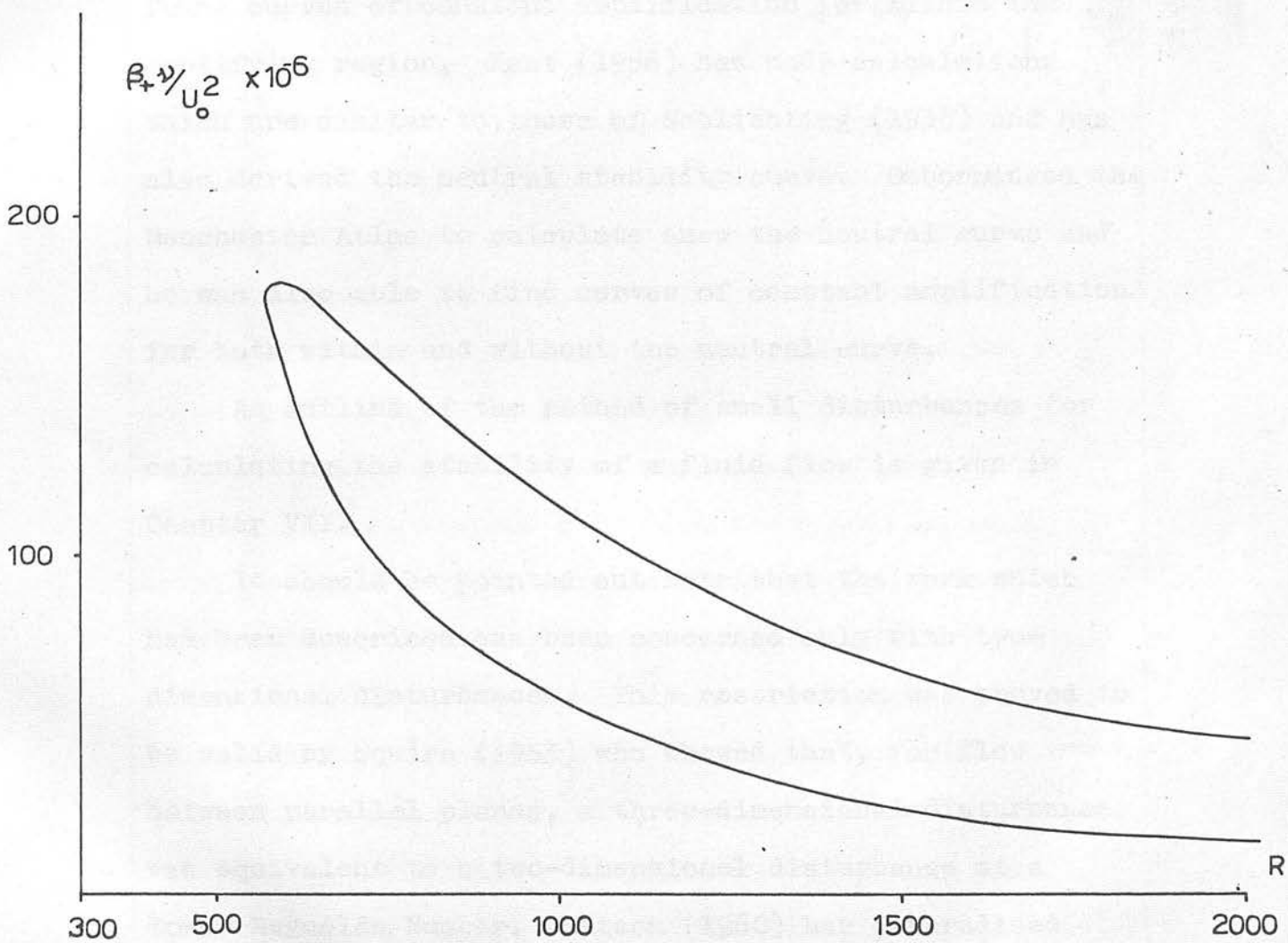

Figure I.1. Neutral Stability Diagram (Tollmein)

oscillations contained within the Neutral Stability curve. Schlichting (1935) also found the amplitude distribution of the small disturbances for two neutral oscillations, one on either of the two branches of the Neutral Stability curve. Lin (1945) and Shen (1954) developed the Tollmein-Schlichting theory. Lin recalculated the neutral curve, whilst Shen, using that curve, found curves of constant amplification for within the amplifying region. Zaat (1958) has made calculations which are similar to those of Schlichting (1935) and has also derived the neutral stability curve. Osborne used the Manchester Atlas to calculate anew the neutral curve and he was also able to find curves of constant amplification for both within and without the neutral curve.

An outline of the method of small disturbances for calculating the stability of a fluid flow is given in Chapter VIII.

It should be pointed out here that the work which has been described has been concerned only with two-dimensional disturbances. This restriction was proved to be valid by Squire (1933) who showed that, for flow between parallel planes, a three-dimensional disturbance was equivalent to a two-dimensional disturbance at a lower Reynolds Number. Watson (1960) has generalised Squire's result. The above work considered small disturbances only. For disturbances of finite size, Meksyn (1964) has shown that three-dimensional disturbances are

more unstable than two-dimensional ones.

Dryden (1936) made the first observations of velocity fluctuations in a laminar boundary layer, but they were irregular and produced transition to turbulence without showing any of the characteristics required by Tollmein-Schlichting theory. Nikuradse (1933), on the other hand, attempted a confirmation of stability theory using a water-tunnel, but the tunnel's general disturbances were too large.

In the decade following Dryden's paper (1936) researchers in the field of fluid dynamics inclined more to Taylor's arguments concerning instability of the laminar boundary layer than to the small disturbance theory of Tollmein and Schlichting. Transition was felt to be necessarily associated with separation of the boundary layer, a view which may be traced back to Prandtl (1914). As has been seen the stability of a boundary layer profile with inflexion had attracted a great deal of theoretical attention. In addition, the theory of Tollmein and Schlichting was thought to have serious deficiencies, notably the assumption that the boundary layer on a flat plate was of constant thickness.

Dryden (1936) did point out, however, that the theories of Taylor and Tollmein and Schlichting were not mutually exclusive but rather that they were supplementary. However he felt that Taylor's theory was the

more valid, as, in his opinion, disturbances of finite size were more usual in practice.

Taylor's theory was confirmed by the measurements of Dryden (1936) on the transition of the boundary layer on a sphere. The work of Hall and Hislop (1938) and Fage (1942) on the transition of the boundary layer on a flat plate with zero pressure gradient and high free stream turbulence indicated the existence of a criterion for transition which depended on the fluctuating pressure gradients in the main stream turbulence. However Hall and Hislop were in some doubt as to whether or not laminar separation took place at the transition point.

The Tollmein-Schlichting theory was finally vindicated by Schubauer and Skramstad (1947). Using the low turbulence wind tunnel at the National Bureau of Standards, Washington, Schubauer and Skramstad after painstaking experiments, discovered disturbance waves in the boundary layer on a flat plate which behaved as Tollmein-Schlichting theory predicted. Schubauer and Skramstad used hot wire anemometers to detect the oscillations in the boundary layer. They then determined the frequency of the most prominent oscillation at various mean wind speeds and positions down the flat plate. The points thus obtained were plotted on the neutral stability curve, and it was found that they all lay close to Branch II of the neutral curve. This was to be expected, for by Tollmein-Schlichting theory the oscillations would have undergone maximum amplification near to Branch II. Having shown the existence of Tollmein-

Schlichting-like waves Schubauer and Skramstad then introduced controlled artificial disturbances into the boundary layer using the vibrating ribbon method. Positions of neutral stability were found that agreed reasonably with the Tollmein-Schlichting neutral curve. Much better agreement may be found when the results are compared with Lin's neutral curve. Perhaps the most striking of Schubauer and Skramstad's results was their confirmation of Schlichting's theoretical prediction for the amplitude distribution of an oscillation through the boundary layer.

Bennett (1953) has clarified the relationship between the theories of Taylor and of Tollmein and Schlichting. Bennett investigated the natural transition of a boundary layer on a flat plate for a range of free stream turbulence levels 0.1°/o to 0.5°/o. He confirmed that Tollmein-Schlichting waves control the initial phase of transition. He inferred that for free stream turbulence levels higher than those used there would be a level where Tollmein-Schlichting waves would play no part in transition and that Taylor's theory might then hold. However Bennett points out that this level is higher than had previously been anticipated.

(c) Non-linear theories

The small disturbance theory of Tollmein and Schlichting was successful in predicting the initial

behaviour of a disturbance in the boundary layer. However, it soon became evident that it was insufficient to give a clear picture of the processes leading to transition. These processes involved disturbances of finite size so that linearisation of the equations describing the flow was no longer valid.

Both Noether (1921) and Heisenberg (1924) considered equations involving non-linear terms. However it was not until Landau (1944) proposed his theory of successive instabilities that any predictions on the effect of the non-linear terms were made.

The theoretical work to be described has considered, in the main, plane Poiseuille flow. In this case the local Reynold's Number is independent of the streamwise position, a feature which introduces a major simplification of the mathematical problem. However, it was hoped that the results might be at least partially valid for boundary-layer flow on a flat plate.

Meksyn and Stuart (1951) gave an approximate method for the solution of the non-linear equations of Noether and Heisenberg. They took account of two non-linear processes, the distortion of the mean flow and the distortion of the distribution of the fundamental, in studying the stability of a disturbance of finite size. For a region, stable according to Tollmein-Schlichting theory, a threshold value for the amplitude of the disturbance

was found. Above that value the disturbance would amplify, and below it would decay. The variation of the critical Reynold's Number with amplitude of the disturbance was also found. Stuart (1958), considering the effect of distortion of the mean flow only, was able to show the existence of a stable disturbance of finite size in a region unstable according to Tollmein-Schlichting theory. Stuart, using energy principles, derived the equation describing the time amplification of a disturbance which was first proposed by Landau. Stuart (1960c) again derived Landau's equation and pointed out the physical significance of the three non-linear terms in its solution. These non-linear terms which control the amplification of the disturbance are the distortion of the mean motion, the generation of a second harmonic of the fundamental wave, and the distortion of the distribution of the fundamental wave. Stuart (1960c) named the cases discussed by Meksyn and Stuart (1951) and by Stuart (1958), "subcritical" and "supercritical" respectively. He then went on to consider the relationship between them when in the region of the neutral curve. Watson (1960) has extended this work and applied the theory to Couette flow. Stuart (1960b) reviewed the work described above. This discussion has omitted work concerned with the generation of a second harmonic of the fundamental wave which will be described fully in a later chapter.

It should be pointed out that the above work has been concerned with the time amplification of two-dimensional finite disturbances. Bradshaw, Stuart and Watson (1960) demonstrated how this work could be extended to amplification in space. However, Klebanoff and Tidstrom (1959) found that the flow on a flat plate showed marked three-dimensional properties before transition. As a result of this work theoretical interest centred on the problem of three-dimensional disturbances in fluid flow.

Benney and Lin (1960) studied the interaction of a two-dimensional wave disturbance with a three-dimensional wave disturbance, a problem prompted by the work of Klebanoff and Tidstrom. They found that the non-linear effects divided naturally into two, the two-dimensional effects which had been examined by Meksyn and Stuart (1951) and Stuart (1958) and the intrinsically three-dimensional effects which included longitudinal vortex motion. Benney (1961) considered the latter effects which comprised two flows both non-periodic (one strictly so and the other non-periodic because of an initial assumption). The vortices had a spanwise periodicity and produced spanwise energy transfer (cf Klebanoff and Tidstrom). Benney discussed the vortex patterns produced for various relative amplitudes of the vortex patterns of the initial waves. As the three-dimensional wave increased

in amplitude the spanwise period of the vortices doubled. Benney and Lin and Benney made their calculations for an inflexional profile. Stuart (1960a) studied the interaction of the two and three-dimensional waves for the case of plane Poiseuille flow. He examined both the non-linear and the three-dimensional effects resulting from the interaction. Stuart also discussed the assumption of Benney that the two waves should have the same frequency and amplification factor. Stuart showed that if this assumption were not made then Benney's results would not be in complete disagreement with those of Görtler and Witting (1958). Benney (1964) acknowledged Stuart's criticism but pointed out that his own results, on this point, had been confirmed experimentally. Benney (1964) extended his previous work to a boundary layer type profile consisting of two straight lines.

A further theoretical approach leading to components with streamwise vorticity has been made by Görtler and Witting (1958). They suggest that the Tollmein-Schlichting wave motion possesses regions where the total flow (mean flow plus oscillation) is unstable due to the action of centrifugal forces, an idea in accord with Landau's theory of successive instabilities. According to their work, streamwise vorticity will develop at positions where the streamlines are concave relative to an observer moving with the wave speed. However, for boundary layer flow it has been observed experimentally

that streamwise vorticity develops at positions where the streamlines are convex. This experimental result is in qualitative agreement with the Lin-Benney theory when the assumption discussed above is made.

Stuart (1960b) discussed a novel cause of instability. He reported on a paper by Raetz (1959) in which the interaction of two strongly three-dimensional waves was considered. It was found that two neutral waves could produce a rapidly amplifying resonance oscillation. Raetz suggested that this phenomenon might account for a growth rate of boundary layer oscillations which was much larger than that given by usual instability theory.

Finally, it seems appropriate to finish this review of the theoretical work on boundary layer stability with a report of a paper by De Santo and Keller (1962). They attempted a numerical integration of the flow equations using a digital computer. The results obtained were not very extensive. However a computer method does offer the opportunity of considering all the non-linear terms simultaneously rather than, as has been done up to now, treating the terms selectively.

d) Experimental work

As has been seen, Schubauer and Skramstad showed that the initial stages of transition could be described by the Tollmein-Schlichting theory. This theory, of

course, was concerned with small disturbances only, and after its confirmation experimental interest turned to the later stages of transition. The behaviour of disturbances of finite size and the breakdown of the laminar boundary layer were then studied.

The picture of the transition process in the boundary layer was clarified greatly by the work of Emmons (1951). Emmons noticed that turbulence in the boundary layer on a water-table was generated at random times and at random positions. The turbulence first appeared as a tiny spot which then grew in both the streamwise and lateral directions as it was washed down the table. In general, spots were formed at a number of spanwise positions, and due to their growth they coalesced at some position downstream so that eventually the whole of the boundary layer on the table became turbulent. Emmons proposed a probability theory to describe the interactions of the turbulent spots in the transition zone, the transition zone being that zone between the position of the first upstream spot and the position where the boundary layer is first fully turbulent. The assumptions made by Emmons in his theory have been confirmed by Schubauer and Klebanoff (1955) and Elder (1960b). A very successful phenomenological theory of the transition zone was established by Dhawan and Narasinha (1958). A fuller discussion of the transition zone, with especial

reference to the lateral growth of the turbulent spots, will be given in a later chapter.

The transition region where the disturbance is of finite size has been studied using both flow visualisation and hot-wire methods. Fales (1955) was the first to perfect a flow visualisation method for this work. The boundary layer on a flat plate, moving at uniform speed through water, was studied by injecting dye from a tube into it. Transition phenomena were seen when a trip was placed parallel to the leading edge of the plate. The uniform dye distribution on passing over the trip gathered into discrete transverse lines. As the dye lines moved downstream their velocity increased and spanwise irregularities formed so that the lines had a sawtooth appearance. Fales considered the concentration of the dye after passing over the trip as being due to the formation of vortices which were comparable to the vortices in a Karman vortex train. The three-dimensional nature of the vortices was studied by Hama, Long and Hegarty (1957). They again made the boundary layer unstable with a trip and found that a weak two-dimensional vortex remained nearly two-dimensional, but that a strong two-dimensional vortex developed three-dimensional properties. The initially straight line vortex became wavy, as observed by Fales, and the peaks were then strongly stretched in the streamwise direction. The plan

shape of the vortex then resembled a series of bottles with sloping shoulders. Shortly after this, bursts of turbulence occurred at the shoulders of the vortex. Turbulence was thus generated at a number of spanwise positions. Hama, Long and Hegarty were able to explain their results by referring to a paper by Lord Kelvin (1880). Kelvin had shown that the plane of a wavy vortex line should rotate in a direction opposite to that of the vorticity. For the case of viscous shear flow the head of the wavy vortex line would then be lifted up from the plate and the tail pushed down. The head would thus have its velocity increased whilst the tail's velocity would be decreased. The vortex line would be stretched and the vorticity therefore increased. By an analysis of their results, Hama, Long and Hegarty were able to show the lifting of the vortex head. However they were unable to explain the cause of the original waviness of the vortex line. Schubauer (1958) discussed the results of Hama, Long and Hegarty in the light of work by Klebanoff and Tidstrom (1959). In this case the boundary layer on a flat plate in a wind tunnel was studied with hot-wire anemometers. Disturbances were introduced into the boundary layer by a vibrating ribbon. Klebanoff and Tidstrom found that the wave front of the disturbance did not noticeably warp, a result in direct opposition to the observations of Hama, Long and Hegarty. Klebanoff and Tidstrom also found that

transition took place before discrete vortices were formed, whereas Hama, Long and Hegarty concluded that the formation of discrete vortices was necessary for transition to take place. Schubauer suggested that the differences might lie in the nature of the disturbances injected into the boundary layer. Hama (1960) therefore used the vibrating ribbon technique to repeat the work of Hama, Long and Hegarty. He found that the initially sinusoidally distributed vorticity did concentrate, as a consequence of wave amplification, to form discrete vortices and that the vorticity concentration took place at the critical layer. For large ribbon amplitudes the results were the same as those of Hama, Long and Hegarty. The underlying assumptions of the Hama, Long, and Hegarty experiment, that an initially small disturbance would roll up to form discrete vortices when amplified and that the vortices from the trip simulated the behaviour of the amplified disturbances, were thus verified. Disagreement therefore still remained between the results of Hama and those of Klebanoff and Tidstrom. Hama (1962a) therefore undertook a theoretical investigation of the behaviour of streaklines in a shear flow for a neutral wave. He found that the streakline which emerged at the critical layer tended to amplify its wavy form and appeared to roll up. A streakline could thus give the incorrect impression that the wave amplified and developed

into discrete vortices despite the fact that the wave was steady and that no discrete vortices existed. Hama pointed out, however, that this result did not necessarily invalidate his previous experimental results as it was quite likely that the streakline would behave similarly when the wave was amplified and when discrete vortices did exist. Hama stated that experimental results favoured the vortex loop concept and in two later theoretical papers reinforced this view. Hama (1926b) computed the progressive deformation of a curved vortex filament by its own induction. The tip of the vortex was found to lift as experiment had shown. Hama (1963) then studied the progressive deformation of a perturbed line vortex filament, a case closely resembling the experimental situation (cf Hama 1960). The results were in close agreement with those found by experiment.

Part of the work of Klebanoff and Tidstrom (1959) has already been discussed in connection with the results of Hama. Klebanoff and Tidstrom followed the work of Schubauer and Klebanoff on turbulent spots with an investigation of the processes leading to the generation of a turbulent spot. They found that the intensity of the wave varied in the spanwise direction and that this spanwise variation was linked with spanwise mean flow variations. Klebanoff and Tidstrom were able to show that these latter variations were, in some way, a function of the smoothing screens. However, they concluded that

disturbance waves had an inherent tendency to form peaks and valleys of intensity which always developed before transition took place. Klebanoff and Tidstrom showed that the intensity variations were due to an energy concentrating mechanism in which energy flowed from a valley to a peak. Turbulent spots were created at the peaks, turbulence then spreading into the valleys.

Tani (1960) and Tani and Komoda (1962) introduced controlled variations into the mean flow. They studied the distribution of the wave intensity through the boundary layer and also the phase of the wave front for a number of spanwise positions. They inferred an energy concentrating mechanism similar to that found by Klebanoff and Tidstrom.

Klebanoff, Tidstrom and Sargent (1962) extended the work of Klebanoff and Tidstrom in a series of fine experiments. The mean flow variations in the spanwise direction were removed by installing new smoothing screens. However the same general behaviour which had been seen by Klebanoff and Tidstrom was observed, They therefore felt that three-dimensional wave behaviour was inherent in transition. As a result they introduced controlled three-dimensional waves into an essentially two-dimensional boundary layer, using an adaptation of the vibrating ribbon method. Spanwise variations in the wave intensity were again found. Surveys of the longitudinal and spanwise components of the mean velocity as well as of the

intensities and instantaneous values of the longitudinal and spanwise fluctuations were made across the boundary layer at different spanwise positions in the region from ribbon to wave breakdown. An evaluation of several theoretical approaches was made. Those considered were the generation of higher harmonics, the interaction of the mean flow and Reynold's stress, the concave streamline curvature associated with the wave motion and the vortex loop. They found that all were inadequate to describe the observed phenomena. However, close agreement was found between their results and the theoretical predictions of Lin and Benney. A system of longitudinal eddies was observed and doubling of the eddy system was inferred as the three-dimensional component of the wave interaction became more dominant. Klebanoff, Tidstrom and Sargent also came to the conclusion that the theoretical assumption, made by Benney, of equal wave velocities for the two interacting waves was reasonable. Klebanoff, Tidstrom and Sargent found that the generation of a turbulent spot was associated with a hairpin eddy system and inflexional instability of the mean velocity distribution. Referring to the work of Kovasznay (1960) they found striking agreement between the instantaneous velocity distribution through the boundary layer for their case and the mean velocity distribution downstream of a roughness element. Finally they showed that their results were equally applicable to natural transition.

(e) Reviews

There have been a number of reviews on the work described in this Chapter and on related topics. They include reviews by Prandtl (1935), Dryden (1955) and (1956), Kuethe (1956), Schlichting (1960) and Stuart (1960b). Books by the following contain relevant material: Lin (1955), Schlichting (1955) and Rosenhead (1963).

I.3. Conclusion

It will have been seen that knowledge of the processes leading to turbulence in a boundary layer is extensive but by no means conclusive. One of the newest theoretical approaches to the problem of transition is by computer analysis, and this method does promise to be successful in relating all the phenomena associated with transition. However, it is imperative that experimental studies should test theoretical results and perhaps also indicate how a problem might best be approached. It is hoped that the present work shows both the above characteristics.

CHAPTER II

HARMONIC CONTENT OF WAVE DISTURBANCES IN THE BOUNDARY LAYER

II.1 Introduction

In the boundary layer the generation of harmonics of a periodic disturbance has, in the main, been considered only for the case of plane Poiseuille flow. The production of harmonics results from the disturbance having a finite amplitude so that the equations describing the motion may no longer be linearised. Distortion of the mean flow is the other main phenomenon associated with disturbances of finite amplitude.

In their paper Meksyn and Stuart (1951) considered the effect of a finite two dimensional disturbance on plane Poiseuille flow. They showed that the interaction of the Reynold's stresses and the mean flow, produced a distortion of the mean velocity profile. In this paper Meksyn and Stuart were studying the transition to turbulence in the flow. On examining the non-linear terms in the relevant equations they concluded that the production of harmonics plays a less important role, in this transition, than the distortion of the mean flow. In their theory they therefore neglected the generation of harmonics.

In a later paper, Stuart (1958) considered the energy balance equation for oscillations of finite amplitude in

plane Poiseuille flow, but again considered only the mean flow.

Lin (1958) concerned himself directly with the problem of harmonic generation in parallel flow. He made an order of magnitude analysis of the non-linear terms involved in the problem and paid especial attention to the region of the critical layer. Lin concluded from his work that "for disturbances in a parallel flow, all the harmonic components of the oscillation simultaneously become important around the critical layer, before the amplitude of the fundamental component is large enough to cause any significant distortion of the mean flow". However, exactly what Lin means by "important" is not clear.

Stuart (1960c) has criticised Lin's conclusion, distinguishing between the cases considered by himself and Lin. Whereas in Stuart's work and that of Watson (1960) the non-linear terms become significant when they are of the same order of magnitude as the whole group of linearised terms, Stuart noted that Lin studied only disturbances such that a typical non-linear term is of the same order of magnitude as some linear term. Stuart concluded that the disturbance amplitudes considered in his earlier work were much smaller than those considered by Lin, and that Lin's analysis did not apply to smaller disturbances. The result of Stuart's analysis as regards harmonic generation is that, with a basic perturbation of

the flow of small order A, the amplitude of the second harmonic and the distortion of the mean flow are of order A^2, and in general the amplitude of the n^{th} harmonic is of order A^n. It is to be remembered that there is a limitation to the above result, namely that $c_i \ll (\alpha R)^{-1/3}$ where $(\alpha R)^{-1/3}$ gives the effective thickness of the critical layer.

It would seem that Stuart's analysis is more closely allied than is Lin's to the physical problem where the growth to finite size of an initially very small periodic disturbance is studied.

Klebanoff and Tidstrom (1959) showed experimentally that three dimensional features were evident when the disturbances in the boundary layer on a flat plate were of finite amplitude. It thus became obvious that consideration of finite amplitude disturbances in two dimensional parallel flow was insufficient. As a result of Klebanoff and Tidstrom's work Benney and Lin (1960) examined theoretically the interaction of a two dimensional Tollmein-Schlichting wave with a three dimensional wave disturbance. They showed that the interaction produces second order effects including the generation of harmonics of the fundamental, modification of the mean flow, and generation of new harmonic components which are non-periodic in time. Benney (1961) carried out more detailed calculations on the perturbations under these circumstances. When the two dimensional wave

is dominant then the secondary flow takes the form of a system of equidistant vortices parallel to the main flow, and when the three-dimensional component becomes dominant then the spacing between the vortices is reduced by a factor of 2.

The other experimental work which has hitherto been published on harmonics in the boundary layer on a flat plate is that by Klebanoff, Tidstrom and Sargent (1962). Periodic three dimensional disturbances were injected into a two dimensional boundary layer, using the vibrating ribbon technique of Schubauer and Skramstad (1947). A hot wire anemometer was used to detect the resulting oscillation downstream. Observations were also made of the boundary layer velocity profile. The results showed that the amplitude of the second harmonic was nowhere of the same order as that of the fundamental before distortion of the mean flow occurred, and that, in general, it was a tenth of the fundamental. In the same paper Klebanoff, Tidstrom and Sargent infer the existence of longitudinal eddy systems of the type suggested by Benney and Lin.

II.2. Acknowledgement

The work about to be described was carried out in conjunction with L. Kersley. A description of the study preliminary to this work, in which the harmonic content of the disturbances was investigated by the analysis of

filmed C.R.O. traces and by the use of sets of filters, has been given by Kersley (1965).

II.3. Description of the apparatus

The work about to be discussed was carried out in an open circuit wind tunnel, a modification of N.P.L. Design No. A 155, with 18 ins. octagonal working section. A vertical flat plate, 6 ft. by 18 ins., of 1/4 in. perspex was mounted centrally in the tunnel. The plate's leading edge was shaped to a symmetrical knife edge and was located 1 ft. upstream of the working section. False walls of 1/16 in. perspex were positioned to obtain zero pressure gradient in the working section. The turbulence level in the free stream was 0.3%.

Disturbances of known amplitude were introduced into the boundary layer on the flat plate, using the vibrating ribbon technique first developed by Schubauer and Skramstad (1947). The phosphor bronze ribbon, 0.001 ins. thick and 0.1 ins. wide, was mounted 0.007 ins. from the plate on drawn glass bridges. The 9 ins. long middle section was free to vibrate at a selected frequency, when driven by an alternating current of this frequency, in the presence of the magnetic field of a permanent magnet, which was mounted on the reverse side of the plate. The ribbon was mounted parallel to and 1 ft. downstream from the leading edge, the centre of the vibrating portion being offset from z = 0 to z = 0.75 ins. The downstream

development of the injected disturbance was studied with constant current hot-wire anemometer system. A tungsten hot-wire was used, 0.0002 ins. diameter and approximately 0.05 ins. long, which was sensitive to the u' component of the fluctuation. High frequency compensation was available but was not employed as the work was limited to frequencies below 200 c/s. The signal from the hot-wire was amplified by a Solartron D.C. Decade Amplifier Type No. AA900. The R.M.S. magnitude of the amplified signal was given by a Bruel & Kjaer Frequency Analyser Type 2107, which was used in its maximum selectivity mode when measuring the magnitude of the individual harmonics.

The description of the apparatus used for the work on the second harmonic content of the boundary layer disturbance has been brief for two reasons. Firstly, the hot-wire equipment and the equipment used to analyse the hot-wire signal is essentially the same as the equipment used in the present tunnel which is described in Chapter V. The ribbon system used differs only in minor details from the one described in Chapter V. Secondly, although the tunnel used is not comparable in design and performance to the present one it has not been felt necessary to give a complete description of it as the results described should be independent of the tunnel used to obtain them. A full description of the design and construction of the open circuit tunnel has been given by Burns (1958). A description of the calibration of the

tunnel and of the traversing mechanism has been given by Kersley (1965).

II.4. Description of the mean flow

The mean velocity in the boundary layer, at constant x and y, was measured. It was found that any variation in the boundary layer thickness, in the spanwise direction, was masked by the mean flow fluctuations resulting from the natural unsteadiness of the tunnel. It was therefore concluded, that if any spanwise variation of the boundary layer thickness did exist, then it was of the order of 5°/o or less. It must be noted that, prior to the wind tunnel smoothing screens being cleaned before the start of the present experiment, measurements of the boundary layer thickness revealed a variation of about 10°/o in the spanwise direction. This spanwise variation had a 'wavelength' of about one inch. Spanwise variation of the thickness of the boundary layer on a flat plate thus appears to be due, at least partly, to the screens. This inference is in agreement with the results of Bradshaw (1964).

Although it was not possible to detect, positively, three dimensional characteristics in the boundary layer, it was found that an injected two dimensional disturbance had different rates of amplification, in the streamwise direction, for different spanwise positions.

The growth of the disturbance intensity in the streamwise direction, for two spanwise positions, is shown in Figure II.1. Growth curves of this type were obtained from hot-wire measurements taken at 1 inch intervals in the x-direction; they are taken with y/δ constant and within the critical layer. The graph clearly shows that the two spanwise positions have different rates of amplification of the disturbance associated with them. It would seem apparent that there is some energy transfer mechanism in operation (in which there is an energy flow from one spanwise position to another.) (cf. Klebanoff, Tidstrom & Sargent 1962). The investigation was made at two positions, 0.5" and 1.0"; the spanwise positions in the vicinity of maximum and minimum rates of growth of the disturbance respectively.

It should be noted here that the entire work was conducted at a wind speed of 25 ft./sec., and with a constant ribbon vibration amplitude, unless specifically stated otherwise. The frequency at which the ribbon was forced is stated on the relevant graphs. The frequencies, 55 c/s and 70 c/s, were used; Branch 1 of the neutral stability curve occurring at $x = 1'4"$ and $x = 1'0"$ respectively, for these two frequencies.

The results of Figure II.1 were obtained with the wire at constant y/δ ; this implies, for no injected disturbance, a constant mean wire resistance. A change

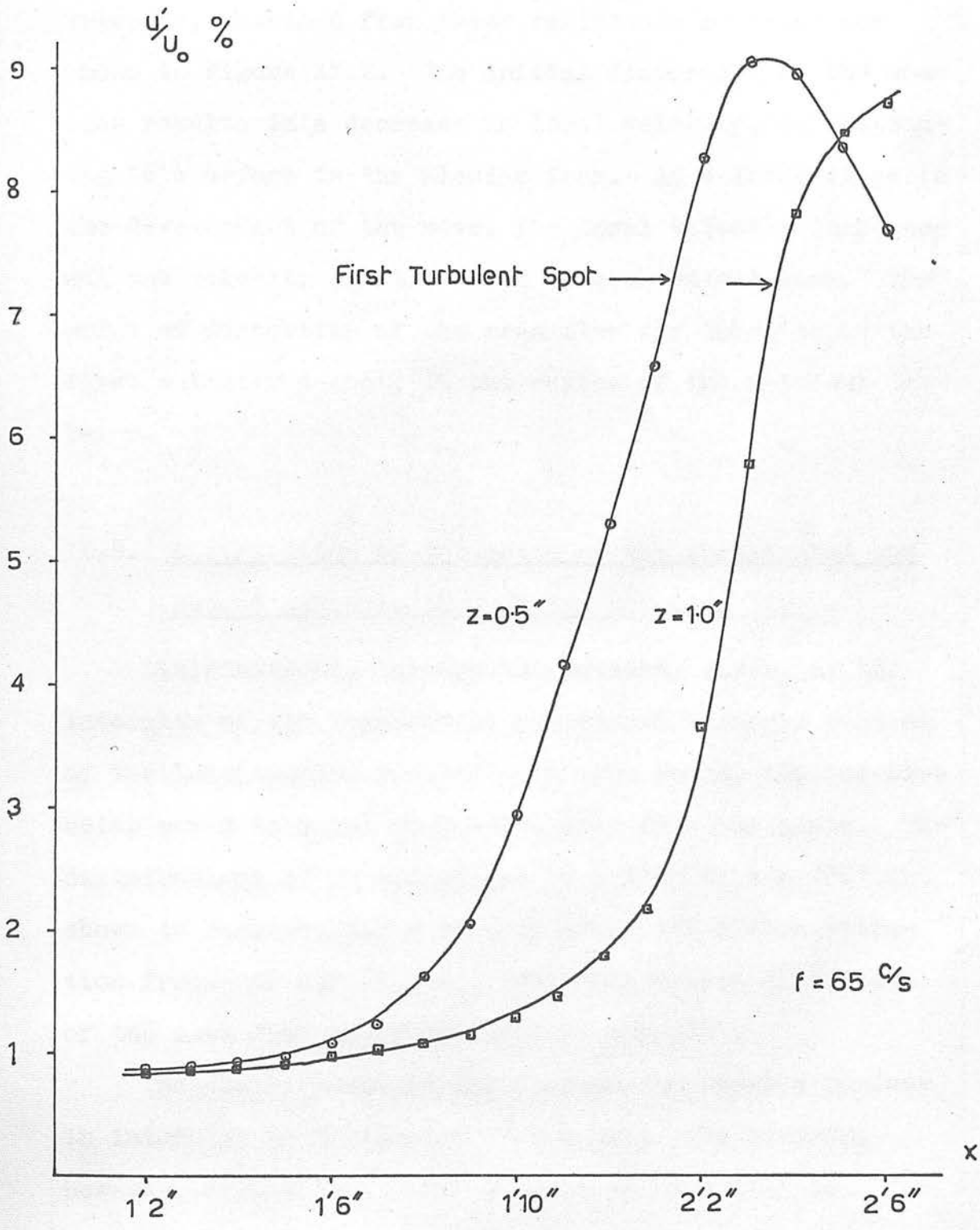

Figure II.1. Downstream Development of Disturbance Intensity at Two z-positions.

in this resistance, when injecting a disturbance, was taken to indicate distortion of the mean flow. Values of local velocity, expressed as a fraction of the free-stream velocity, obtained from these resistance readings are shown in Figure II.2. The initial distortion of the mean flow results in a decrease in local velocity, corresponding to a defect in the Blasius form. At a later stage in the development of the wave, the local velocity increases and the velocity profile tends to a turbulent form. The point of distortion of the mean flow was taken to be the first velocity defect, in the region of the critical layer.

II.5. Distribution of intensity of the fundamental and second harmonic through the boundary layer.

Distributions, through the boundary layer, of the intensity of the fundamental and second harmonic content of the longitudinal fluctuations were found, the hot-wire being moved in steps of 0.005", away from the plate. The distributions at $z = 0.5"$ for $x = 1'4"$ to $x = 2'2"$ are shown in Figures II.3 - 8 (for which the ribbon vibration frequency was 55 c/s). For this series distortion of the mean flow occurred first at $x = 2'0"$.

The distribution of the fundamental shows a maximum in intensity in the region $y/\delta = 0.2$. The minimum, however, shifts from $y/\delta = 0.85$ at $x = 1'4"$ to

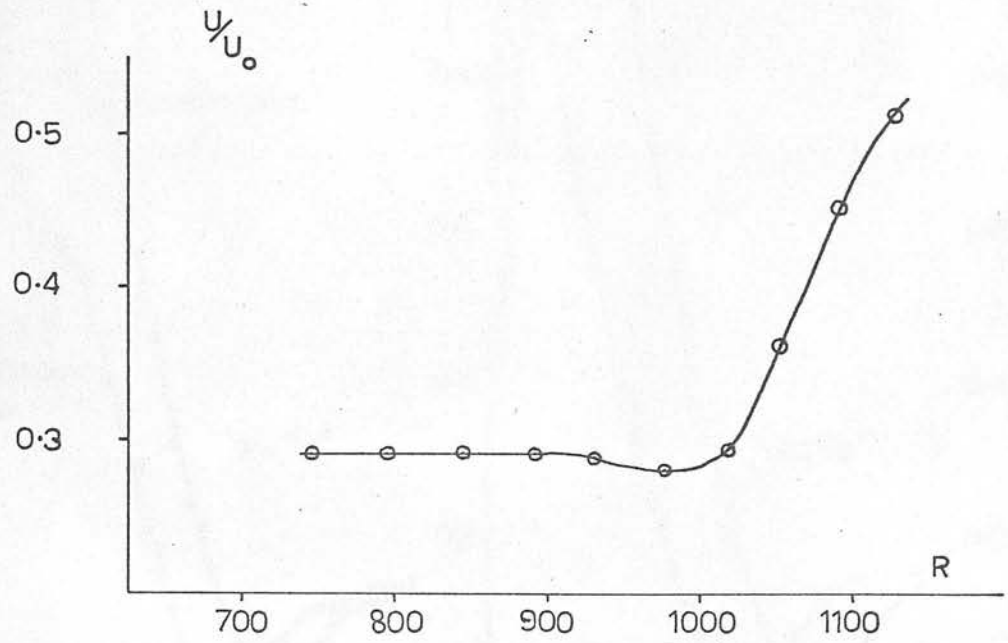

Figure II.2 Downstream Change in Local Mean Velocity.

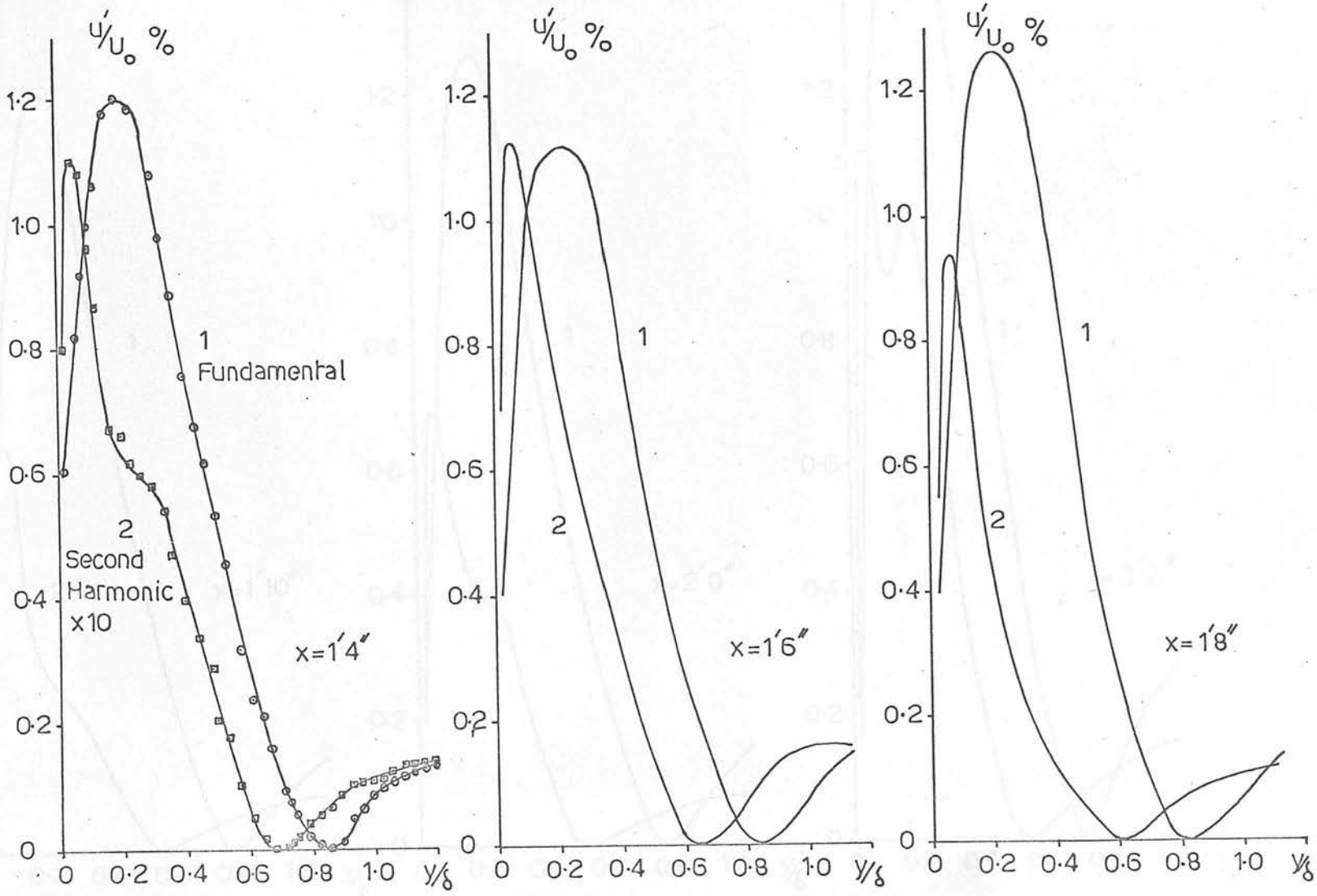

Figures II.3-5 Distribution of Fundamental and Second Harmonic Intensities through the Boundary Layer, s = 0.5" and f = 55 c/s.

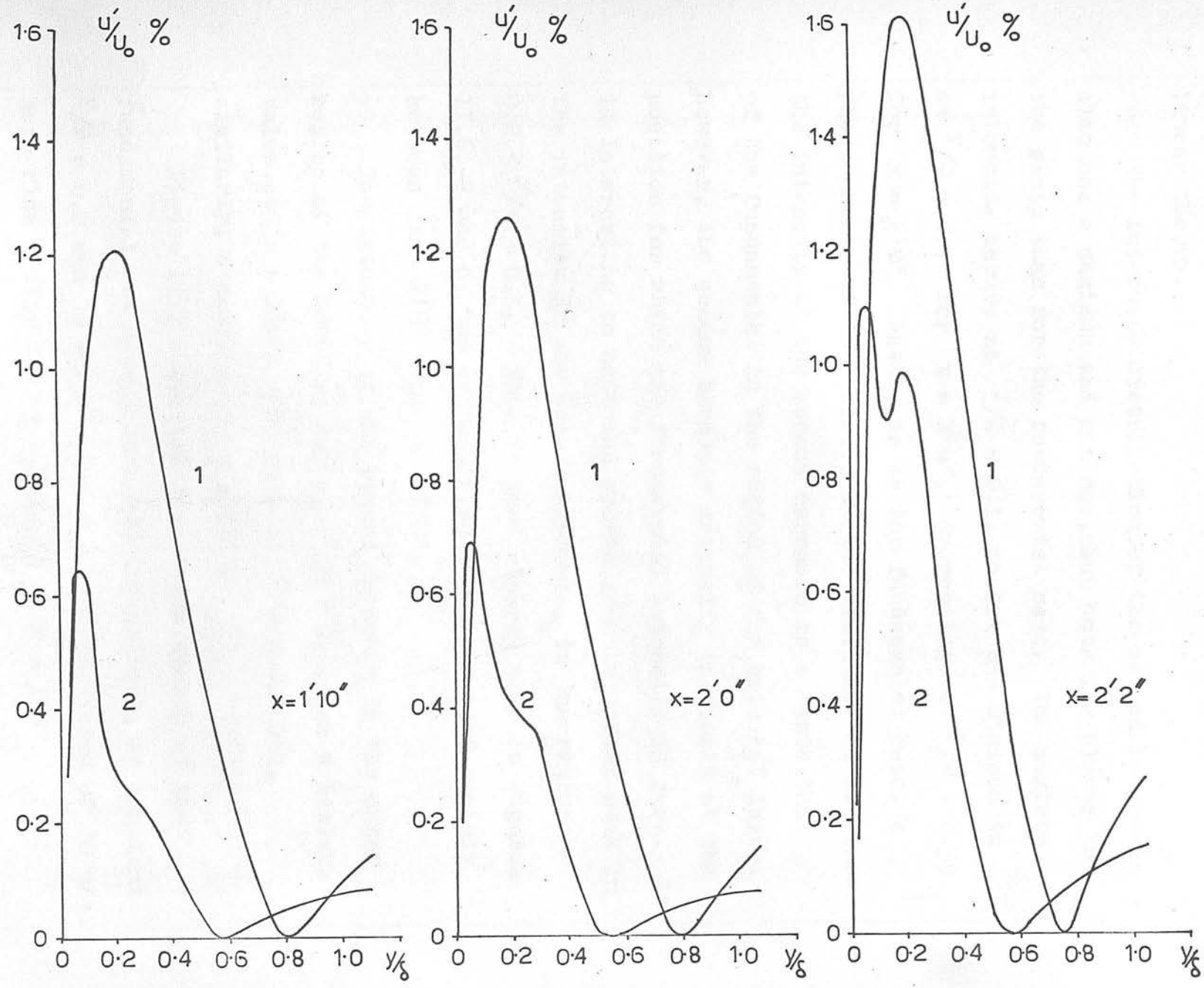

Figures II 6-8 Distribution of Fundamental and Second Harmonic Intensities through the Boundary Layer, s=0.5" and f=55 c/s.

$y/\delta = 0.75$ at 2'2". A phase change of 180° occurs at the minimum. These results agree with the predictions of linear theory.

The intensity distribution of the second harmonic also has a maximum and minimum, but both lie closer to the plate than for the fundamental case. The maximum intensity occurs at $y/\delta = 0.1$, whilst the minimum is at $y/\delta = 0.7$ for $x = 1'4"$, decreasing to $y/\delta = 0.55$ for $x = 2'0"$. Again, as in the fundamental case, a phase change of 180° occurs at the minimum. In all cases the intensity of the second harmonic is a tenth that of the fundamental in the region of the critical layer. However, the second harmonic intensity is finite at the position for which the fundamental intensity is zero. It is interesting to note the growth of a secondary peak in the intensity of the second harmonic, in the region $0.2 < y/\delta < 0.3$. This is most clearly seen in Figures II.6, 7 and 8, the secondary peak growing most rapidly between $x = 2'0"$ and $x = 2'2"$.

The intensity of the second harmonic in the outer region of the boundary layer, $y/\delta > 0.8$, has a maximum value at $x = 1'6"$. The peak at $y/\delta = 0.1$ has, similarly, a maximum at $x = 1'6"$.

Figure II.9 shows the downstream growth of the fundamental and second harmonic intensities, at constant $y/\delta = 0.2$ and $z = 0.5"$, for a ribbon frequency of 70 c/s. Mean flow distortion first occurs at $x = 1'9"$.

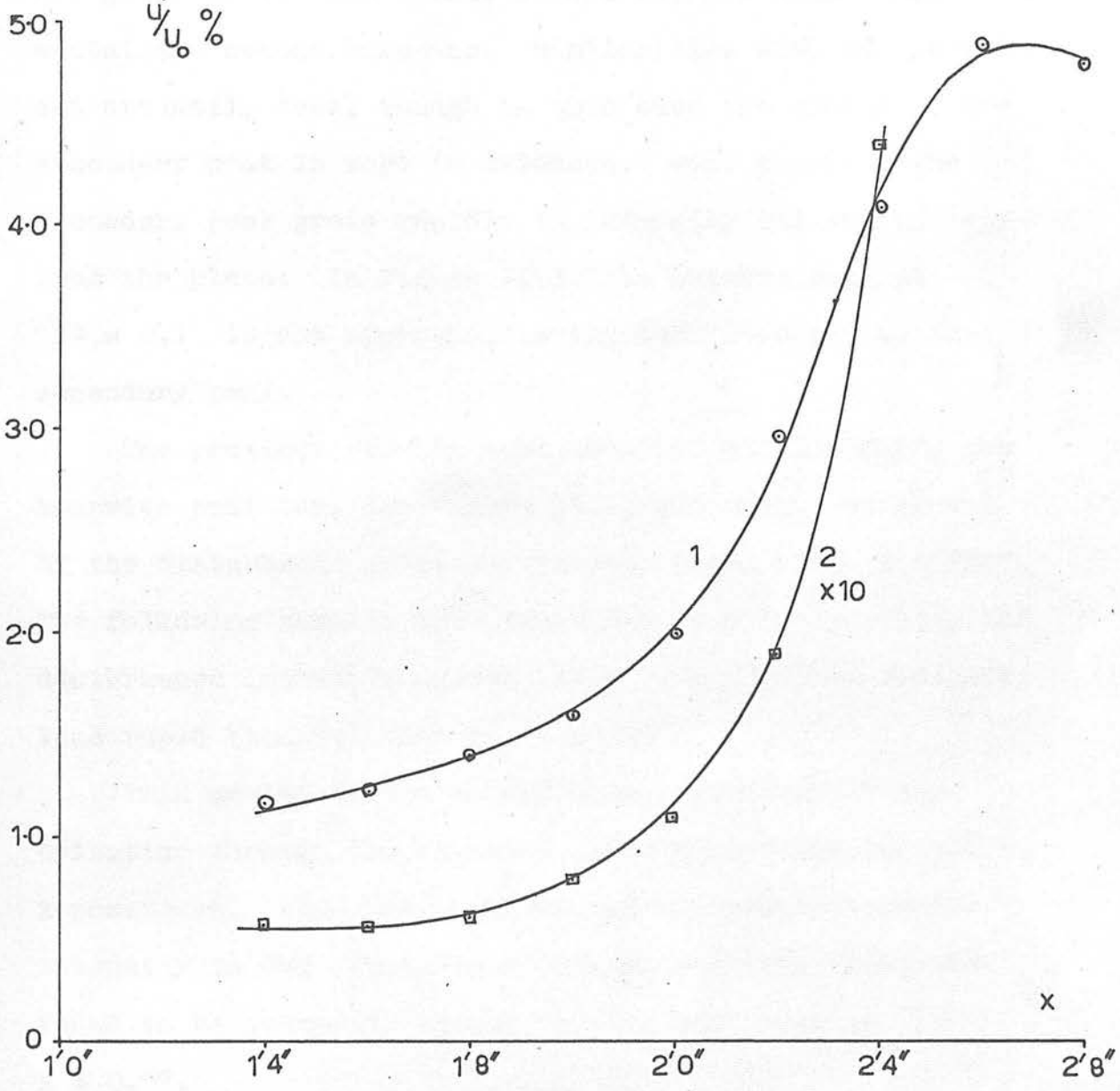

Figure II. 9 Downstream Growth of the Fundamental and Second Harmonic Intensities, a = 0.5" and f = 70 c/s.

Distributions of intensities, through the boundary layer, are given in Figures II.10, 11 and 12, for both fundamental and second harmonic. Similarities with the previous set are easily seen, though in this case the growth of the secondary peak is more in evidence. Once present, the secondary peak grows rapidly in intensity and shifts away from the plate. In Figure II.12 the primary peak at $y/\delta = 0.1$ is not apparent, having been absorbed by the secondary peak.

The previous results were obtained at $z = 0.5"$, the spanwise position, see Figure II.1, for which the growth of the disturbance intensity is very rapid after $x = 2'0"$. The following results were found for $z = 1.0"$, where the disturbance intensity growth after $x = 2'0"$ was decidedly less rapid than for that at $z = 0.5"$.

Twin maxima in the second harmonic intensity distribution through the boundary layer were found for all x-positions. Also the magnitude of the second harmonic intensity in the outer region of the boundary layer was found to be generally larger at $z = 1.0"$ than at $z = 0.5"$.

The growth of the secondary peak in the second harmonic intensity distribution can be seen most clearly in Figures II.13 - 18. The magnitude of this peak appears to remain approximately constant until an x-position of $1'10"$ is reached. It then grows rapidly, and moves away from the plate.

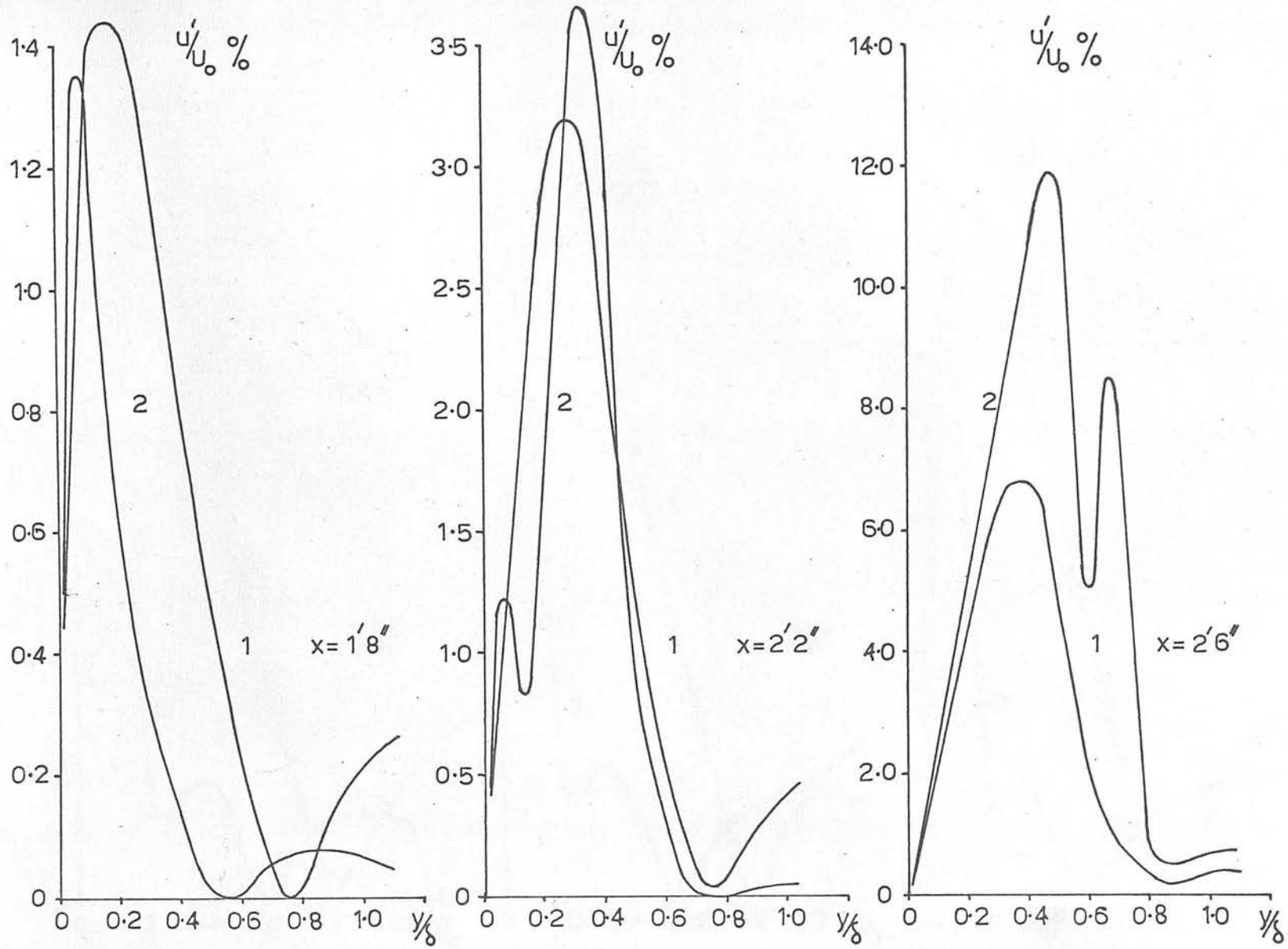

Figures II 10-12 Distribution of Fundamental and Second Harmonic Intensities through the Boundary Layer, s = 0.5" and f = 70 c/s.

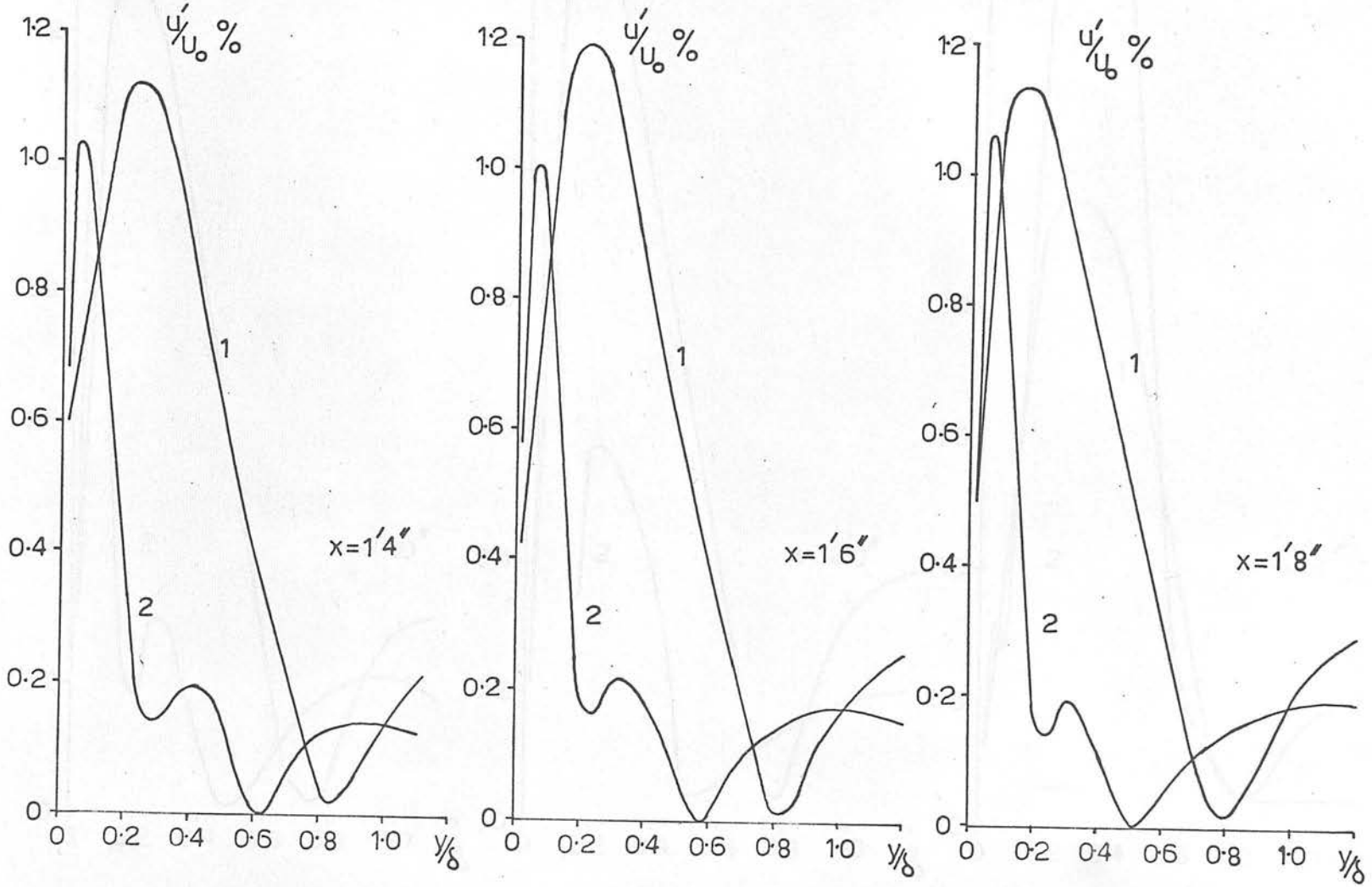

Figures II 13-15 Distribution of Fundamental and Second Harmonic Intensities through the Boundary Layer, s = 1.0" and f = 70 c/s.

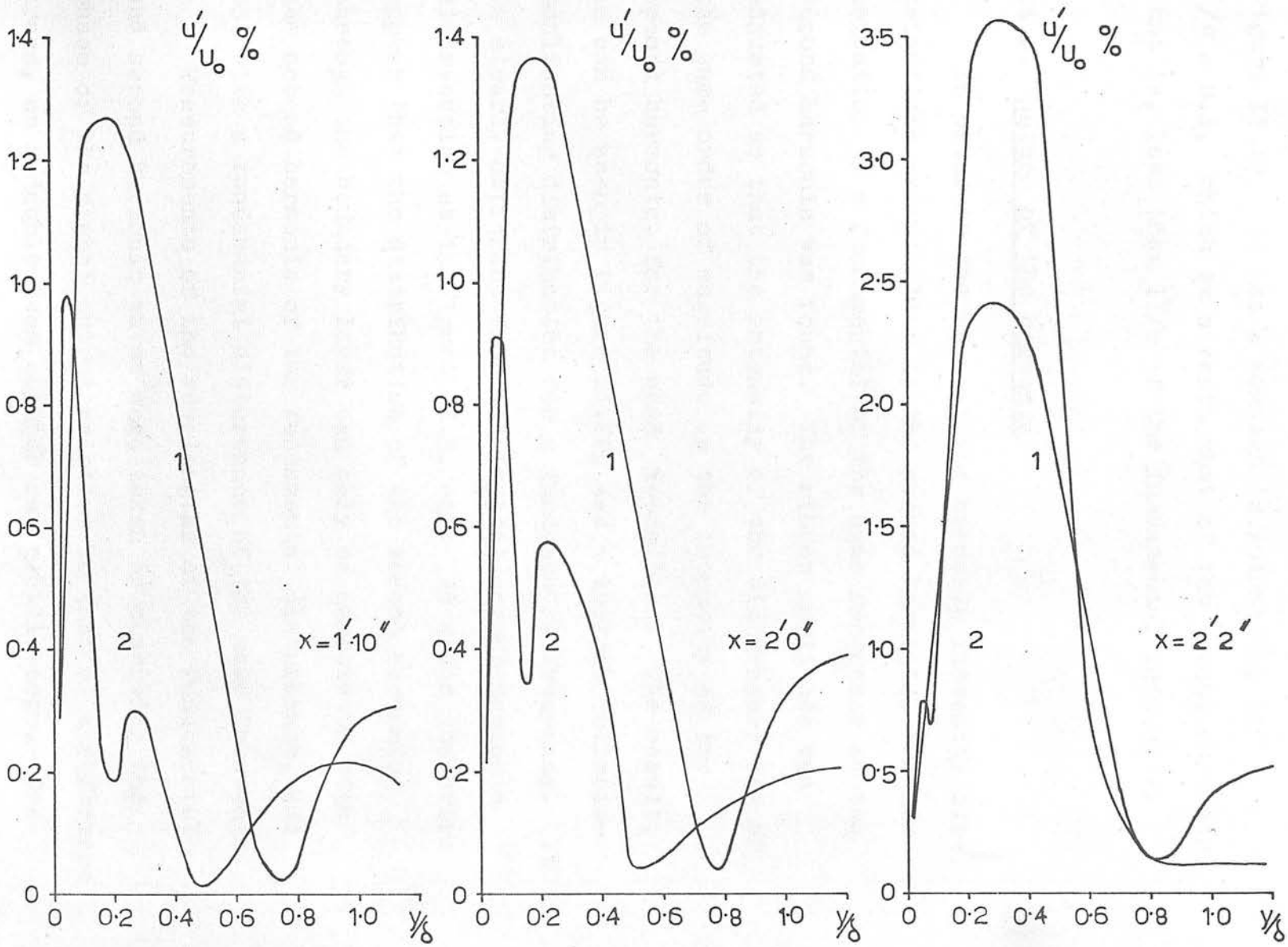

Figure II 16-18 Distribution of Fundamental and Second Harmonic Intensities through the Boundary Layer, x = 1.0" and f 70 c/s.

A distribution, through the boundary layer, of the third harmonic at $x = 1'6"$ and $z = 0.5"$ is shown in Figure II.19. It has a maximum in intensity, at $y/\delta = 0.1$, which is a tenth that of the second harmonic; that is, less than $1^{o}/o$ of the fundamental intensity.

II.6. Nature of the harmonic

In order to ensure that the harmonic intensity distributions are peculiar to the second harmonic, the distribution of a fundamental of the same frequency as the second harmonic was found. The ribbon amplitude was adjusted so that the intensity of the disturbance was of the same order of magnitude as the intensity of the second harmonic, for the same x-position. The result, as can be seen in Figure II.20, was a typical Tollmein-Schlichting distribution for a fundamental frequency. It is clearly different from the typical second harmonic distribution as in Figure II.5, say. It would therefore appear that the distribution of the second harmonic through the boundary layer can only be associated with the second harmonic of the fundamental disturbance, and not with a fundamental disturbance of the same frequency.

Measurements of the wavelengths of the fundamental and second harmonic waves were taken by observing the phase of the signal output relative to that of a reference trace, on a double beam cathode ray oscilloscope. The

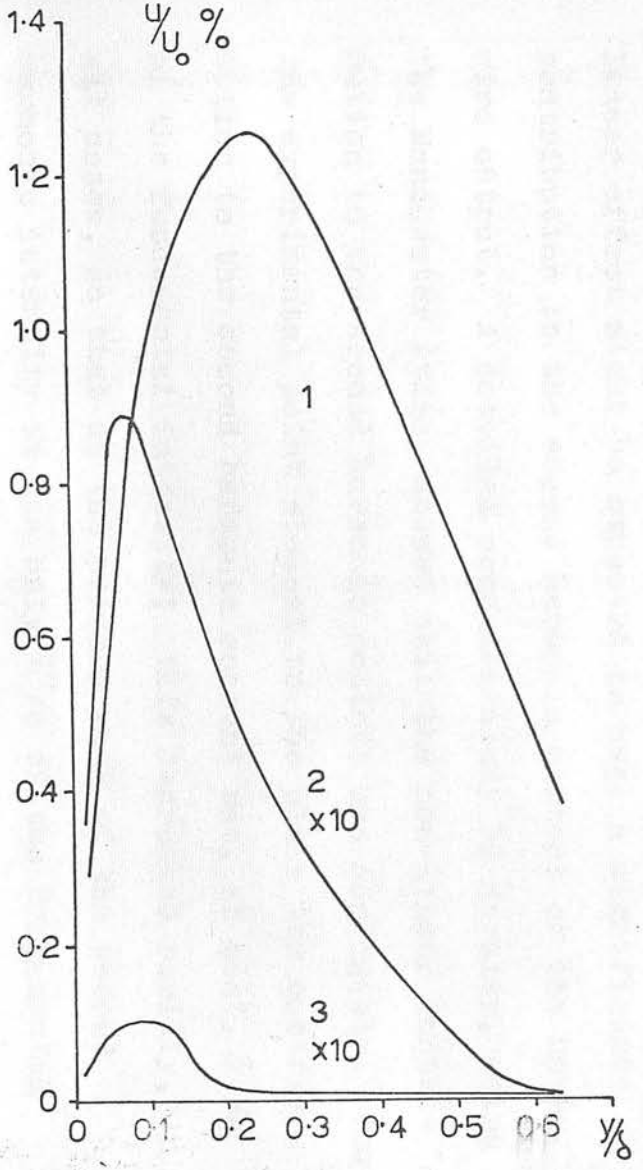

Figure II.19 Distribution of Fundamental, Second and Third Harmonic Intensities through the Boundary Layer, δ = 0.5", f = 70 c/s and x = 1'6".

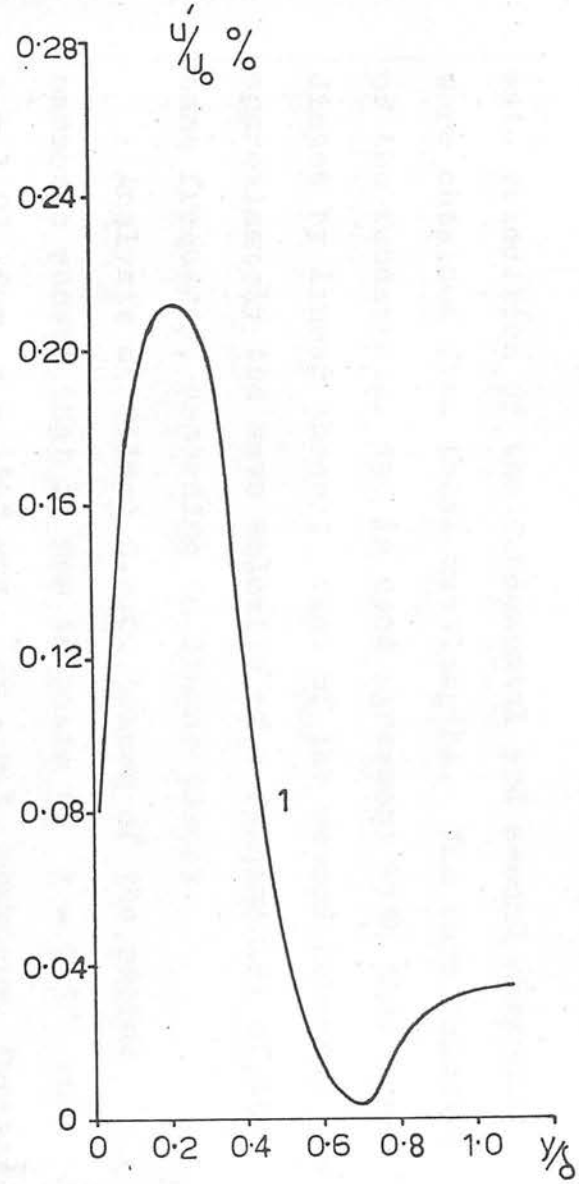

Figure II.20 Distribution of Fundamental Intensity through the Boundary Layer for a Frequency of 110 c/s, δ = 0.5" and x = 1'8".

wave velocities of the fundamental and second harmonic were obtained from these wavelengths. The wave velocity of the fundamental was in good agreement with that predicted by linear theory; that of the second harmonic was approximately the wave velocity of a fundamental of the same frequency, according to linear theory.

Analysis of filmed C.R.O. traces of the second harmonic showed that it was in phase at $z = 0.5"$ and $z = 1.0"$ for $x = 1'6"$ and $y/\delta = 0.1$. However, further downstream, in the region of the rapidly developing peak at $y/\delta = 0.3$, a phase difference of 120° was found between the second harmonic at the two spanwise positions.

Klebanoff et al. have stated that the effect of the non-linearity of the hot-wire is such that it would tend to contribute to the harmonic content. The primary peak of the second harmonic distribution occurs at a position where the mean velocity is low; a position where the non-linear effect might be expected to make a significant contribution to the second harmonic content of the hot-wire output. A detailed computer study by Kersley, using the Manchester Atlas, showed that the non-linear contribution to the second harmonic content was negligible. For the experimental point closest to the plate the contribution to the second harmonic content was, at most, $2^{o}/o$ of the fundamental intensity; this decreased rapidly, in all cases, so that at the primary peak of the second harmonic intensity it was only $\frac{1}{2}^{o}/o$ of the fundamental intensity.

As has already been discussed in the introduction Stuart has suggested that Lin's work (1958), on the generation of harmonic in the critical layer, only applies to large initial disturbances. For small initial disturbances we have seen that the intensity of the second harmonic is no greater than 10°/o that of the fundamental, in the region of the critical layer and before distortion of the mean flow. The ribbon amplitude was therefore doubled, and a boundary layer traverse made at a position just upstream of distortion of the mean flow. It was found that the percentage of second harmonic intensity, compared with fundamental intensity, increased by only a factor of two on our previous cases, see Figure II.21. The intensity of the second harmonic in the boundary layer, therefore, does appear to be a function of the amplitude of the initial disturbance, though in no case could it be made large enough to satisfy Lin's predictions.

II.7. Harmonic content of the ribbon vibration

The input signal to the ribbon was found to contain approximately 2°/o of second harmonic. The extent to which this is introduced into the boundary layer is open to conjecture. Nevertheless it is reasonable to assume that some second harmonic is injected into the boundary layer by the ribbon. However it is unlikely that this can explain all the second harmonic present which is, in

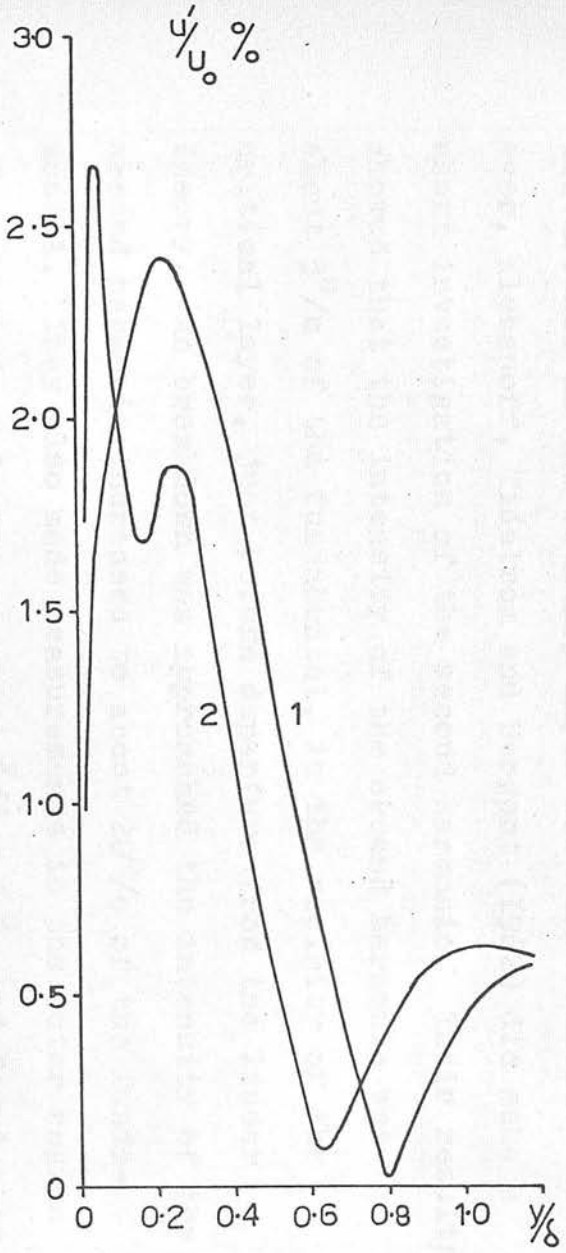

Figure II 21 Distribution of Fundamental and Second Harmonic Intensities through the Boundary Layer for Increased Ribbon Amplitude.

general, 10°/o of the first harmonic. If it did, it is difficult to see why the distribution of the second harmonic should differ from that of the fundamental. That some second harmonic is injected into the boundary layer by the ribbon in no way detracts from the importance of the results obtained for the intensity distributions of the second harmonic through the boundary layer.

II.8. Discussion on the second harmonic distribution through the boundary layer.

In the Introduction to this chapter it was pointed out that knowledge of the second harmonic content of a disturbance in the boundary layer was very limited. However, Klebanoff, Tidstrom and Sargent (1962) did make a short investigation of the second harmonic. Their results showed that the intensity of the second harmonic was about 5°/o of the fundamental, in the vicinity of the critical layer, just before departure from the linear theory. As breakdown was approached the intensity of the second harmonic increased to about 20°/o of the fundamental. They also made measurements in the outer region of the boundary layer, at about $y/\delta = 0.6$, and found that the harmonic content was of the same order as the harmonic content in the vicinity of the critical layer, and that at breakdown it was even larger. These results are in broad agreement with those reported here. However, it does seem fortuitous that the two chosen positions in

the boundary layer should have given harmonic contents which were of the same order. Klebanoff, Tidstrom and Sargent concluded that there was no real evidence of any strong harmonic content occurring before distortion of the mean flow.

Stuart (1960c) has made an order of magnitude analysis for the production of harmonics and found that for a fundamental of small order A, the amplitude of the second harmonic would be A^2, and in general the amplitude of the n^{th} harmonic would be of order A^n. The present results show that when the fundamental intensity is approximately 10°/o of the local mean velocity, at the y/δ position corresponding to the second harmonic peak close to the plate, the second harmonic intensity is 10°/o, and the third harmonic intensity 1°/o of the fundamental intensity, Fig. II.19. Good agreement is found therefore with Stuart's analysis.

The main features of the second harmonic distribution through the boundary layer are the peak at $y/\delta = 0.1$ and the phase reversal at $y/\delta = 0.6$. The presence of the secondary peak at $y/\delta = 0.3$ appears to be dependent on both the spanwise position and the proximity of the wave to breakdown. The main features are markedly similar to those of the distribution of the fundamental. It was thought therefore, that the peak in the second harmonic distribution might coincide with a singularity similar to the singularity which occurs at the peak in the fundamental distribution. That is, that the wave velocity

of the second harmonic might be equal to the local mean velocity at $y/\delta = 0.1$. It would therefore be less than the wave velocity of the fundamental. Measurements of the second harmonic wave velocity showed, however, that it was greater than that of the fundamental. That the peak in the second harmonic distribution does not coincide with the "critical layer" of the second harmonic indicates, perhaps, that the second harmonic is linked with the fundamental rather than being independent of it. This would seem reasonable as the second harmonic is produced when the intensity of the fundamental is no longer small according to linear theory.

A discussion of the second harmonic distribution is now given in which it is proposed that the distribution is made up of two components. It is suggested that the basic component is similar to the distribution shown in Figure II.10. The distribution has a peak at $y/\delta = 0.1$ and a phase reversal at $y/\delta = 0.6$. The secondary component of the distribution is such that it produces the peak at $y/\delta = 0.3$. The two components superimposed result in the typical distribution shown in Figure II.17.

The production of second harmonic is associated with a fundamental wave of finite size. Klebanoff, Tidstrom and Sargent have shown that the boundary layer then exhibits a periodic variation in thickness and that associated with that variation are longitudinal eddies. It is suggested that the basic component is the result of

a finite sized fundamental wave, whilst the secondary component is produced by the longitudinal eddies. Klebanoff, Tidstrom and Sargent showed that the action of the eddies was to produce more second harmonic at a valley than at a peak. The valley and peak positions correspond approximately to the spanwise positions $z = 1.0"$ and $z = 0.5"$ respectively for the results reported here. The streamlines of the eddies have been plotted by Klebanoff, Tidstrom and Sargent and it appears that the effect of the eddy, in producing second harmonic, is localised at about $y/\delta = 0.3$ for the initial stages of the development of the eddy. Later on in the development of the eddy, however, a much larger part of the boundary layer is affected and a drift outwards of the centre of the interaction between the eddy and the fundamental wave takes place. The development of the second harmonic distribution downstream agrees well with the development expected if the secondary component is produced by an eddy system. For instance, the distributions for the 70 c/s fundamental wave show a secondary peak at $x = 1'8"$ for $z = 1.0"$ but no peak for $z = 0.5"$. The growth and outward drift of the secondary peak is clearly seen for $x > 2'0"$.

Further support for the proposed two-component explanation of the intensity distribution is given by Kersley (1965). He found that at $y/\delta = 0.1$ the second harmonic oscillations were in phase at both z-positions

for all x-stations where measurements were taken. He found, however, that a phase difference of approximately 120° was present between the second harmonic waves at the two z-positions for $y/\delta = 0.3$ at an x-position where the peak in the second harmonic intensity, at this position, was growing rapidly. This observation is consistent with the view that the second harmonic peak in the region of $y/\delta = 0.3$ results from an eddy system.

CHAPTER III

THE WIND TUNNEL

III.1a. The Wind Tunnel

The tunnel was designed for experiments which required a low turbulence, low speed wind tunnel. It was decided that Reynold's Numbers up to 8.10^6 should be attained with a maximum wind speed of 140 feet/sec. The maximum power available was 30 h.p., which allowed a working section of 4 foot octagonal cross-section. An axisymmetric working section was chosen as this allowed the widest range of experiments to be performed. A closed circuit tunnel was chosen for two reasons. Firstly, the size of the building made a low turbulence open circuit tunnel an impossibility. Secondly, the tunnel was to be used for hot-wire anemometer measurements and a closed circuit tunnel was likely to contain cleaner air than an open circuit tunnel. Figure III.1 is an airline diagram of the tunnel.

III.1b. The Working Section

The working section was 10 feet long with a basic 4 foot square cross-section. Set diagonally into the corners of the working section, and along its length, were perspex fillets making the actual cross-section octagonal. The perspex fillets could be flexed through

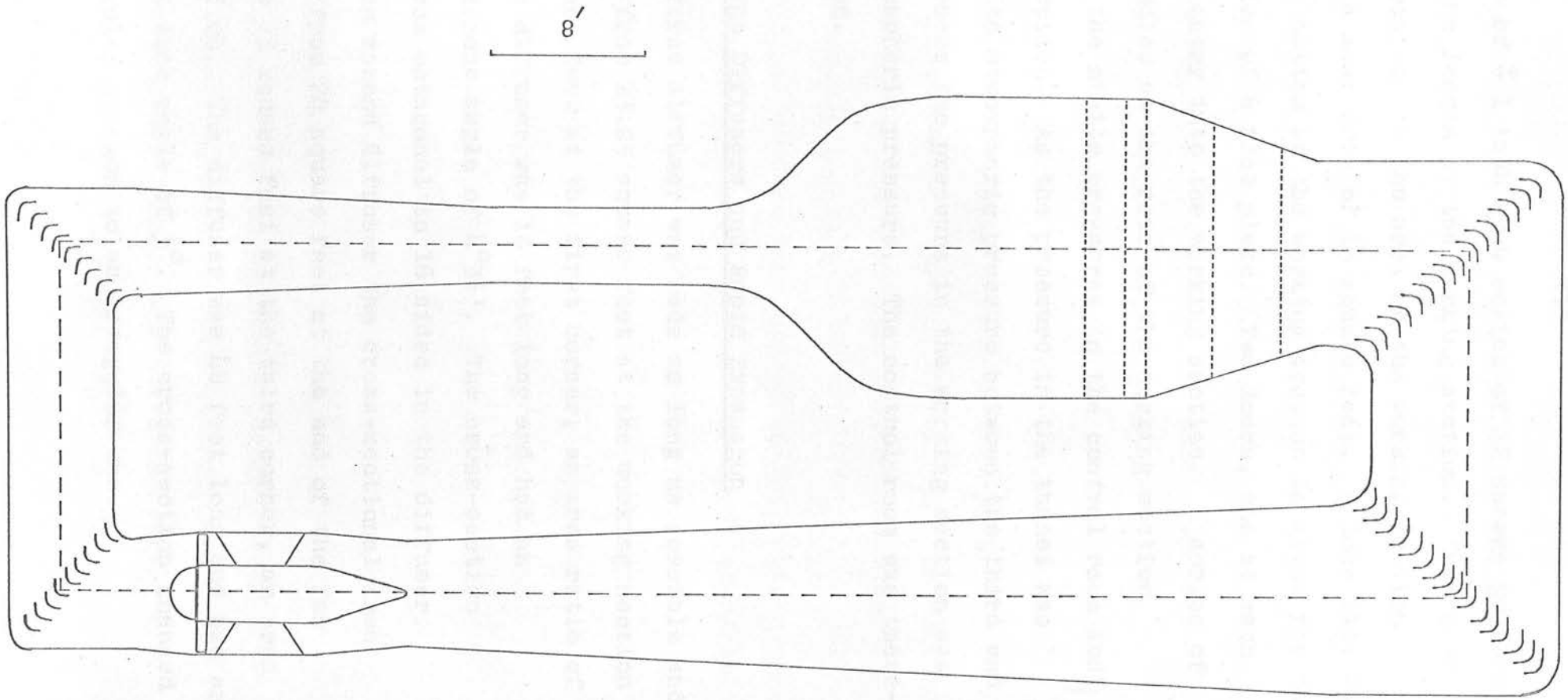

Figure III.1. Airline Diagram of the Wind Tunnel.

a distance of $\pm$ 1 inch by 4 series of 12 screws positioned along the length of the working section. This gave a $\pm$ 2% variation in the area of the working section which had a mean area of 13 square feet. A long slit was cut in the bottom of the working section to allow for the introduction of a flat plate. Two doors, one at each end, gave entry into the working section. A series of breather holes at the rear of the working section equalised the static pressures in the control room and working section. As the pressure in the tunnel was equalised to atmospheric pressure between the third and fourth corners the pressure in the working section was below atmospheric pressure. The control room was therefore sealed.

III.1c. The Diffusers and Rapid Expansion

The first diffuser was made as long as possible and increased from 13.25 square feet at the working section to 24 square feet at the first corner, an area ratio of 1.81. The diffuser was 18 feet long and had an equivalent cone angle of $4^{\circ}36'$. The cross-section changed from octagonal to 16 sided in the diffuser.

In the second diffuser the cross-sectional area increased from 24 square feet at the end of the fan section to 73 square feet at the third corner, an area ratio of 3.04. The diffuser was 48 feet long and had an equivalent cone angle of 5°. The cross-section changed from a regular octagon to an irregular one.

The cross-sectional area of the tunnel remained constant between the first and second and the third and fourth corners.

The area expansion ratio in the rapid expansion was 2.73 : 1 in a length of 9 feet. Three fixed screens were placed in this section, equally spaced 3 feet apart, the last one being at the end of the expansion. The screens were held in the vertical plane.

III.1d. The Screens

The smoothing screens were made from 38 mesh, 36 s.w.g. phosphor-bronze wire. The blockage coefficient was 0.506. The screens were made from 4 foot wide panels butt welded together.

Three fixed screens were placed in the rapid expansion section and provision was made for three moveable screens in the settling section, equally spaced a foot apart. Only two moveable screens have been used, and these were placed in the first and last positions, the first position being 1 foot downstream of the last fixed screen. The screens were cleaned at regular intervals.

III.1e. The Corners

All four corners had hardboard turning vanes of circular-arc section with straight extensions at the leading and trailing edges. The subtended angle of the circular arc was 86° and the trailing edge was set

parallel to the centre line of the tunnel. Provision was made for minor adjustment of the setting of the vanes. Both the leading and trailing edges were shaped. The gap-chord ratio in all the sets was 1/4.

III.1f. The Fan Section

The diameter of the four bladed fan was 6.28 feet whilst the nacelle diameter was 3 feet. The tubular steel frame-work on which the motor and fan were mounted was independent of the tunnel and the motor and fan themselves had an anti-vibration mounting on to the framework. The fan spinner was an aluminium hemisphere, 3 feet in diameter, and the motor was housed in a streamlined cowling.

The area of the fan duct was constant throughout its length. The section changed from 16 sided at the second corner to circular at the fan via 32 sides. From the fan the section went to 14 sides to 8 sides at the beginning of the second diffuser.

Seven straightener vanes were installed behind the fan. They were attached to the tunnel walls and terminated just off the cowling. The angle of attack of the vanes could be adjusted. Three of the vanes covered the frame support of the motor and fan.

III.1g. The Contraction

The contraction area ratio was 15 : 1 and the shape of the contraction was designed, with a slight modification, using a method due to Bloomer (1947).

III.1h Access to the Tunnel

Trapdoors provided access to all parts of the tunnel.

III.2a. The Tunnel Drive and Control

A block diagram of the tunnel drive and control is shown in Figure III.2. The drive motor and pump were developed by Burns and the engineers of F.W. Baggett and Co. Ltd., the hydraulic drive system being based on an N.E.L. design. The drive provided a complete hydraulic analogue to the Ward-Leonard system. The 35 h.p. squirrel cage induction motor drove the pump at constant speed and the fan was designed to absorb 30 h.p. at 750 revs./min., giving a maximum wind speed of 140 feet/sec.

Coarse power control, and therefore fan speed control, was given by varying the swash plate angle in the pump. Fine control was achieved by an electrically controlled variable aperture valve, a Moog valve, parallel to the hydrostatic motor. The flow through the valve was proportional to the pressure in the hydraulic system so that it gave an approximately constant percentage control

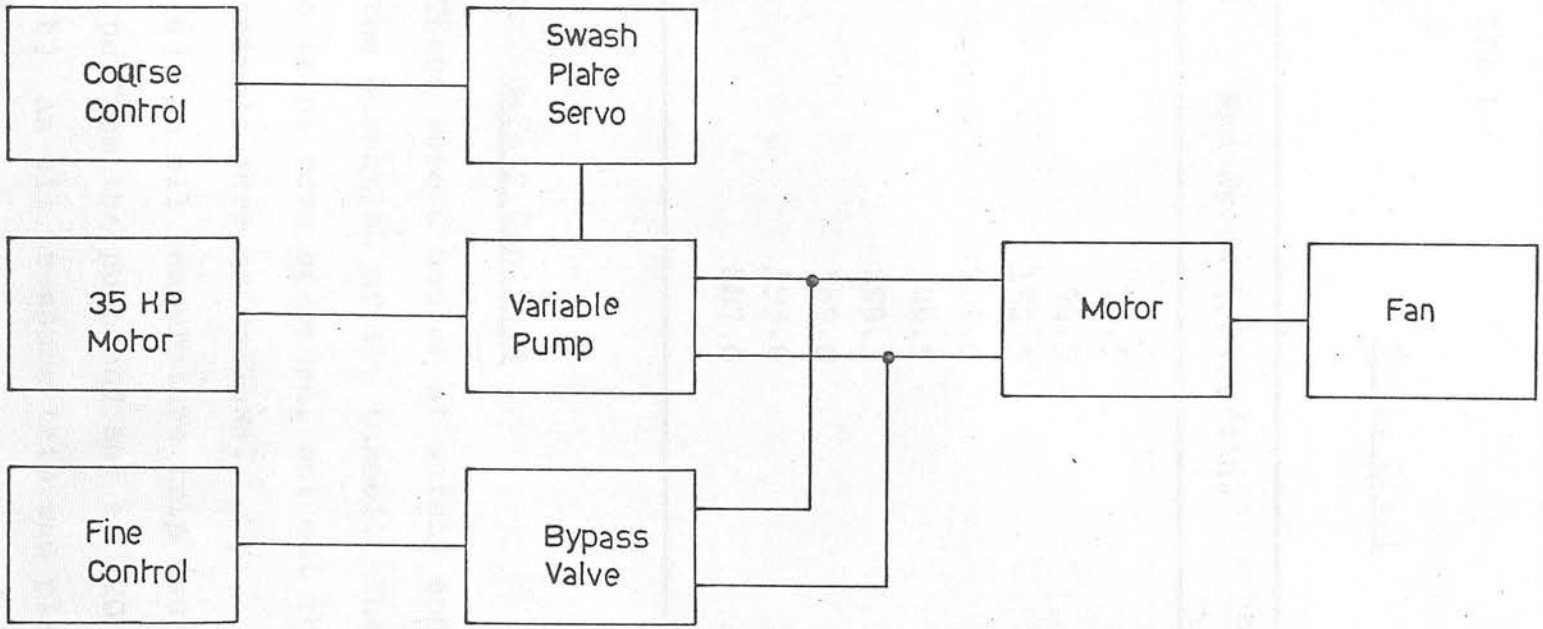

Figure III.2 The Tunnel Drive and Control.

III.1g. The Contraction

The contraction area ratio was 15 : 1 and the shape of the contraction was designed, with a slight modification, using a method due to Bloomer (1947).

III.1h Access to the Tunnel

Trapdoors provided access to all parts of the tunnel.

III.2a. The Tunnel Drive and Control

A block diagram of the tunnel drive and control is shown in Figure III.2. The drive motor and pump were developed by Burns and the engineers of F.W. Baggett and Co. Ltd., the hydraulic drive system being based on an N.E.L. design. The drive provided a complete hydraulic analogue to the Ward-Leonard system. The 35 h.p. squirrel cage induction motor drove the pump at constant speed and the fan was designed to absorb 30 h.p. at 750 revs./min., giving a maximum wind speed of 140 feet/sec.

Coarse power control, and therefore fan speed control, was given by varying the swash plate angle in the pump. Fine control was achieved by an electrically controlled variable aperture valve, a Moog valve, parallel to the hydrostatic motor. The flow through the valve was proportional to the pressure in the hydraulic system so that it gave an approximately constant percentage control

of the fan speed and therefore of the wind speed, see Table III.1.

Table III.1

Fan Speed (revs./min.)	% Control
70.5	± 10.60
96.5	± 6.95
152.5	± 5.59
203.0	± 4.90
246.5	± 4.66
299.5	± 4.50
349.0	± 4.30
393.0	± 4.07
447.0	± 3.80

III.2b Safety Controls

There were a number of safety controls associated with the operation of the tunnel. The controls, if one of the trips were operated, cut out the drive motor. The controls were as follows:

(a) An oil temperature trip was placed on the output pipe from the pump and set at 120°F.

(b) An oil pressure trip was placed in the output pipe from the pump and set at 3000 lbs./square inch.

(c) Trip wires were placed on the inside of the walls at the fan position. If the fan blades touched the walls they would first cut the wires.

(d) Provision has been made for a wide grid of fine trip wires at the end of the first diffuser. If an object came loose from the working section it would cut these wires.

Finally, an interlock was placed on the swash plate control to prevent the swash plate going to negative angles.

III.2c. Feedback Control

Although a constant feedback control of the wind speed has yet to be developed it is, perhaps, not irrelevant to discuss the form it will take. A block diagram of the projected control is shown in Figure III.3. A suitable device measuring either wind speed or dynamic pressure sends an error signal to the Moog valve control which adjusts the fan speed and therefore the wind speed. An investigation by Burns, using an analogue computer, indicated that a simple "bang-bang" control was sufficient for the control of the wind speed in this tunnel. A suitable signal would indicate when the wind speed lay outside the operational range of the valve and the swash plate angle would then be manually adjusted to bring it inside that range. A warning system will be used to indicate that the control is in operation and a logic interlock fitted to the recording equipment to prevent measurements being taken until the required wind speed is attained.

Three types of wind speed indicators have been

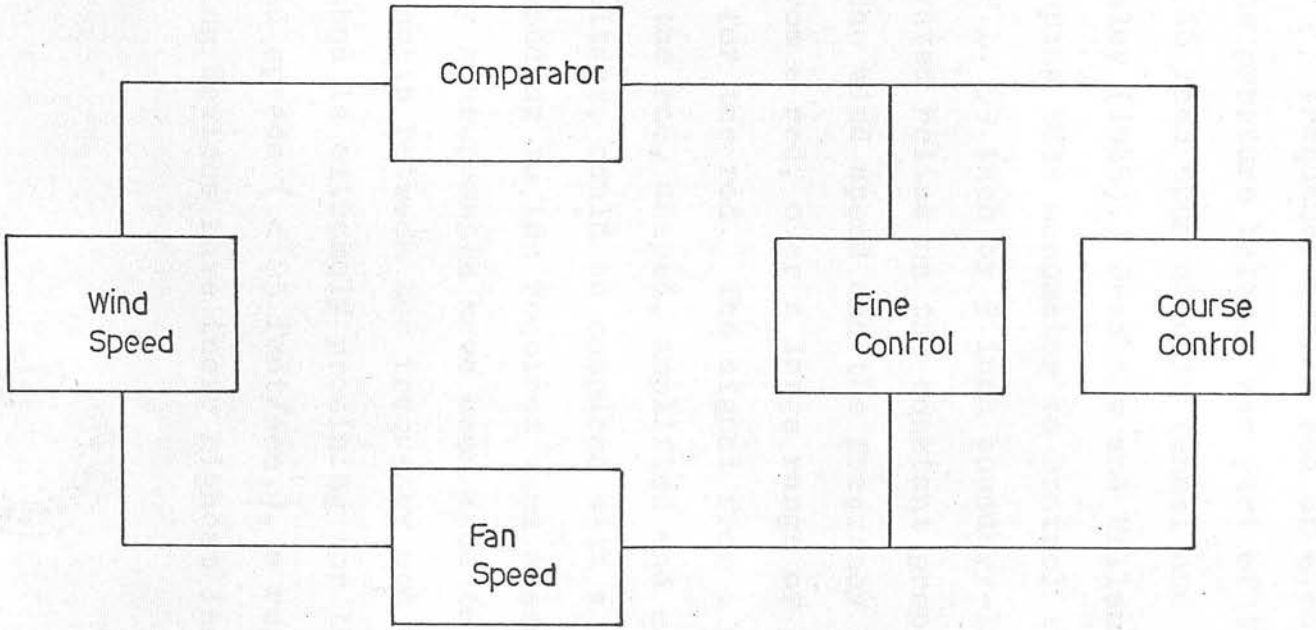

Figure III.3 The Feedback Control.

considered so far. As yet, no decision has been made as to which one will be incorporated into the feedback control. The three instruments are:

(a) Pressure balance

(b) Sloping tube manometer

(c) Hot wire measurement of the eddy shedding frequency from a rod of circular cross-section.

The pressure balance was part of the control system of the 18 inch open circuit tunnel and has been described by Kersley (1965). Bradshaw and Hellens (1964) have used the sloping tube manometer to control the wind speed in the N.P.L. 59 inch by 9 inch boundary-layer tunnel. The last system relies on the constant proportionality between the wind speed and the frequency of the eddies shed from a rod, over a large range of Reynold's Number for the rod. The signal from a hot-wire placed behind the rod, shaped, amplified and converted to a d.c. voltage, could be compared with a d.c. voltage corresponding to the required wind speed. Some preliminary measurements have been made to test the relationship between the frequency and the windspeed. The method is extremely promising for the control of low wind speeds (< 25 feet/sec.), a region where other measuring devices have their highest inaccuracies.

III.3. The Measurement of Wind Speed

The fan speed was measured by fitting a disc to the fan shaft. Sixty holes were drilled symmetrically in the disc at a constant radius position. A narrow beam light source was placed on one side of the disc and on the other, a photo-electric cell. Each revolution of the fan produced, therefore, sixty pulses from the cell. The pulses were shaped, amplified and either counted by a Venner Frequency Meter or converted to a d.c. voltage by a frequency to voltage converter to give a dial reading. The wind speed varied linearly with the fan speed and could be set to within $\pm$ 1 ft./sec. of the required speed using the dial reading or $\pm$ 0.5 ft./sec. using the frequency meter.

When a set of measurements was being taken steady running conditions were first achieved. The wind speed was found by measuring the dynamic pressure from a pitot tube with a Chattock gauge. The pitot tube was stationed 5 feet from the leading edge of the flat plate, 1 foot and 4 inches from the plate and 9 inches above the centre line. The wind speed was measured at the end of the set and while the measurements were being taken the fan speed was kept constant to $\pm$ 0.2 revs./min. by using the fine control. The temperature of the air was measured by a thermometer in the working section. The atmospheric pressure was also measured so that the density and kinematic viscosity of the air could be found.

The greatest error in the measurement of the wind speed occurred at the lowest attainable wind speed, 10 ft./sec., and was estimated to be $\pm$ 3%. The allowed variation of $\pm$ 0.2 rev./min. at 80 revs./min (= 10 ft./sec.) was well within this limit. The allowed variation did not become comparable with the error in the pressure measurement until a wind speed of 90 ft./sec. was attained.

This discussion has been concerned with hand control of the wind speed only. If an automatic feedback control system were used it might be found that a practical dead space allowed a greater variation than that discussed above. A correction factor could be introduced by recording the fan speed each time a reading was taken. The frequency meter has a binary coded output which, if fed through the encoder of the Digital Voltmeter, could be recorded on paper tape. As the relationship between the wind speed and the fan speed is well known the small deviation could be adequately corrected.

III.4a. Mean Flow Measurements in the Tunnel

An investigation of the mean flow of the tunnel was made. This investigation was designed to find, if present, large scale defects in the flow, such as flow separation. To this end it was sufficient to use a cup anemometer to measure wind speed, and simple flow visualisation was provided by a blob of cotton wool tied

to a length of cotton. Each cotton wool streamer was tested in the working section for satisfactory behaviour Measurements were made downstream of the fan and thereafter following each set of turning vanes. The streamers were attached to the motor cowling and also the trailing edges of both the turning and straightener vanes. The cup anemometer was attached to the end of an extending pole.

The best angle of attack for each of the seven moveable straightener vanes was determined by adjusting the angle of each until the streamers attached to the trailing edge were most nearly steady in a wind.

Mean velocity measurements made 3 feet before the third set of turning vanes showed a concentration of velocity in the top outside region. Measurements then taken of the wind velocity immediately following the second set of vanes, in front of the fan, showed a separation of the flow at the inside corner. An extra turning vane was fitted close to the inside wall, correcting the flow separation and improving the velocity profile downstream of the fan.

Similar velocity measurements taken between the first and second vanes showed a velocity concentration to the inside of the centre line, with a tendency for the velocity to be higher at the top than at the bottom. This was largely corrected by taping over four of the bottom pressure equalisation holes at the rear of the working section. This also corrected a flow

asymmetry found immediately in front of the first vanes.

The velocity profile 3 feet downstream of the last moveable screen was found to be flat to within $\pm$ 3%.

After these minor modifications close attention was paid to the mean flow in the working section.

III.4b. Mean Flow Measurements in the Working Section

Extensive mean velocity measurements were made at two positions in the working section, 2 feet 6 inches and 6 feet 6 inches from the beginning of the working section. Measurements were made with a pitot tube and a sloping tube manometer which was read by a travelling microscope. The pitot tube was attached to a brass slide which moved on a steel bar, ½ inch by 3/8 inch by 4 feet. The steel bar could be held in a variety of horizontal or vertical positions by brackets fixed to the side walls of the working section, or to the roof and floor. At the forward position no detectable variation in the velocity of flow could be found in an area 2 feet square about the centre point of the section at 60 ft./sec. Near the tunnel walls the velocity was 1% greater than the velocity at the centre. The results from the rear position showed no noticeable difference from those at the forward position. The mean flow in the working section was considered satisfactory and the flat plate and traversing mechanism were then installed.

III.5a. The Traversing Mechanism.

The requirements of a traversing mechanism were that it should be able to move a hot-wire along the three axes, x, y and z. The setting of the hot-wire was to be accurate to 0.05 inch in the x-direction, 0.02 inch in the z-direction and 0.001 inch in the y-direction. Two traversing mechanisms were built so that two hot-wires could be moved wholly independently of each other. They were made identical as this simplified their construction and the movements in the x- and z-directions were made as near kinematic slides as was practically possible.

III.5b. The x-movement.

The carriages moved on a bottom rail of circular cross-section and were held at the top against a T-section rail. The aluminium alloy T-section rail was set with its centre line $4\frac{7}{16}$ inches from the top of the flat plate, and screwed directly to the roof of the working section. The rail was $\frac{3}{16}$ inch thick and extended $1\frac{1}{2}$ inches from the roof. The silver steel rod, 1 inch in diameter and 11 feet long, was set vertically below the top rail. The rod was set in the horizontal plane with packing pieces and was supported by 12 equally spaced saddles, each $1\frac{1}{2}$ inches long, which were the split sections of $1\frac{1}{8}$ inch square brass rod with a 1 inch diameter bore down its centre. The rod was fixed to the

floor by bolts passing through the rod, saddles and packing pieces.

The traversing mechanism is shown in Figure III.4. The main carriage, made from 1 inch square section aluminium alloy, was 3 feet 6 inches by $9\frac{5}{8}$ inches, see Figure III.8. The carriage rested on the bottom rail on two supports each of which consisted of two ball races, 4.5 cm diameter, set at right angles to each other, see Figure III.5. At the top the carriage was held against the T-rail by a spring loaded bracket, see Figure III.6.

The carriage was moved in the x-direction by a friction drive system. Bowden cable, 0.025 inches diameter, was attached to the front support of the main carriage and ran above the bottom rail to an inclined pulley at the end of the rail. The cable then returned along side the rail and was fed out to the capstan through a breather hole at the rear of the working section. The cable returned through the breather hole and passed to the rear end of the rail and thence to the rear support of the carriage, see Figure III.7. The 1 inch diameter capstan was driven by a 24 volt d.c. motor through a 100 : 1 reduction ratio right-angled gear box and a 5 : 1 reduction ratio set of gear wheels. The cable was tensioned by mounting the drive system on a wooden board which was hinged to the floor of the control room. A heavy weight was then placed on the board. The motor speed was 5,400 rpm so that the carriage moved 0.57 inches/sec. It is planned to provide a two speed drive,

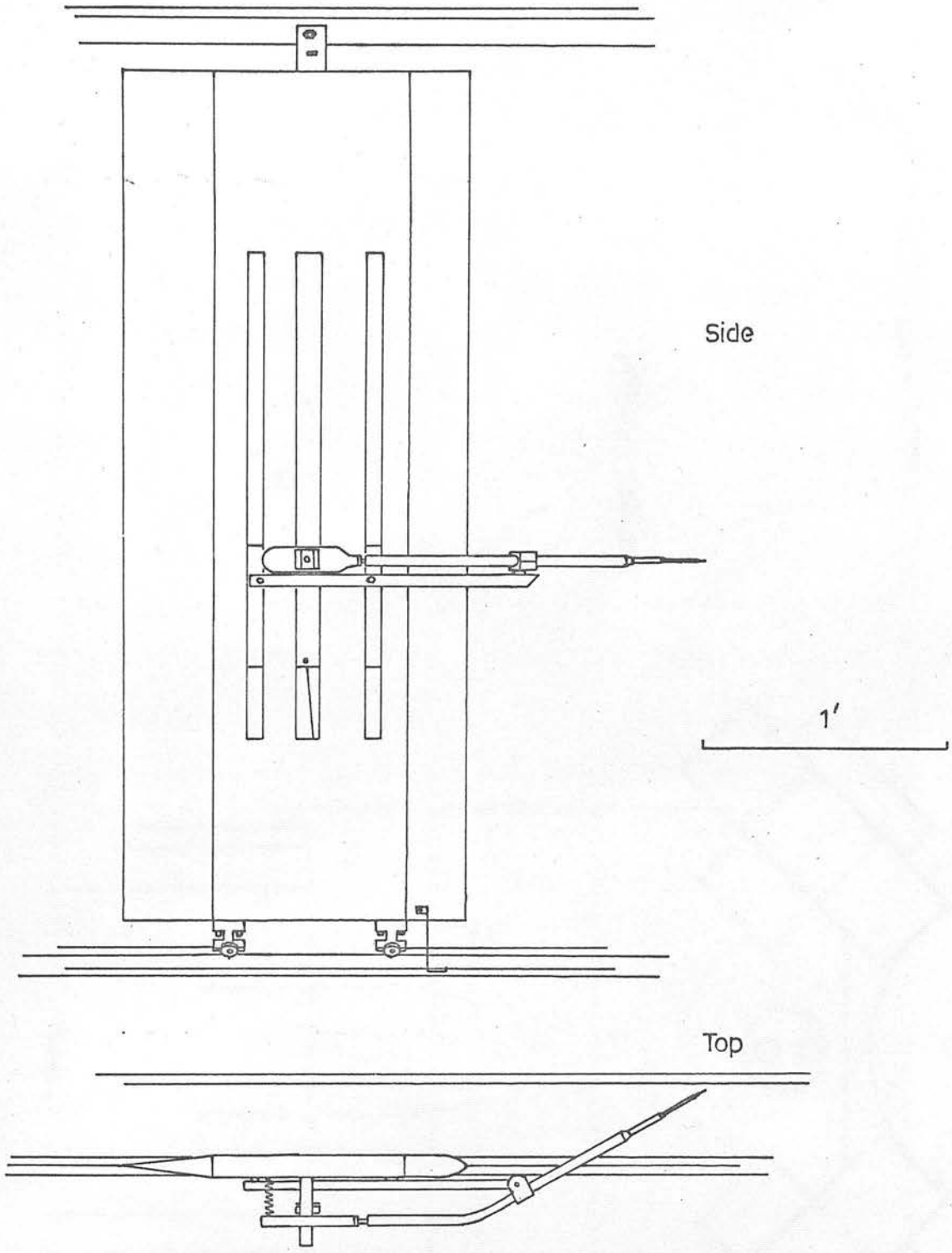

Figure III.4 The Traversing Mechanism

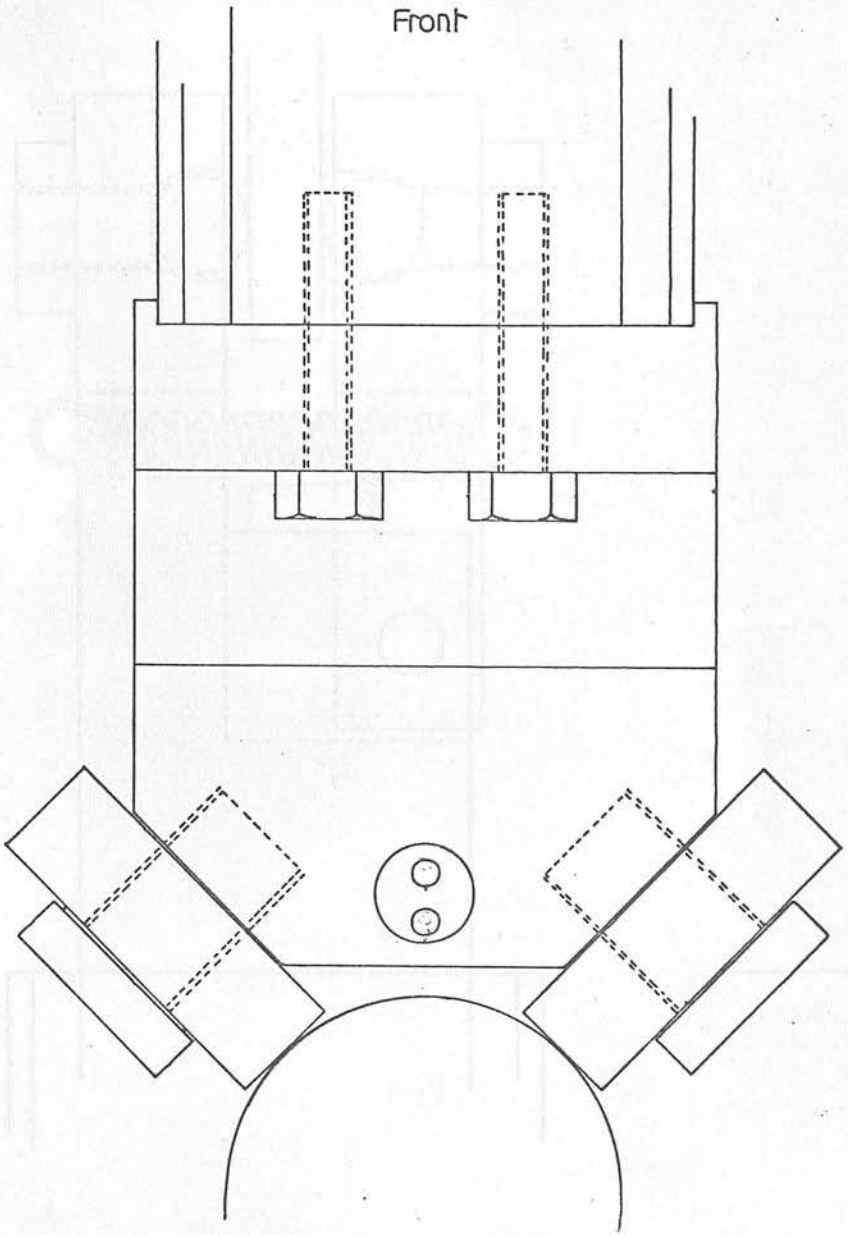

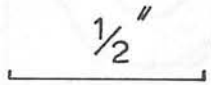

Bottom Support

Figure III.5 Bottom Support

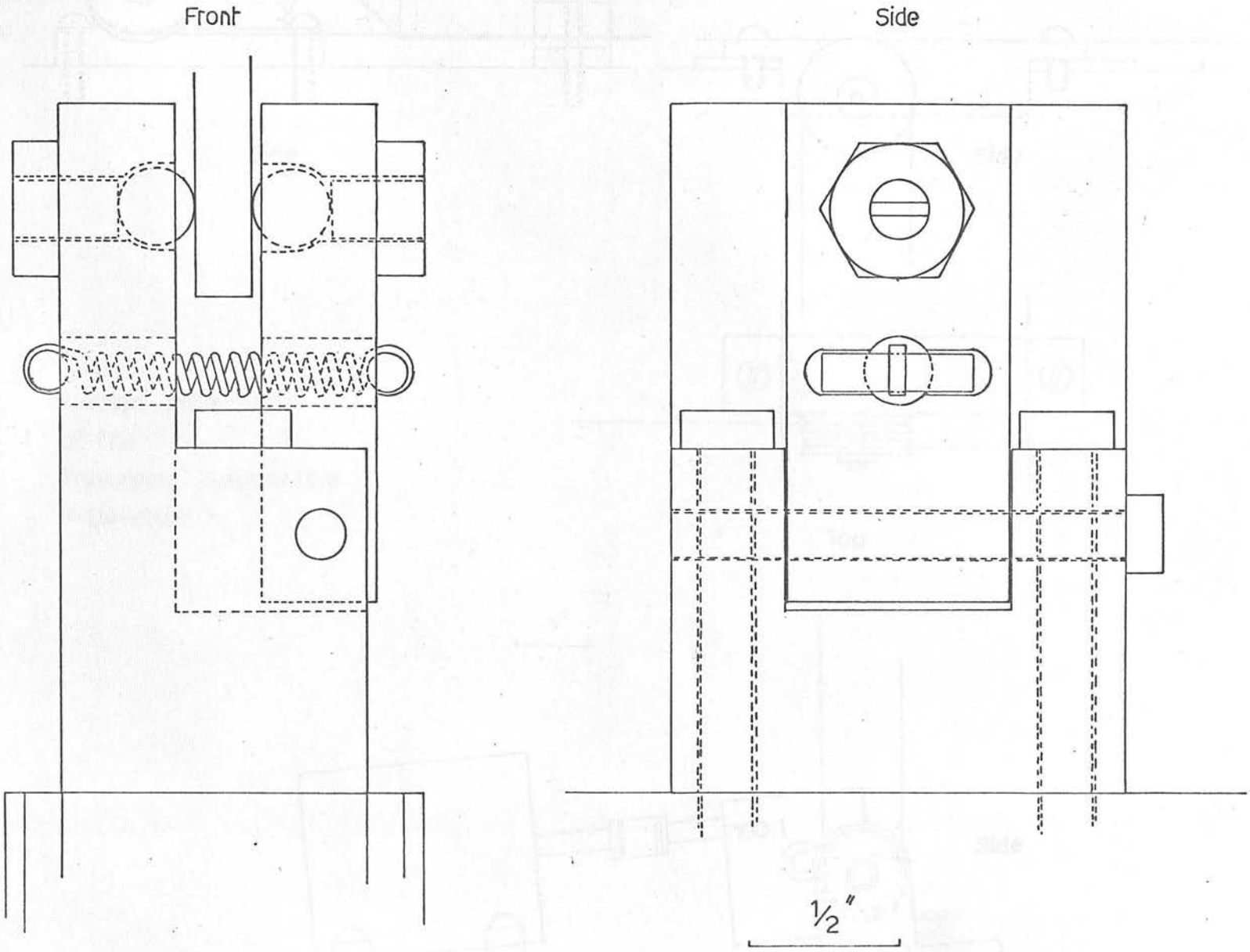

Figure III.6 Top Bracket

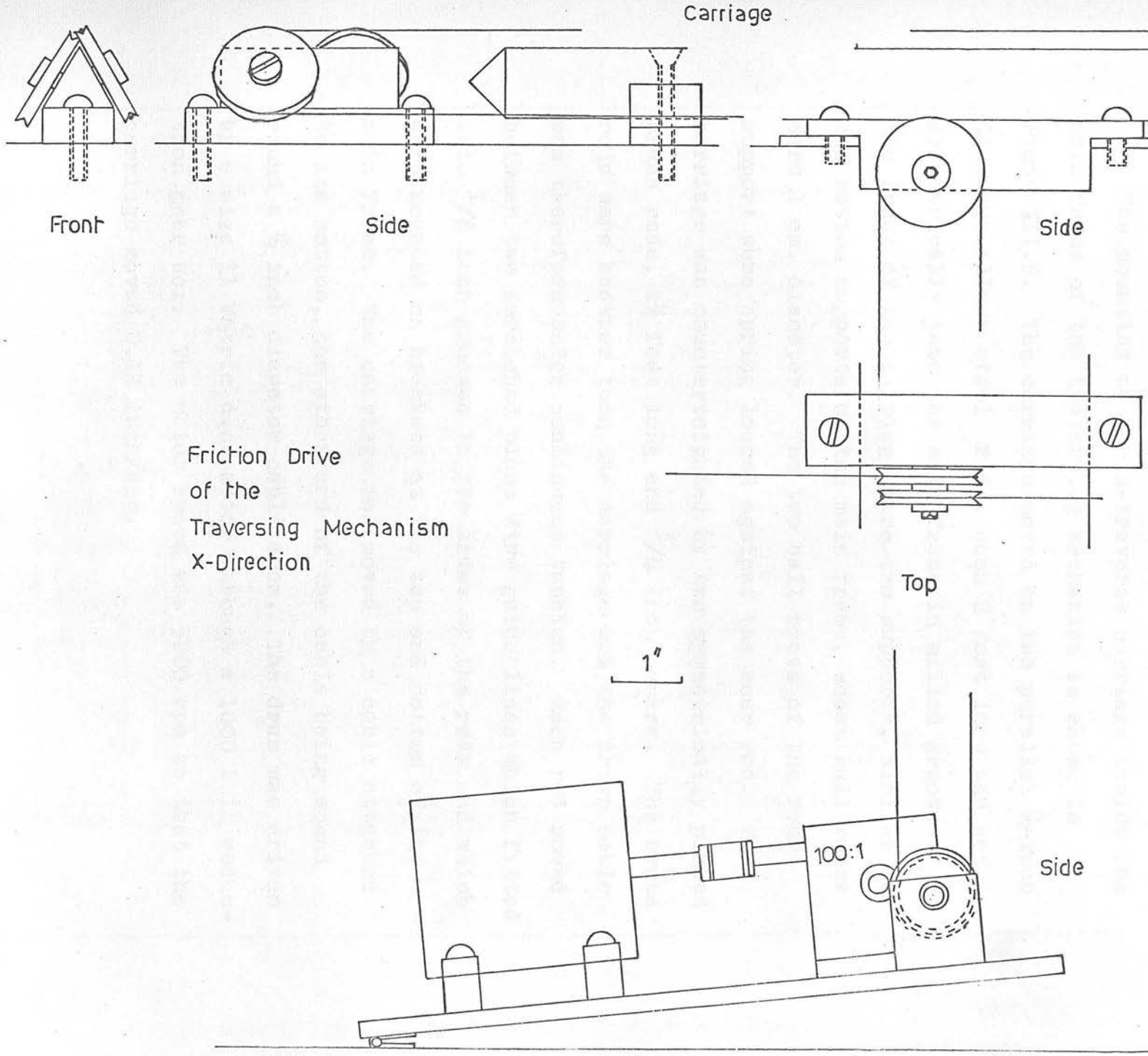

Figure III.7 The x-Drive.

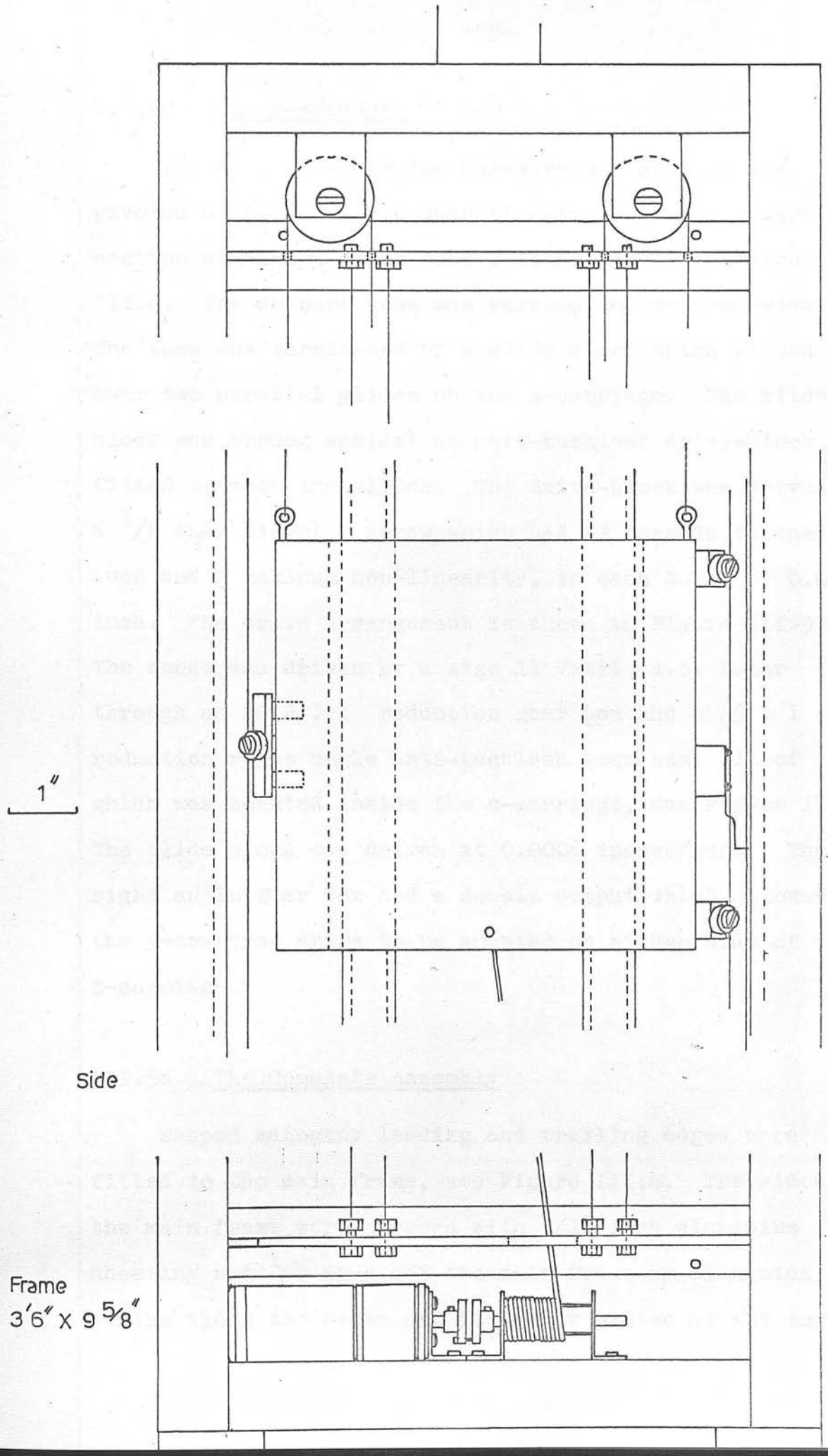

Figure III.8 Main Frame and Z-Traverse Carriage

III.5d The y-movement

The boom on which the hot-wire was mounted was pivoted at the end of a support beam, a ½ inch square section aluminium rod 1 foot 2 inches long, see Figure III.4. The support beam was screwed to the z-carriage. The boom was terminated by a slide block which fitted over two parallel slides on the z-carriage. The slide block was sprung against an anti-backlash drive-block fitted between the slides. The drive-block was driven by a 1/4 inch diameter screw which had 52 threads to the inch and a maximum non-linearity, in each turn, of 0.001 inch. The drive arrangement is shown in Figure III.9. The screw was driven by a size 11 Vatric d.c. motor through an 80.2 : 1 reduction gear box and a 25 : 1 reduction right angle anti-backlash gear box, all of which was mounted inside the z-carriage, see Figure III.10. The slide block was driven at 0.0008 inches/sec. The right angle gear box had a double output which allowed the y-traverse drive to be mounted on either side of the z-carriage.

III.5e The Complete Assembly

Shaped mahogany leading and trailing edges were fitted to the main frame, see Figure III.4. The sides of the main frame were covered with 1/16 inch aluminium sheeting set 1/8 inch off the main frame by aluminium strips along the sides and stiffener plates at the top and

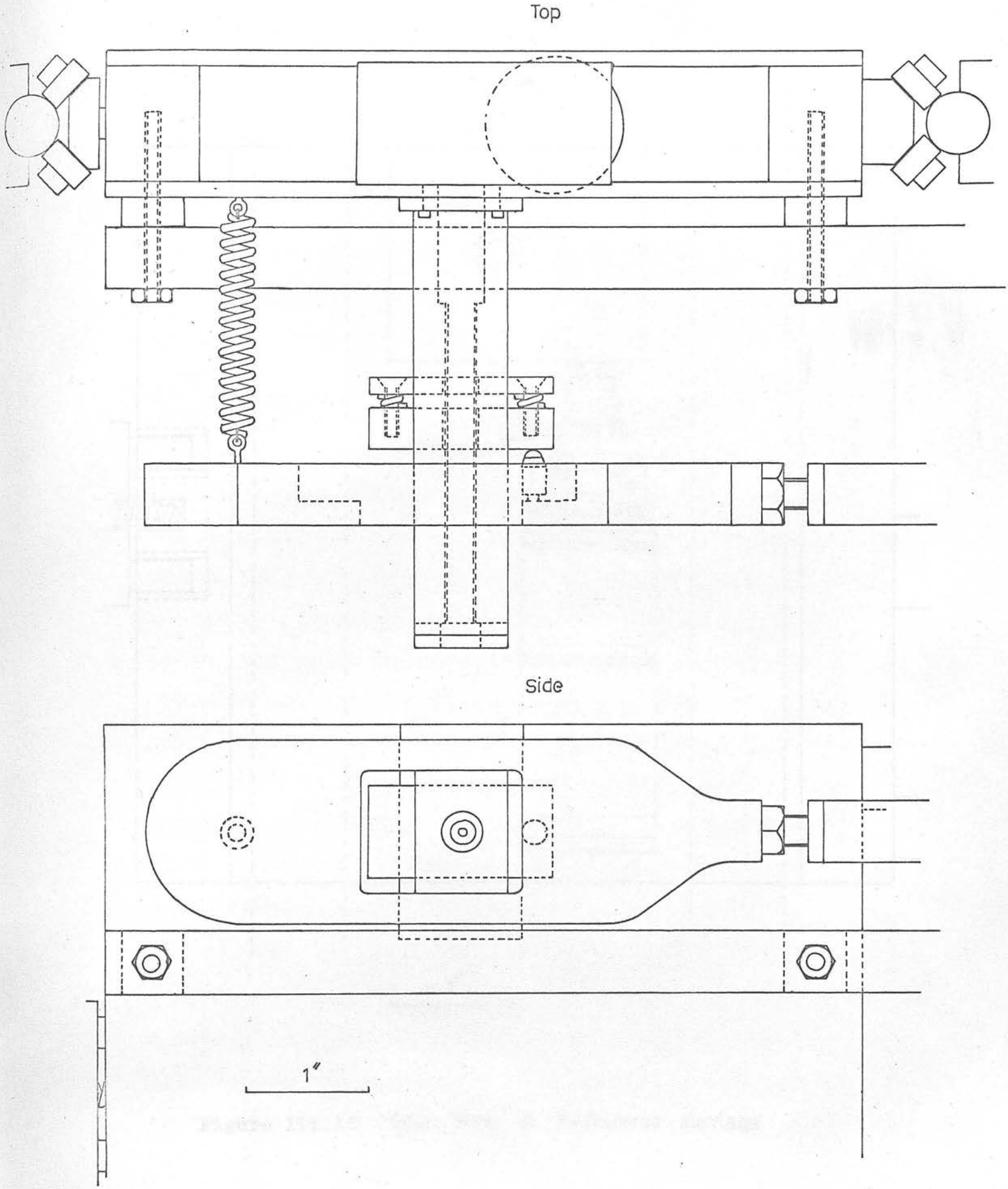

Figure III.9 Y-Traverse Drive

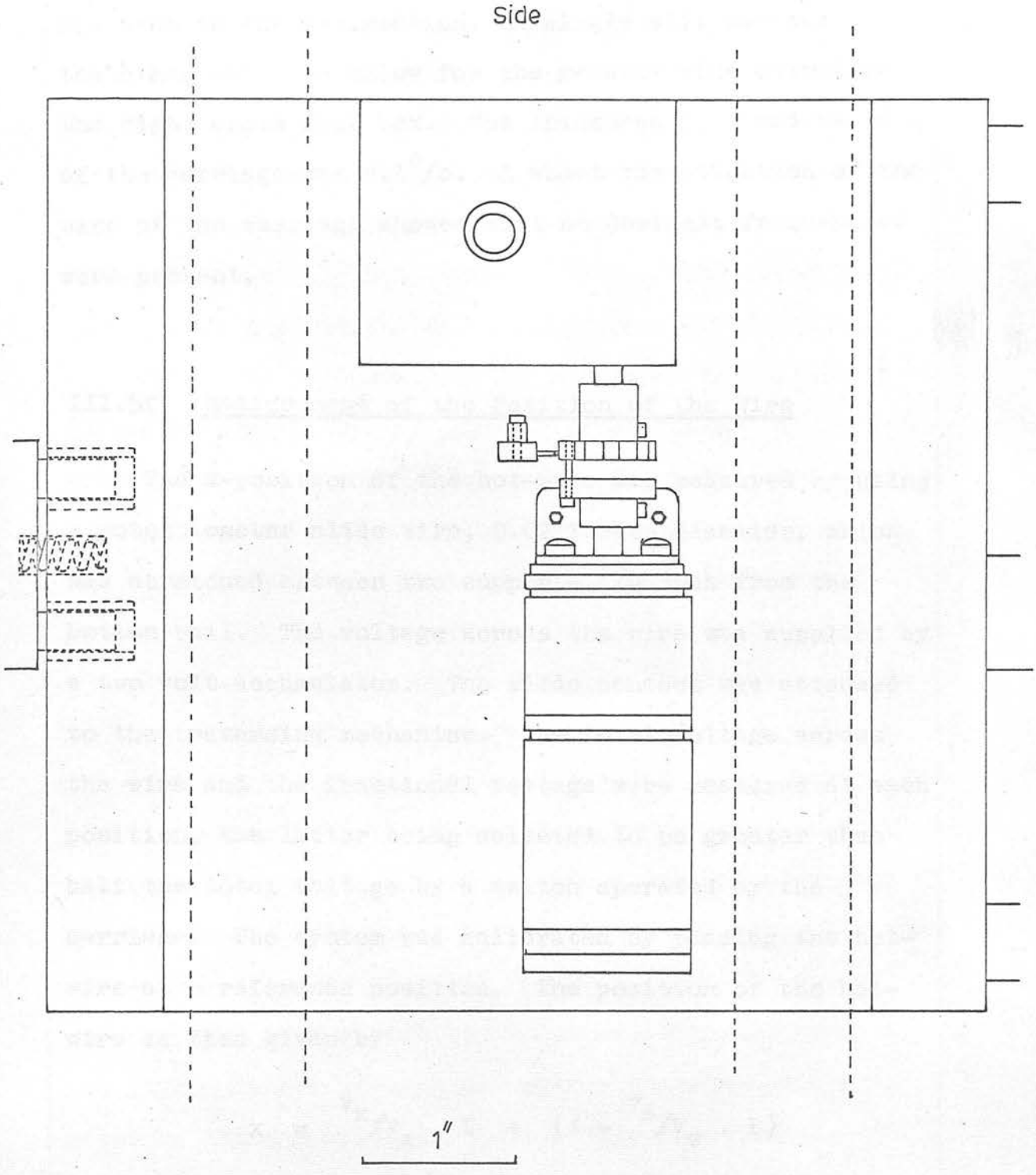

Figure III.10 Open View of Z-Traverse Carriage

bottom. Three slits were cut in the cover to allow for movement in the z-direction. A single slit was cut in the other cover to allow for the reverse side output of the right angle gear box. The thickness to chord ratio of the carriage was 8.1°/o. A short investigation of the wake of the carriage showed that no dominant frequencies were present.

III.5f Measurement of the Position of the Wire

The x-position of the hot-wire was measured by using a potentiometer slide wire, 0.02 inches diameter, which was stretched between two supports 1/4 inch from the bottom rail. The voltage across the wire was supplied by a two volt accumulator. The slide contact was attached to the traversing mechanism. The total voltage across the wire and the fractional voltage were measured at each position, the latter being selected to be greater than half the total voltage by a switch operated by the carriage. The system was calibrated by placing the hot-wire at a reference position. The position of the hot-wire is then given by

$$x = {}^{v_x}/_{V_x} \cdot L + (\ell - {}^{v_s}/_{V_s} \cdot L)$$

where L is the length of the slide wire, v_x and v_s are the fractional voltages at any position and the reference position respectively, V_x and V_s are the total

voltages at any position and the reference position respectively and ℓ is the x-coordinate of the reference position. L was measured by recording v_x and V_x at two inch intervals down the slide wire and measuring the distance of each position from an arbitrary position. A least squares straight line was calculated and L was found to be 98.34 ± 0.03 inches. The residuals of the voltage all lay within the reading error of the digital voltmeter. By manipulating the ranges of the digital voltmeter the system was capable of measuring x with an error of the order of $\pm$ 0.05 inch. The x-position was found, once the system was calibrated, by recording V_x and v_x on paper tape, using the digital voltmeter and punch.

A system, similar to the one described above, will be used to measure the z-coordinate.

The y-position was found by measuring the number of revolutions made by the output from the first gear in the y-traverse drive. An eight lobed cam composed part of the coupling on the input to the right angle gear box and operated a micro-switch, see Figure III.10. The pulses were counted by a reversible electro-mechanical counter, but it is planned to make the pulses operate a stepping motor to which a helical potentiometer is attached. The voltage could be measured by the digital voltmeter and recorded on paper tape. The system was calibrated by measuring the distance moved by the hot-wire with a

travelling microscope and recording the number of pulses or potentiometer voltage.

The system described above measured the distance moved by the wire in the y-direction. A method to convert this into a direct y-measurement has yet to be decided upon. The problem would be trivial if it were possible to move the hot-wire parallel to the flat plate. However, this method had to be rejected because of the complexity of the engineering which would be involved. Two alternatives are left which are:

(a) To measure the y-position at one place and map the surface of the flat plate with reference to the traversing mechanism.

(b) To reference the hot-wire at all positions.

Method (a) was investigated first. It was decided that to measure the y-coordinate of the hot-wire at one place would be straight forward using a simple optical system. The flat plate was then mapped by clamping a clock guage to the z-carriage and recording the arbitrary readings of the gauge over an area 2 feet 6 inches (x-direction) by 1 foot 4 inches (z-direction). The readings were repeated with a wind speed of 30 feet/sec. A least squares cubic surface was fitted to the results and was found to represent the surface adequately. By referring to the cubic surface, in a computer programme, the y-position could be found at all x- and z-positions. However, it was found that the two maps differed due to the plate flexing in a wind. Method (b) was therefore

investigated although method (a) has not been entirely rejected. The wind speed on the reverse side of the plate was 10°/o higher than the speed on the working side. If the plate were held more rigidly and the wind speeds on the two sides of the plate made nearly equal method (a) might then become possible.

Kersley (1965) has described how the hot-wire could be referenced in the y-direction at all positions. He brought the ends of the prongs of the hot-wire head against the flat plate, the hot-wire being soldered a short distance from the ends. The distance of the wire from the plate was then known, it having been measured with the hot-wire head in an external mounting. This method was rejected because of the fragility of platinum wires (Kersley used tungsten wires). However, it is proposed to investigate a similar method in which a micro-switch could be operated by coming into contact with the flat plate. The switch will be mounted on the boom close to the hot-wire because of surface variations in the flat plate and it will therefore have to be small so as not to interfere with the flow at the wire. A suitable switch has been found with a light action and a repeatability within 0.001 inch. The y-position when the switch operates will be found at one position using an optical system.

When the natural state of the boundary-layer is laminar the zero position of the wire can be found by extrapolating the measured Blasius profile. As this is

the condition for a large part of the experimental work envisaged this measurement will provide a useful check on the measurement of the y-position.

CHAPTER IV

THE FLAT PLATE

IV.1. The Flat Plate

The perspex flat plate was nine feet long, four feet wide and ½ inch thick. It was symmetrically tapered at one end, being milled at two angles which decreased from the leading edge. Each cut was 2.75 inches wide and the shoulders left by the cuts were removed by polishing. The edge was polished to a semicircle 1/32 inch in diameter. The plate was tapered at one angle on just one side at the other end. The taper was 7.5 inches wide and the edge was 1/64 inch in diameter. Again the shoulder was removed by polishing. The two different tapers at the ends allowed a choice of leading edge but the symmetrically tapered edge has been the only leading edge used to date.

The plate was suspended at the roof from a heavy L-shaped duralumin bracket which was bolted to the roof and off-set from the centre line of the working section by 1/4 inch. The leading edge of the plate was 5½ inches from the beginning of the working section. The bracket was 2 inches by 3 inches by 10 feet and was 1/4 inch thick. Its leading edge was sharpened. The plate was wedged along its bottom edge by small aluminium brackets, screwed to the floor of the working section, so that it was parallel to the bottom rail of the traversing mechanism

to within $\pm$ 0.005 inches.

With the plate installed an investigation was made of the pressure gradient down the plate, of the turbulent wedges on the plate and of the laminar boundary layer.

IV.2 The Pressure Gradient

The pressure gradient along the flat plate was adjusted by means of the diagonal flexible perspex fillets in the working section. The fillets were adjusted until an approximately zero pressure gradient was obtained.

The pressure gradient was measured using two pitot static tubes. One of the pitot static tubes, $^5/_{16}$ inch in diameter, was fixed 1 foot downstream of the leading edge of the plate, 6 inches from the flat plate and 18 inches above the floor of the tunnel. The other pitot static tube, $^1/_8$ inch in diameter, was mounted on the traversing mechanism so that it moved down the mid-line of the plate and 4 inches from it. Comparison of the static pressures was made using a paraffin filled sloping tube manometer. Readings were taken at six inch intervals along the plate.

A graph showing the pressure distribution for two wind speeds is plotted in Figure IV.1. The static pressure has been made non-dimensional. There is a small stabilising pressure drop from 5 feet to 6 feet 6 inches after which there is a pressure rise. The Pohlhausen shape factor (Λ) for the pressure decrease has a maximum of + 0.8 and for the increase - 4.4. The

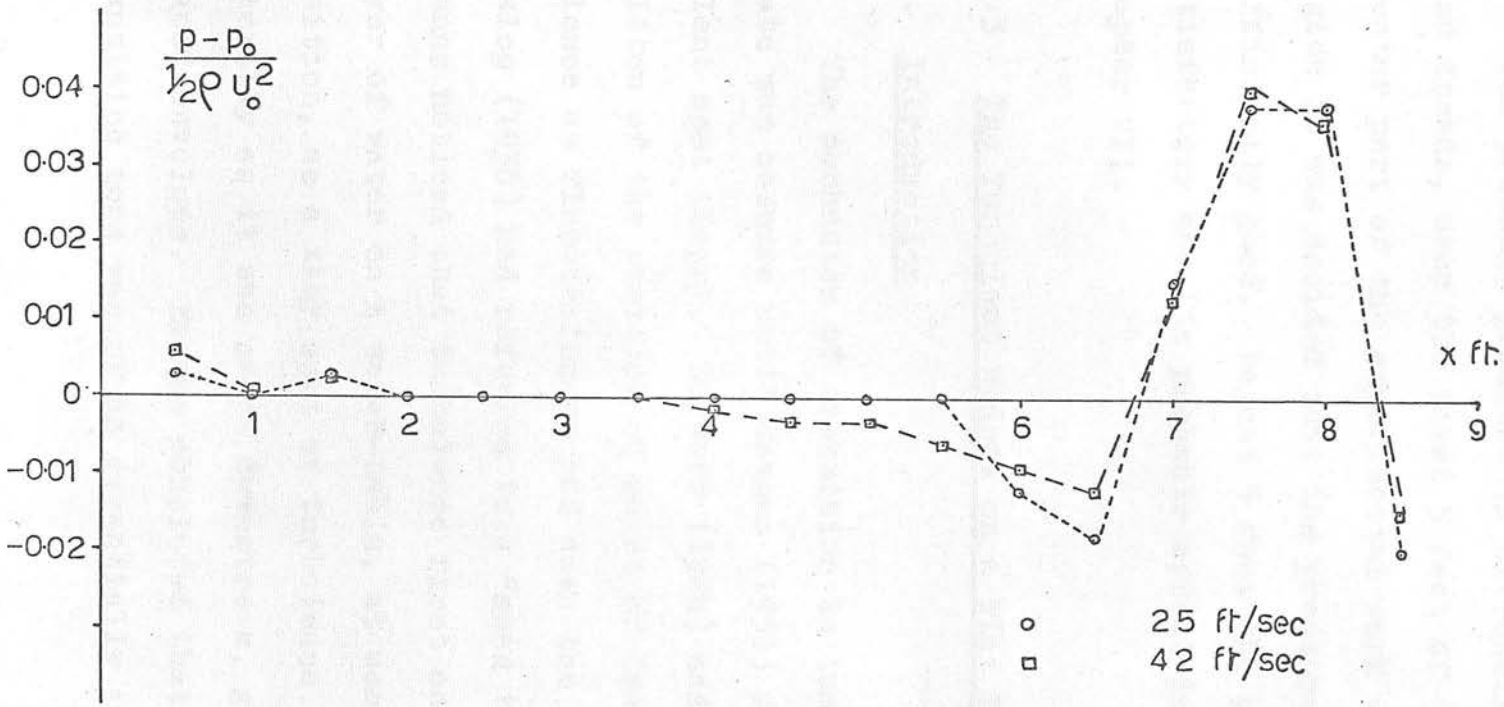

Figure IV.1 Pressure Distribution down the Flat Plate

Pohlhausen shape factor is a parameter which indicates the effect of a pressure gradient on the stability of a boundary layer, and is given by

$$\Lambda = \frac{\partial^2}{\nu} \cdot \frac{dU_o}{dx} \quad .$$

The pressure gradient is extremely small, for both wind speeds, over the first 5 feet of the plate. As the greater part of the experimental work would be in that region it was decided that the pressure gradient was sufficiently good. Beyond 5 feet the gradient is less satisfactory and its probable effect is discussed in Chapter VII.

IV.3 The Turbulent Wedges on a Flat Plate

3a. Introduction

The mechanism of transition to turbulence on a flat plate was obscure until Emmons (1951) suggested the turbulent spot theory. Burgers (1924) had, for instance, written of the position of onset of transition to turbulence as fluctuating up and down the plate, and Hall and Hislop (1938) had referred to a "mean transition position". Emmons noticed that turbulence first occurred, in the thin layer of water on a water-table, at some random instant and position, as a tiny spot of turbulence. The spot grew laterally as it was swept downstream, generating a wedge-shaped envelope. Emmons concluded that turbulence in the transition zone was of an essentially intermittent nature

and proposed a theory for the growth of turbulent spots. He made four assumptions which were:

(a) A point-like breakdown of the boundary layer.

(b) A sharp boundary between the turbulent fluid of a spot and the surrounding laminar flow.

(c) A uniform rate of spot growth.

(d) No interaction between spots.

Assumptions (c) and (d) imply that if turbulent spots are produced at a particular position on a flat plate then they will spread out, wedge like, downstream from that position. Schubauer and Klebanoff (1955) have shown that assumptions (a) and (b) are correct and that (c) is, if the initial spot is of sufficient intensity and the Reynolds Number high enough. Elder (1960b) has verified assumption (d). In both investigations the initial turbulent spot was produced artificially by discharging a spark through the boundary layer, a technique first developed by Mitchner (1954) and which allows a single spot to be examined. Turbulent spots have been produced by other methods. Townsend (1958) and Elder (1960a) described an investigation into the stability of the boundary layer at the free edge of a flat plate. They noted the production of turbulent spots at the free edge, and their subsequent downstream spread into the boundary layer on the flat plate. Turbulent spots arise, of course, in natural transition and in the special case where turbulence is induced by the introduction of a sinusoidal

oscillation into the boundary layer. Schubauer and Klebanoff also produced a continuous train of spots by placing a 1/8 inch sphere on the surface of the flat plate. They found a permanent wedge of turbulence which originated at the obstruction. It appears reasonable to expect similarities in the properties of turbulent spots produced in all the above ways.

Turbulent wedges growing from the extremities of the leading edge of a flat plate, when the plate entirely spans the working section of a tunnel, have been observed for many years. In fact, where a wind tunnel has been designed with an investigation of boundary layer stability in mind, the required length of turbulent free boundary layer on the plate has determined the width, or height, of the working section. Charters (1943) was the first to investigate these wedges. He found that they were due to transverse contamination of the laminar boundary layer on the flat plate by the turbulent boundary layers on the roof and floor of the working section. He found also that the lateral spread of the turbulence took place at an approximately constant rate which varied slowly with the velocity of the main flow. Charters showed that similar wedges of turbulence could be produced by the wake of a rod, or aerofoil, placed against the plate. Emmons has pointed out the connection between a turbulent spot and the turbulent wedges observed by Charters.

An investigation has been made of the turbulent wedges on the flat plate in this tunnel, and the relationship between the wedge angle and wind speed examined.

3b. Previous results for the wedge angle

Details are given below of previous results for the wedge angle or semi-angle of the turbulent spot envelope. The method by which the initial spot was produced is described and the Reynold's Number ($\equiv U_o x/\nu$) of a spark or obstruction, if used, is given.

The results for the wedge angle, α, lie in the range 7.5° - 11.3°, and although they are not all consistent α does appear to be a weak function of Reynold's Number. It is also probable that α is a weak function of the method by which the turbulent spots were first produced.

Turbulent spot produced by a spark

Author	Reynolds Number of the spark position	α	Wind Speed ft./sec.
Schubauer & Klebanoff (1955)	$1.6 \cdot 10^4$	8.6°	10
	$4.8 \cdot 10^4$	10°	30
	$4.3 \cdot 10^5$	11.3°	30
Elder (1960b)	$1.4 \cdot 10^5$	10.5°	27
Mitchner (1954)	$2.4 \cdot 10^5$	8.6°	46

Turbulent spot produced by the wake behind an obstruction.

Author	Reynold's Number of the obstruction position	Obstruction	α	Wind Speed ft./sec.
Charters (1943)	$1.1 \cdot 10^5$	1/4 inch rod	9.3°	51
	$1.1 \cdot 10^5$	Aerofoil	7.5°	24.1
	$1.6 \cdot 10^5$		9.5°	34
	$2.4 \cdot 10^5$		11.3°	51
Schubauer & Klebanoff (1955)	$1.0 \cdot 10^6$	1/8 inch sphere	10.6°	80

Turbulent spot produced by tripping the layer of water on a water table.

Author	α	Water speed ft./sec.
Emmons (1951)	9.7°	
Mitchner (1954)	6.6°	1.46

Turbulent spot produced at the free edge of a flat plate.

Author	α
Townsend (1958)	
Elder (1960a)	7.9°

Turbulent spot produced by transverse contamination.

Author	α	Wind Speed ft./sec.
Charters (1943)	8.3°	24.1
	10°	34
	11°	51
Burns (1958)	10.5°	70

IV.3c The determination of the wedge angle

The position of onset of transition, x_T, was found by traversing a surface total head pitot tube longitudinally down the flat plate, parallel to the centre line. x_T was found for seven transverse positions, at two inch intervals, between $z = -6$ inches to $z = -18$ inches. The surface pitot tube was made of hypodermic tubing, 0.028 inches outside diameter and 0.0165 inches inside diameter. The end of the tube was flattened so that the orifice was approximately oval shaped with axes 0.024 inches and 0.007 inches.

Traversing downstream, the pressure, which was measured using a sloping tube manometer, fell slowly due to the boundary layer growth and then quickly rose due to the modification of the mean velocity profile of the boundary layer with the onset of transition to turbulence. The position of minimum pressure was taken as the point of onset of transition. Dhawan and Narasinha (1958) have shown that this point corresponds to the first appearance of a turbulent spot.

A least squares best straight line was calculated for each set of results, and sets for four wind speeds were found. Table IV.1 gives the results for α. The straight lines were extrapolated to $z = -24$ inches and the "origins" of the wedges are also given in Table IV.1.

Table IV.1

Wind Speed ft./sec.	α	"Origin" inches
40.0	$10.8^{\circ} \pm 0.2^{\circ}$	1.9 ± 0.9
58.0	$10.9^{\circ} \pm 0.1^{\circ}$	1.1 ± 0.5
67.5	$11.7^{\circ} \pm 0.2^{\circ}$	3.4 ± 0.9
76.5	$12.2^{\circ} \pm 0.3^{\circ}$	3.6 ± 1.2

The position of the wedge from the roof was also measured and it was found that the wedges from the roof and floor were symmetrical about the centre line of the flat plate.

IV.3d Discussion of the results

The turbulent wedge angles found agreed with the results of Charters and showed that the average angle was approximately $\tan^{-1} 0.2$. If natural transition to turbulence did not occur on the flat plate, the boundary layer therefore remained laminar along the centre line over the whole length of the plate.

The small increase in wedge angle with increase in wind speed confirms the work of Charters and shows the angle to be a weak function of Reynolds Number.

Schubauer and Klebanoff investigated the rate of lateral growth of a turbulent spot initiated by a spark

3 inches from the leading edge of a flat plate. The rate of growth was initially small and did not attain its constant final value for several inches. It will be seen from Figure IV.2 why the extrapolated "origins" of the wedges lie downstream of the leading edge. However, in contrast to Schubauer and Klebanoff's results, the present results indicate that the "origin" shifts downstream with increase of wind speed. If the turbulent wedge originates at the intersection of the flat plate leading edge and the outer region of the turbulent boundary layer on the floor and roof, then it would be expected that the "origin" of wedges at high speed would be displaced downstream compared to those at low speed. The thickness of the turbulent boundary layers of course decreases with increase in the wind speed. The estimated thickness of the turbulent boundary layer on the floor of the working section, assuming a 3 feet long turbulent boundary layer before the flat plate, is 0.32 inches and 0.28 inches at wind speeds of 40 ft./sec. and 75 ft./sec. respectively (see Pankhurst and Holder (1952)). However, this explains a shift of only 0.2 inch. The discrepancy might be explained by a variation of pressure gradient in the immediate vicinity of the leading edge with wind speed.

Dryden (1956) has suggested that the growth of a turbulent spot might be inhibited until the critical Reynold's Number was attained ($R_\delta = 525$). Schubauer and Klebanoff obtained results which partially confirmed this

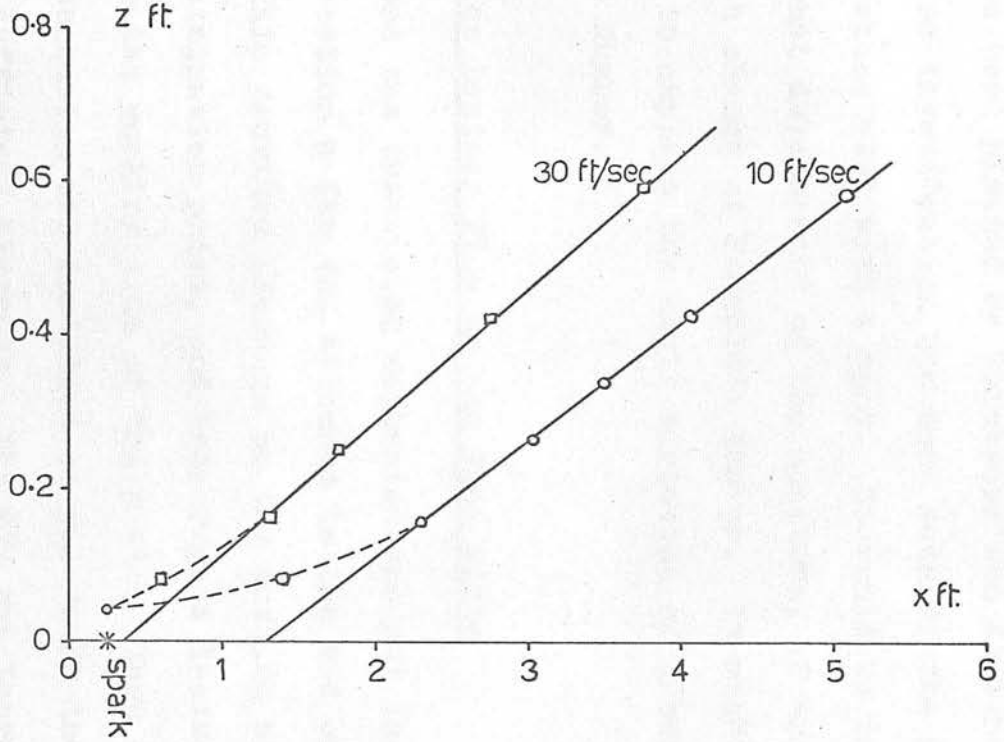

Figure IV.2 Envelopes of Spot Growth (Schubauer and Klebanoff)

suggestion. Taking the true origin to be the intersection of the wedge with the estimated edge of the turbulent boundary layer then its Reynold's Number lies between 450 and 750 for the present results.

IV.3e Suggestion for a further investigation

The growth of turbulent spots in a boundary layer merits further investigation. The physical structure of a spot has been plotted by Schubauer and Klebanoff. However, no investigation has been made of the frequency spectrum associated with a spot. It would be interesting to know what development of the spectrum, if any, took place with change of Reynold's Number. It might then be possible to explain the small variation of growth rate with Reynold's Number.

IV.4. The Laminar Flow on the Flat Plate

Before the traversing mechanism was put into the working section a fin was attached to the end of the flat plate. This provided blockage on the working side, keeping the stagnation point, and therefore a laminar boundary layer, on the working side of the plate. When the traversing mechanism was installed it was found that it provided sufficient blockage. The fin was therefore removed.

Traverses with a total head pitot tube, see Section 3c, were made through the laminar boundary layer at

several Reynold's Numbers. The static pressure was measured with a static tube attached to the support beam of the y-traverse so that it was at the same x-position as the total head tube. The pressure difference was measured by a sloping tube manometer. A typical set of results for the mean flow profile is shown in Figure IV.3 compared with the Blasius profile.

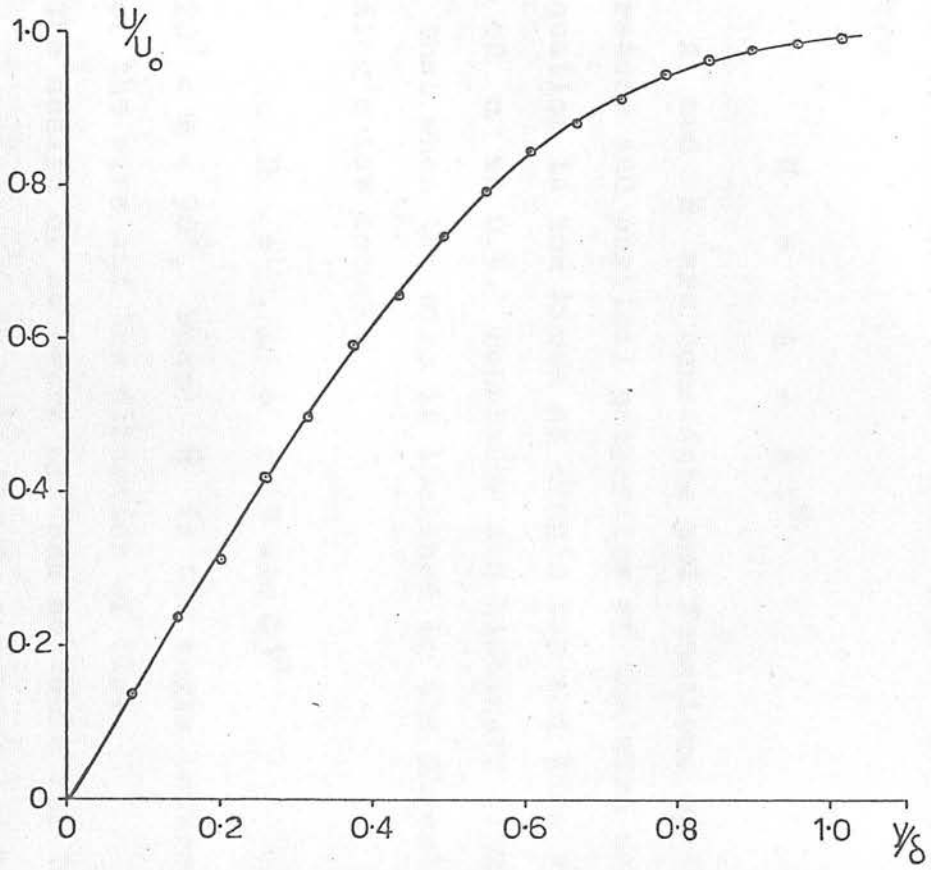

Figure IV.3 The Mean Flow Profile of the Laminar Boundary Layer compared with the Blasius Profile

CHAPTER V

THE HOT-WIRE ANEMOMETER AND THE RIBBON

V.1 The Hot-wire Method

The hot-wire anemometer is a fine electrically heated wire which is cooled convectively when placed in an air-flow. King (1914) showed that the rate of loss of heat from a wire placed normal to the flow (H) was related to the velocity of the fluid flow (U) by an equation of the form

$$H = A + B U^n$$

where A and B are constants and functions of the temperature and physical properties of the wire and fluid. The equation is now known as King's Law and King gave the value of n as 0.5. Schubauer and Klebanoff (1946) have shown that when the wire is inclined to the direction of flow King's Law becomes

$$H = A + B (U \sin \Theta)^n$$

for $20^\circ < \Theta < 90^\circ$, where Θ is the angle between the axis of the wire and the direction of flow.

The design of hot-wire systems suitable for turbulence measurements in both the free stream and boundary layers has been thoroughly investigated, and comprehensive papers have been written by Schubauer and Klebanoff (1946), Cooper and Tulin (1955) and Kovasznay (1953).

V.2 The Components of the Hot-Wire Anemometer

The apparatus required to make measurements of turbulence or disturbances in the boundary layer may be divided into three sections which are:

(a) The hot-wire probe.

(b) The control circuit and amplifier which may include a compensating unit.

(c) The recording, analysing and measuring equipment.

These sections will now be discussed in greater detail.

V.3 The Hot-Wire Probe

In the present work studies have been made of the three components of turbulence in the free stream and of the longitudinal component of a disturbance in the boundary layer on a flat plate. In the former case both single and V-wires were used, whilst in the latter a single wire was sufficient.

a) The hot-wire head

(i) The single wire head

The requirements of the single wire head were that it should be durable, easy to detach from the boom and simple to reproduce. In the design eventually decided upon the head screwed into a co-axial plug which was set into the boom of the traversing mechanism. A diagram of the head and plug is shown in Figure V.1.

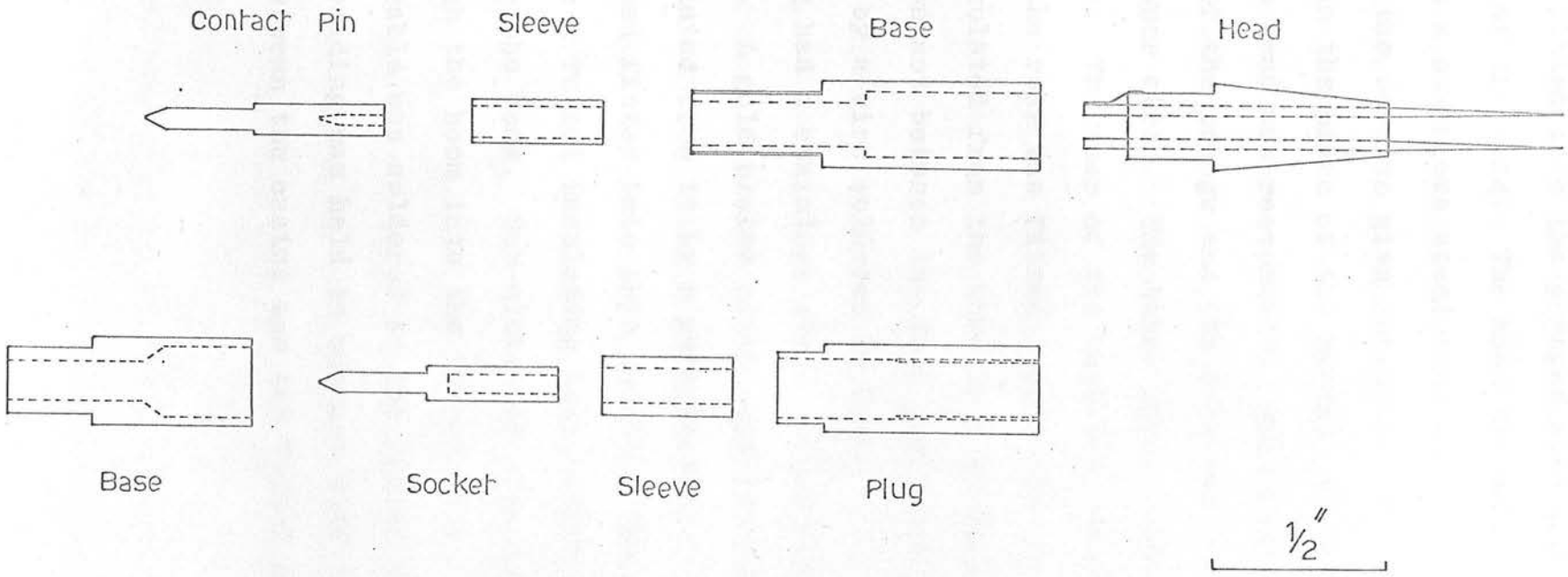

Figure V.1. Head and Plug for a Single Wire.

The prongs, two nickel plated No. 6 sewing needles, were tightly fitted into the perspex head and araldited at both ends of the head. The head was made to have a push-fit into a stainless steel base and it was also araldited to the base to give solidity. The head was filed down, in the plane of the prongs, so that the air flow over the head was reasonable. Electrical contact between one of the prongs and the base was made by a thin beryllium copper strip. The other prong remained isolated from the base. The rear of the base was threaded 2 B.A. size. Into the rear was fitted a gold plated contact pin which was insulated from the base by a perspex sleeve. Electrical contact between the free prong and the contact pin was made by a wire soldered to both.

The plug had a stainless steel casing into which the head screwed. A gold plated socket was set into the casing and insulated from it by a perspex tube. The contact pin of the head fitted into this socket. The casing had a push fit into a Tufnol insulating base, which insulated the plug from the boom. Sub-miniature co-axial cable passed through the boom into the Tufnol base. The centre wire of the cable was soldered to the end of the socket whilst the braiding was held in contact with the casing at the fit between the casing and the Tufnol base.

(ii) The V-wire head

The V-wire head was considered as a "one-off" piece of equipment to be used to measure the v' and w' components of turbulence in the free stream. A V-wire arrangement measures the fluctuating components of velocity of the air flow over a larger volume of air than does an X-wire arrangement. The latter might therefore be preferred. However, measurements of the u' component had indicated that a wire arrangement with a typical length $^1/_4$ inch would be suitable. The V-wire was therefore chosen as it was thought that the mounting and etching of the Wollaston wire would be easier with a V-arrangement rather than an X-arrangement. A diagram of the V-wire head is shown in Figure V.2.

The prongs, three nickel plated No. 6 sewing needles, were tightly fitted into the perspex head and araldited at both ends of the head. The head was made to have a push-fit into a stainless-steel base and it was also araldited to the base. The head was filed down in the plane of the prongs. The rear of the base was threaded 1 B.A. size and screwed into the boom of the support mechanism. Two sub-miniature co-axial cables passed through the boom and rear of the base. The braidings of the two cables were joined to the centre prong. The centre wires were soldered to the outside prongs.

The V-wire head used in the initial measurements of the turbulence components had three prongs araldited into

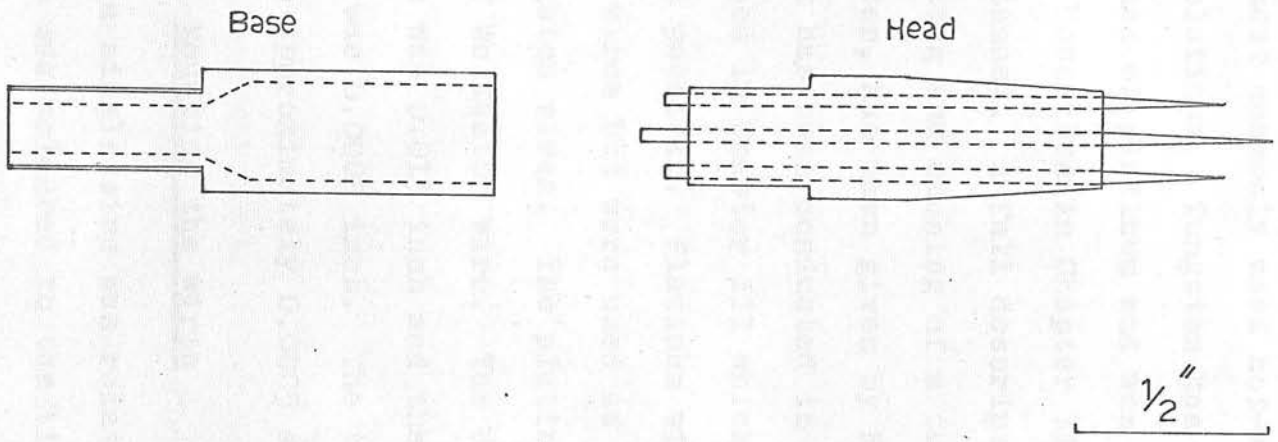

Figure V.2 Head for a V-Wire

a brass plug. The plug fitted directly into the boom. This crude system suffered from prong vibration and the prongs had to be araldited together over half their lengths. No prong vibration was observed in the head described above.

b) The wire

The two most commonly used hot-wire materials are tungsten and platinum. Tungsten has a tensile strength seven times that of platinum and was therefore used in the investigation described in Chapter II which employed an open circuit tunnel. A full description of the copper plating, mounting and etching of a tungsten wire, 0.0002 inch in diameter, has been given by Kersley (1965). The remaining work has been conducted in the closed circuit tunnel described in Chapter III which made the use of platinum wires possible. Platinum wires are more fragile than tungsten wires but were used as they were easier to make than tungsten wires. The platinum wire used here was in the form of Wollaston wire. The diameter of the Wollaston wire was 0.013 inch and the diameter of the platinum wire was 0.0002 inch. The time constant of the wires used was approximately 0.0005 sec.

c) Mounting the wires

Mounting a single wire was relatively simple. The Wollaston wire was soldered to the tips of the prongs and at right angles to the prongs. A straight piece of wire

had to be chosen for mounting as the platinum wire could not be tensioned. The mounting of the wire for a V-wire proved a somewhat more difficult task. The first limb was mounted in the same way as a single wire with the Wollaston wire extending beyond the centre prong. The wire was then bent round to make the second limb. However, this limb had to be straight for if it had even a slight bow the platinum wire fractured when the silver coating was etched away.

d) Etching the wires

The silver coating of the Wollaston wire was removed by electrolytic etching. The hot-wire head was held in a jig and positioned by hand so that a fine jet of 10°/o nitric acid played on the wire. The acid was stored in a burette with a finely drawn nozzle. A terminal of the wire was connected to the anode of a 9 volt dry cell and the cathode was joined to a platinum electrode placed in the nitric acid reservoir. The length of wire etched for a single wire was approximately 0.04 inch and for a V-wire was approximately 0.06 inch. The resistances of the two limbs of a V-wire, which had to be equal to within 10°/o, were measured with a bridge circuit. It was found that further fine etching of the wires could be controlled quite satisfactorily by eye. In fact the two V-wires used had limb resistances which differed by less than 4°/o. A low power microscope was used both to examine the wires and, in the case of a V-wire, to compare the etched

lengths of the two limbs.

V.4 The Control Circuit and Amplifier.

Two two channel hot-wire units were used. The first unit was designed and built by Kersley and only a brief description of it will be given. The second unit was a low noise system which was built for the measurement of the free-stream turbulence.

a) The first unit

The unit was a two channel system with a 12 volt d.c. power supply. The stability of the system was such that a 1°/o change in hot-wire resistance resulted in a $^{1}/_{300}$ °/o change in hot-wire current. The mean resistance of the hot-wire was measured with a Wheatstone Bridge circuit. The hot-wire current was found by measuring, with a Tinsley Type 3184 D potentiometer, the voltage across a standard 10 Ω resistance in series with the hot-wire. The resistances of two hot-wires which differed by up to 20°/o could be matched and their outputs then added or subtracted. The basic amplifier in each channel was a Solatron D.C. Decade Amplifier Type No. AA900 and the compensation amplifier provided compensation for frequencies up to 12 Kc/s. The electronic noise of the unit was approximately 10 μv.

b) The second unit

A circuit diagram of the two channel low noise unit is shown in Figure V.3. The power supply of the unit was 240 volt d.c. provided by H.T. batteries or 180 volt

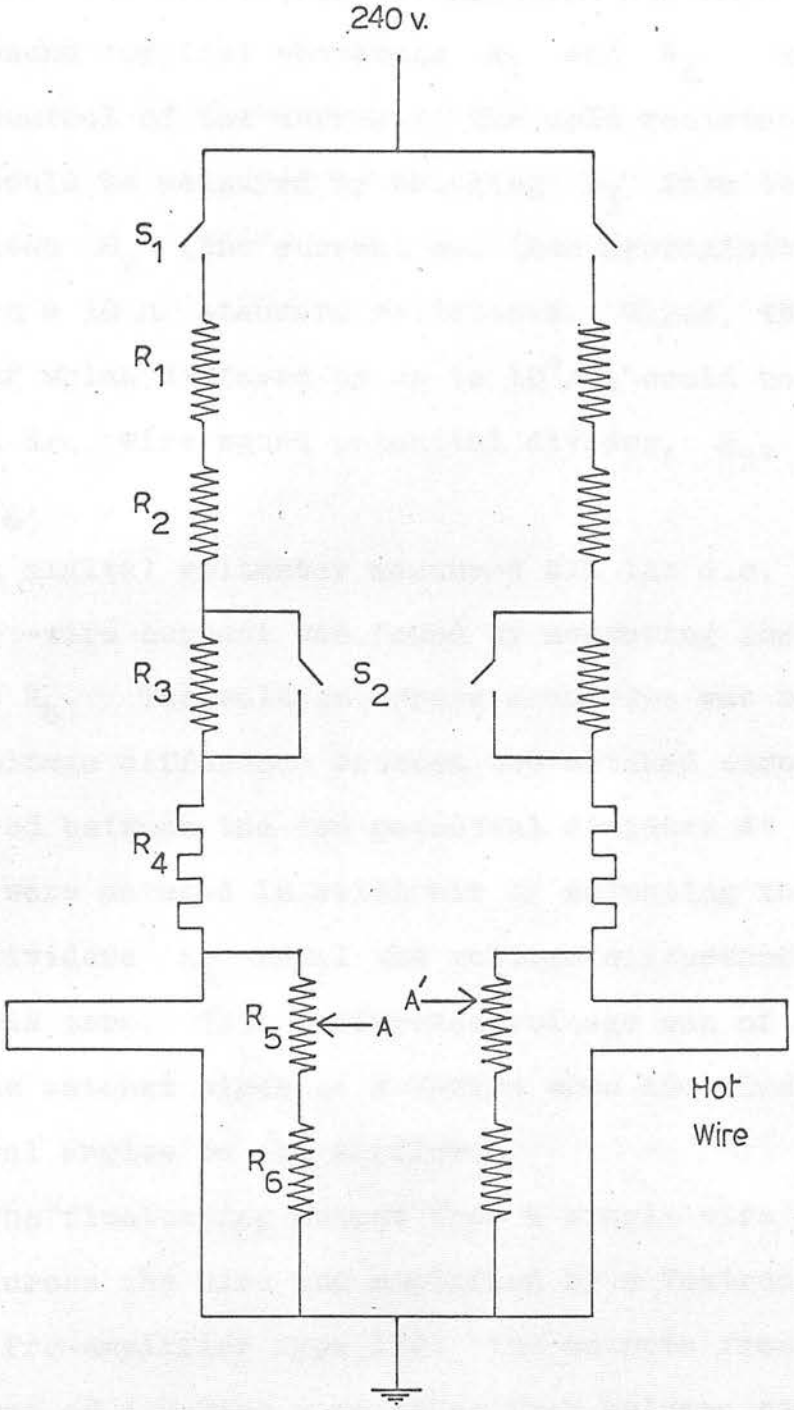

Figure V.3 The Second Hot-Wire Unit

d.c. provided by the Department supply. The latter supply was unsatisfactory when also being used for some other purpose. The current in the hot-wire was adjusted by two wire wound toroidal rheostats R_1 and R_2. R_2 provided fine control of the current. The cold resistance of the wire could be measured by bringing R_3 into the circuit by switch S_2 (the current was then approximately 2 mA). R_4 was a 10 Ω standard resistance. Wires, the resistance of which differed by up to 10°/o, could be matched by a 1 KΩ wire wound potential divider, R_5, in series with R_6.

A digital voltmeter measured all the d.c. variables. The hot-wire current was found by measuring the voltage across R_4. The voltage across each wire was measured and the voltage difference between two matched wires was measured between the two potential dividers at AA'. Wires were matched in still air by adjusting the potential dividers R_5 until the voltage difference across AA' was zero. This difference voltage was of course zero for the matched wires of a V-wire when the wires were set at equal angles to the airflow.

The fluctuating output from a single wire was taken from across the wire and amplified by a Tektronix Low Level Pre-Amplifier Type 122. The outputs from the matched wires of a V-wire were taken from between earth and A and A'. The outputs were amplified by a Tektronix Pre-Amplifier set in its differential mode. The amplifiers output was therefore the amplified difference of the

fluctuating voltages across the two matched wires. Further amplification of the signal was provided, if required, by the amplifiers in a Brüel and Kjaer Frequency Analyser Type 2107.

No frequency compensation was used with this system.

The electronic noise of the system was 3μv to 4μv when the u' component of turbulence was measured and was 1μv to 2μv when the v' and w' components were measured.

V.5 The Recording, Analysing and Measuring Equipment

All the d.c. variables of the system were converted, if not already in that form, to voltages and then measured by a Solatron Digital Voltmeter, Type L.M. 1420. The voltmeter had twenty channels and could be used to monitor just one channel, or to examine automatically 5, 10 or 20 channels in turn. The values could be recorded on seven hole paper tape using a Creed Punch.

The a.c. signal, after amplification, could be recorded on magnetic tape using an E.M.I. Emidata system employing frequency modulated recording. The recorded signal could then be analyzed by a Brüel and Kjaer Frequency Analyser Type 2107 and a Brüel and Kjaer Level Recorder Type 2305. For frequency analysis the lower limit of the frequency analyser, 20 c/s, could be effectively lowered by using a play back speed on the tape deck higher than the recording speed.

A fuller description of the characteristics of the above equipment is given in Appendix I.

V.6 Calibration of the Hot-Wire

a) The single wire

King's Law may be given in the form

$$H = (T_W - T_\infty)(D + F\,U^n) \qquad (1)$$

where D and F are constants and depend on the thermal conductivity, density and specific heat of the air and on the dimensions of the wire. Kovasznay (1953) has shown that if the mass of a wire is small and temperature fluctuations slow equation (1) reduces to

$$\rho = \rho_o + F_1\,U^n \qquad (2)$$

If the wire is operated at constant current then for a given wire and current ρ_o and F_1 are constants. King gave the value of n as 0.5.

Collis and Williams (1959) have suggested a relation between H and U which differs from that given by King's Law, namely that

$$N(T_m/T_\infty)^{-0.17} = A + B\,R^n \qquad (3)$$

which is equivalent to

$$H(T_m/T_\infty)^{-0.17} = (T_W - T_\infty)(A' + B'\,U^n) \qquad (4)$$

Collis and Williams have shown that the best agreement

with experimental results is given when $n = 0.45$. It can be seen that the only difference between equations (1) and (4) is the temperature loading factor in equation (4). Equation (4) obviously reduces to

$$e' = (T_m/T_\infty)^{0.17} (e_o' + F_1' U^n) \qquad (5)$$

where e_o' and F_1' are constants.

The relationship taken for the present work was

$$e = e_o + F_1 U^{0.45} \qquad (6)$$

The temperature loading factor $(T_m/T_\infty)^{0.17}$, for the platinum wires used at present, varied by only 3°/o in the calibration range. In fact the error in e_o for a typical calibration of the wire was approximately $\pm$ 0.5°/o. However, the estimated variation in the factor for a typical boundary layer traverse was 6°/o. It is now planned to use the relation given by equation (5) and also to make an investigation to determine the best value of n for the wires used.

Kersley (1965) has shown that if equation (6) is used then the fluctuating component u' of a disturbance is given by

$$u'/U_o = (e - 1)^2 e'/0.45 \; i \; R_a (e - e_o) \qquad (7)$$

where e' is the r.m.s. voltage fluctuation.

A single wire was calibrated by placing it in the freestream and measuring the wire resistance, at the operating current, at a number (≥ 12) of windspeeds

between 10 ft./sec. and 75 ft./sec. The value of the "cold" resistance was found with the wire in the air-stream. A least squares straight line was calculated for the relationship between $\varrho = R_W/(R_W - R_a)$ and $U_o^{0.45}$ and ϱ_o found.

b) The V-wire

Schubauer and Klebanoff (1946) showed that v'/U_o $w'/U_o = \sqrt{e_b^2}/\triangle E_b$, where $\sqrt{e_b^2}$ is the r.m. s. difference of the fluctuating voltages across the two limbs of the V-wire and $1/\triangle E_b$ indicates the sensitivity of the pair of wires to the v' or w' components of turbulence. E_b, the difference of the mean voltages across the pair of wires, is a function of windspeed and of the angle, θ, of the V-wire to the flow. $\triangle E_b$ is the rate of change of E_b with θ expressed in volts/radian. The V-wire is therefore calibrated for a given wind speed by finding the variation of E_b with θ. Figure V.4 shows the mean voltages for the two limbs of the V-wire as a function of θ at $U_o = 48$ ft./sec. The difference voltage, E_b, is also plotted. It can be seen that while the curves for the individual wires are far from linear in the neighbourhood of $\theta = 0^o$, E_b is a linear function of θ when $-15^o \leq \theta \leq 15^o$. $\triangle E_b$ is found from the straight line calculated by a least-squares fit. Figure V.5 shows the variation of E_b with mean wind speed and hence gives a more general calibration of the wire.

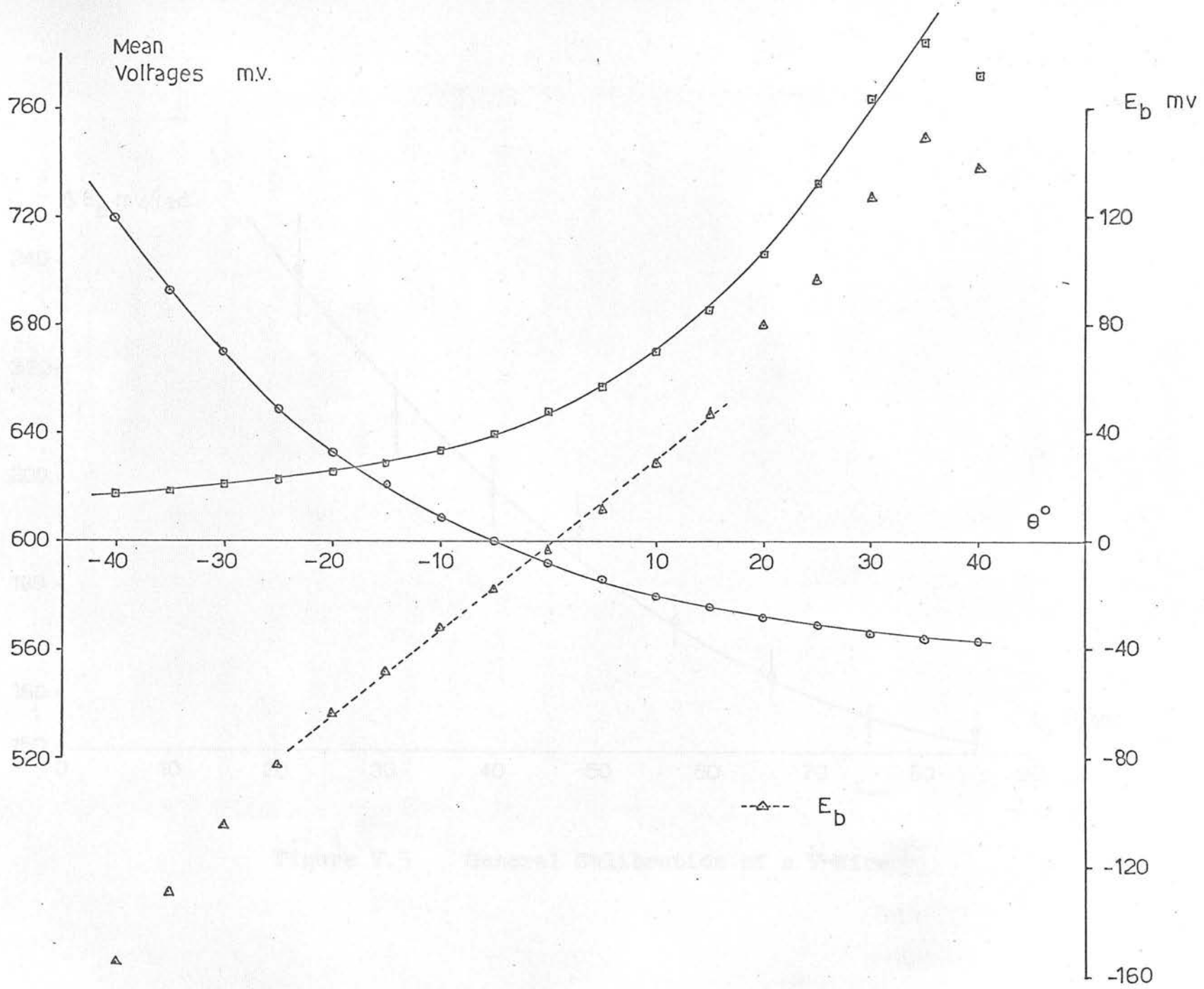

Figure V.4 Calibration of a V-Wire.

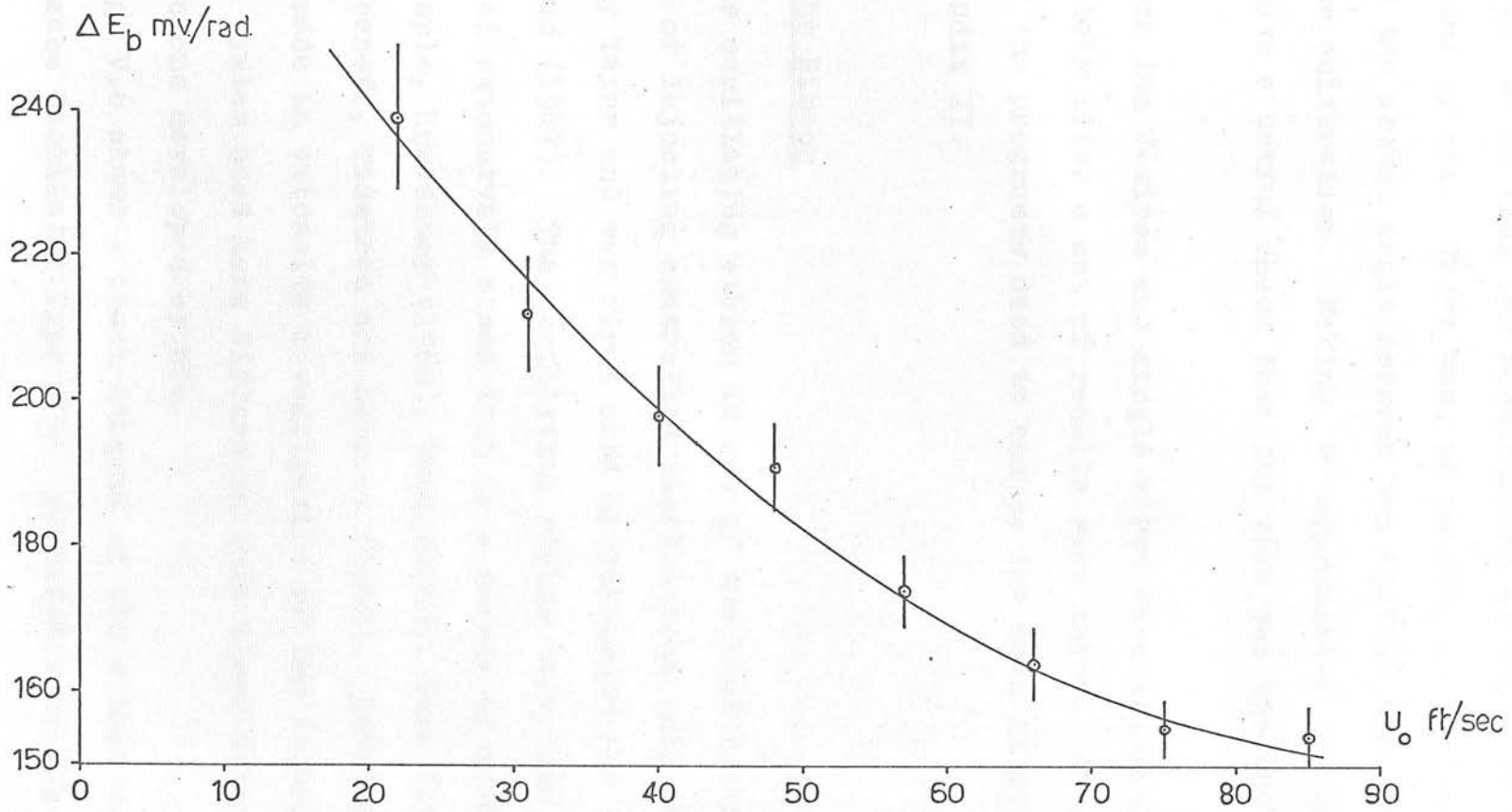

Figure V.5 General Calibration of a V-Wire

It will be seen in Chapter VI that θ was an arbitrary value. The reference position, $\theta = 0^{o}$, was designated by putting the boom support of the wire horizontal by eye. There was, of course, no necessity to know the actual angle between the airflow and the wire for calibration. Making θ approximate to this angle gave a useful check that the wire was working correctly.

Both the V-wires and single wires were calibrated immediately after a set of results were taken. An outline of the programme used to reduce the data is given in Appendix II.

V.7 The Ribbon

The oscillating ribbon is one of the best known methods of injecting controlled oscillations into the boundary layer and was first used by Schbuauer and Skramstad (1947). The oscillating ribbon technique has been used extensively since then by a number of workers, for example, Kovasznay (1960), Tani (1960), Hama (1960) and Klebanoff, Tidstrom and Sargent (1962). Kersley (1965) made an extensive investigation of the technique and the system used here differs in only minor detail from the one developed by him.

Fig. V.6 shows a block diagram of the ribbon circuit. The Advance Oscillator Type J-1 provided a single

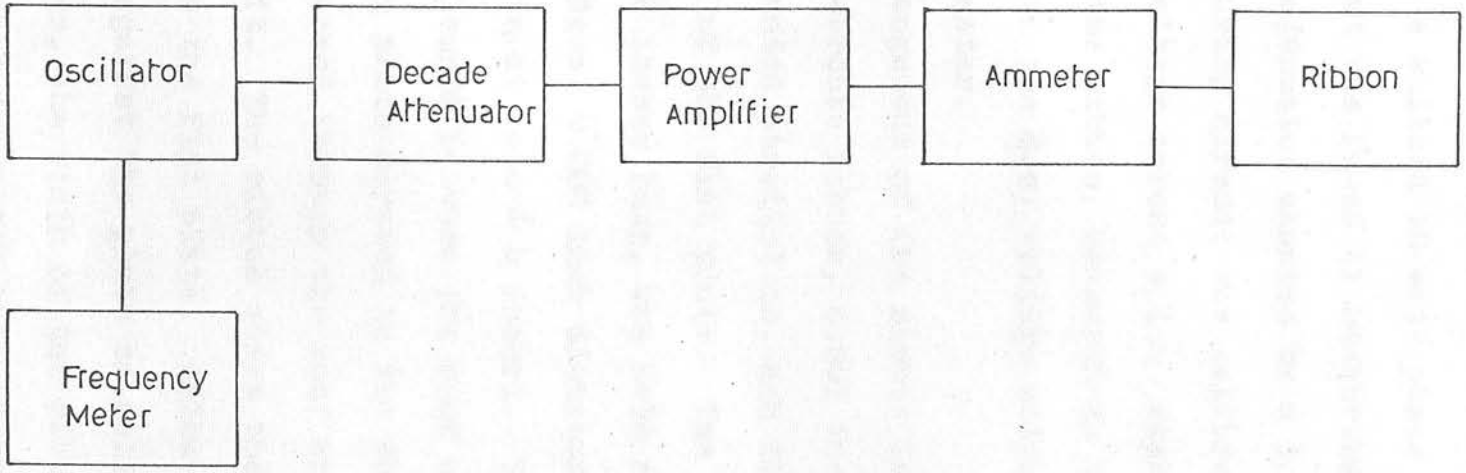

Figure V.6 The Ribbon Circuit

frequency signal which was measured by a Venner Frequency Meter Type T.S.A.3336/2. The signal passed through a decade attenuator which allowed the chosen current to be varied in accurately known steps and was amplified by a Mullard 10 watt power amplifier. The ribbon current was found by measuring the d.c. voltage from a thermojunction shunted by a 1 Ω resistance. The current measuring circuit was calibrated by comparing the r.m.s. voltage across a 1 Ω standard resistance in series with the ribbon, measured by the Frequency Analyser, with the d.c. voltage output, measured by the digital voltmeter.

The arrangement of the ribbon is shown in Figure V.7. The phosphor-bronze ribbon, 0.001 inch thick by 0.1 inch wide, was mounted parallel to, and 12 inches from, the leading edge of the flat plate. The centre portion of the ribbon, 8 inches long, was held away from the plate by glass bridges, 0.008 inch diameter, sellotaped to the flat plate at $z = \pm 4$ inches. The top end of the ribbon was clamped between the roof of the tunnel and a small perspex plate screwed to the roof. A wire soldered to the end passed through the roof and connected to the ribbon circuit. The ribbon above the top bridge was sellotaped to the flat plate. Below the bottom bridge it was held against the plate by sellotape which had a strip of paper, the width of the ribbon down its length. This arrangement prevented transverse movement of the

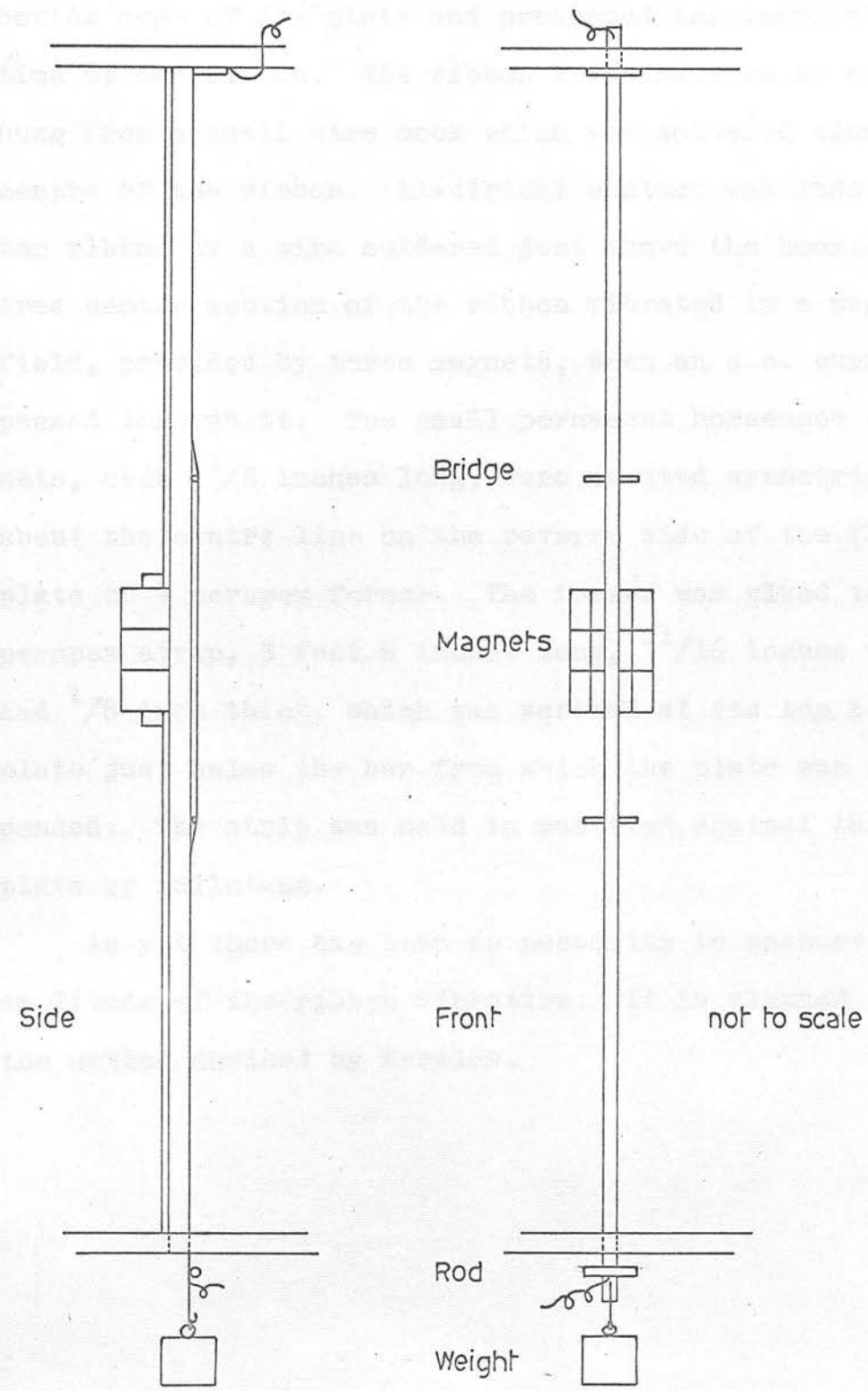

Figure V.7 The arrangement of the Ribbon

ribbon but allowed a longitudinal tension to be placed on the ribbon. A small rod held the ribbon against the bottom edge of the plate and prevented torsional vibration of the ribbon. The ribbon was tensioned by weights hung from a small wire hook which was soldered along the centre of the ribbon. Electrical contact was made with the ribbon by a wire soldered just above the hook. The free centre section of the ribbon vibrated in a magnetic field, provided by three magnets, when an a.c. current passed through it. The small permanent horseshoe magnets, each $1\frac{1}{8}$ inches long, were mounted symmetrically about the centre line on the reverse side of the flat plate on a perspex former. The former was glued to a perspex strip, 3 feet 6 inches long, $\frac{11}{16}$ inches wide and $\frac{1}{8}$ inch thick, which was screwed at its top to the plate just below the bar from which the plate was suspended. The strip was held in position against the plate by sellotape.

As yet there has been no necessity to measure the amplitude of the ribbon vibration. It is planned to use the method devised by Kersley.

CHAPTER VI

MEASUREMENT OF THE FREE STREAM TURBULENCE

VI.1. Introduction

The total turbulence level is given, as a fraction of the mean velocity, by $\frac{100}{U_o}\left[\frac{1}{3}(u'^2 + v'^2 + w'^2)\right]^{\frac{1}{2}}$ % so that to define it the values of u'/U_o, v'/U_o and w'/U_o for the free stream must be measured. A single hot-wire, set transverse to the wind direction, was used to measure u'/U_o. The measurement of the v'/U_o and w'/U_o components required two hot-wires set in either an X or V formation. The latter arrangement was used in this case. Platinum wires, 0.0002 inches in diameter, were used for hot-wires throughout the investigation, their time constant, under typical working conditions being 0.0005 sec. The greater part of the turbulence energy will be seen to fall below a frequency of 200 c/s; compensation of the wires was therefore felt not to be necessary.

A full description of the design and manufacture of the hot-wire heads and of the calibration of the wires is given in Chapter V.

The measurement of the free stream turbulence divides itself into two parts, a preliminary study and a fuller investigation which gave more reliable results for the turbulence level and also turbulence spectra unaffected by vibration of the hot-wire.

The preliminary study was made at a position 1 foot 6 inches downstream of the leading edge and 6 inches from,

and opposite the mid-line of, the flat plate. The second study was made at the beginning of the working section, 2 feet from the floor and 6 inches from the centre point of the working section. Traverses were also made which showed that there was no significant variation in the u'/U_o component of turbulence within $\pm$ 1½ feet of the centre point of the working section, in both the horizontal and vertical directions.

VI.2 Preliminary Study of the Free Stream Turbulence

a) Measurement of the u'/U_o component

Measurements of the u'/U_o component were made with the head for the single hot-wire mounted on the traversing mechanism.

It was found that the noise level of the two channel hot-wire system built by Kersley (see Chapter V) was too large to make free stream turbulence measurements possible. A temporary low noise system, essentially the same as that described in Chapter V, was therefore built. As there was severe pick-up of 50 c/s in the leads to the hot-wire both arms of the system were used, hot-wire A in one and hot-wire B in the other. The leads to the two wires were made identical, and the wires themselves had resistances equal to within 5°/o. Hot-wire A was mounted on the traversing mechanism, whilst hot-wire B was sealed in a test tube which was sellotaped to the tunnel floor. The signals from the two hot-wires were subtracted and

amplified by a Tektronix low level preamplifier Type F.M. 122 used in its differential mode. The amplifier gave a gain of 1000, and the frequency range used was 0.2 c/s to 1000 c/s. The RMS output was measured with a Bruel and Kjaer Frequency Analyser Type 2107. The measurement of the noise of the system was made under still air conditions. However, it was found necessary, because of draughts in the tunnel, to place a protective can over hot-wire A whilst this noise measurement was being made. Measurements of the u'/U_o component of turbulence were made for different wind speeds and the results are given in Figure VI.1. The frequency spectrum of the u'/U_o component was found also, using a Bruel and Kjaer Level Recorder Type 2305 and the Frequency Analyser.

b) Measurement of the v'/U_o and w'/U_o components

The V-wire head was attached to a short steel tube boom. The boom itself was mounted on a wooden beam, which was securely bracketed to the ceiling and floor of the working section of the tunnel, so that it could be pivoted in a vertical plane. The angle of the boom, relative to a fixed datum line on the beam, was measured with a 360^o protractor which rotated with the boom. The arrangement is shown in Figure VI.2.

The hot-wire system used was identical to that used to measure the u'/U_o component, except that the hot-wires A and B became the two wires of the V-arrangement. The v'/U_o or w'/U_o component of the turbulence

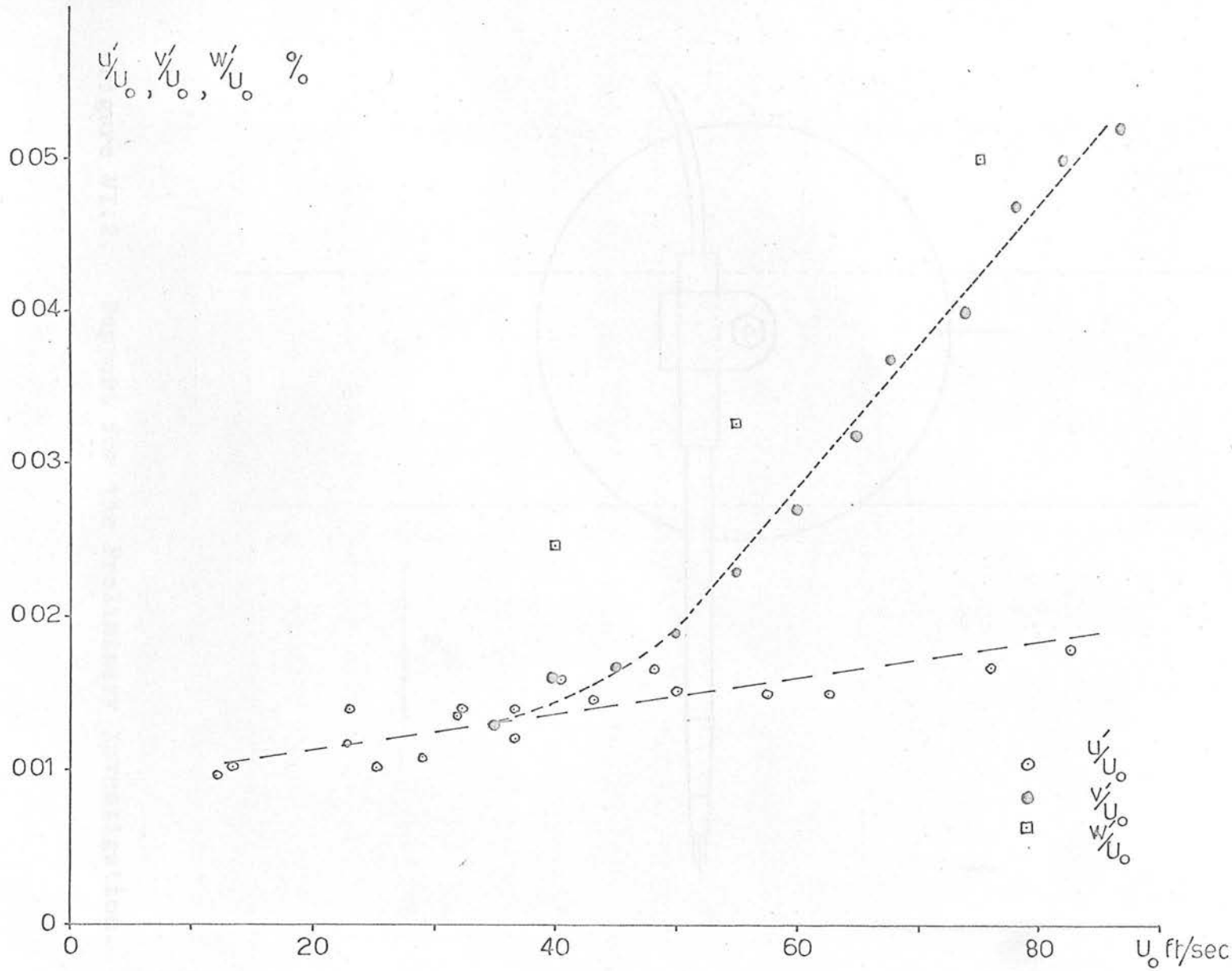

Figure VI.1. Preliminary Results for the Turbulence Level.

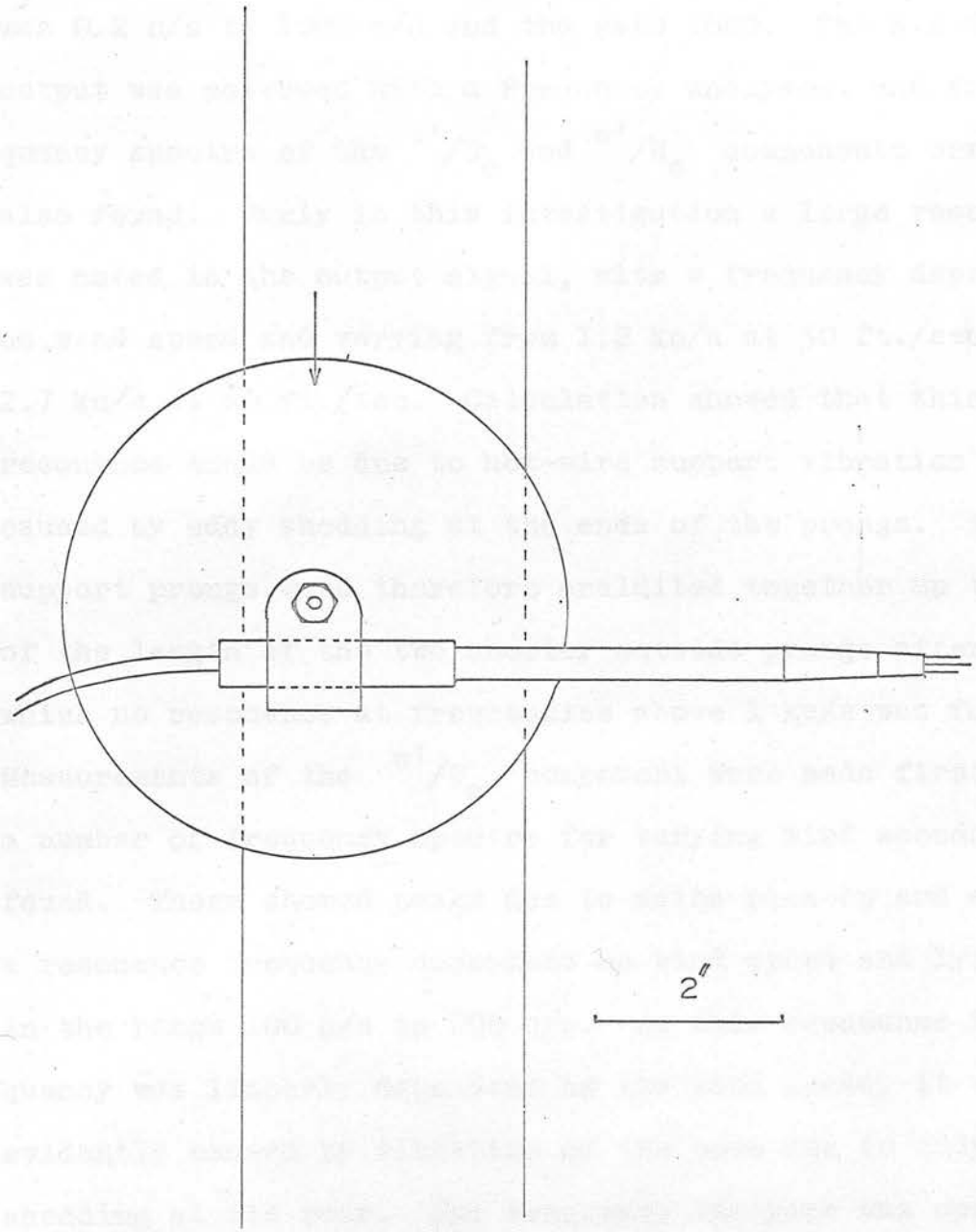

Figure VI.2. Support for the Preliminary Investigation.

was found by subtracting and amplifying the signals from the two component wires of the V-wire using a preamplifier in its differential mode. The band width of the amplifier was 0.2 c/s to 1000 c/s and the gain 1000. The R.M.S. output was measured with a Frequency Analyser, and frequency spectra of the v'/U_o and w'/U_o components were also found. Early in this investigation a large resonance was noted in the output signal, with a frequency dependent on wind speed and varying from 1.2 kc/s at 30 ft./sec. to 2.7 kc/s at 60 ft./sec. Calculation showed that this resonance could be due to hot-wire support vibration caused by eddy shedding at the ends of the prongs. The support prongs were therefore araldited together up to ½ of the length of the two shorter outside prongs after which no resonance at frequencies above 1 kc/s was found. Measurements of the w'/U_o component were made first, and a number of frequency spectra for varying wind speeds were found. These showed peaks due to mains pick-up and also a resonance frequency dependent on wind speed and lying in the range 100 c/s to 200 c/s. As this resonance frequency was linearly dependent on the wind speed, it was evidently caused by vibration of the boom due to eddy shedding at its rear. The Frequency Analyser was operated in its Frequency Rejection mode whilst measuring the w'/U_o component of turbulence, with the wind speed dependent resonance being rejected. The results are given in Figure VI.1.

The v'/U_o component of the turbulence was more

difficult to measure than the w'/U_o component. The wire placed in the horizontal plane was very sensitive to vibrations of the main beam. Three resonances were observed and the v'/U_o component was measured with the largest of these resonances rejected. No great dependence can therefore be put on the three values of v'/U_o obtained.

VI.3. a) Final Study of the Free Stream Turbulence

The preliminary study had produced reasonably reliable results for the u'/U_o component of turbulence. However the results for the two other components were unsatisfactory due to resonances in the support arrangement. A new support for the hot-wire was therefore made, and is shown in Figure VI.3. The boom pushed into a 30 lb. lead block which was suspended within a solid wood frame from two springs. Vibrations of the lead block were damped out by a dash-pot placed below the block. Leading and trailing edges similar to those of the traversing mechanism were fitted to the wood frame and the sides were covered with $^1/_{32}$ inch thick aluminium sheet. The wood frame was wedged between the roof and floor of the working section. The vibrational frequency of the lead block was approximately 2 c/s.

The low noise hot-wire system described in Chapter V was used in this final study of the free stream turbulence. The apparatus used is shown in the block diagram of Figure VI.4.

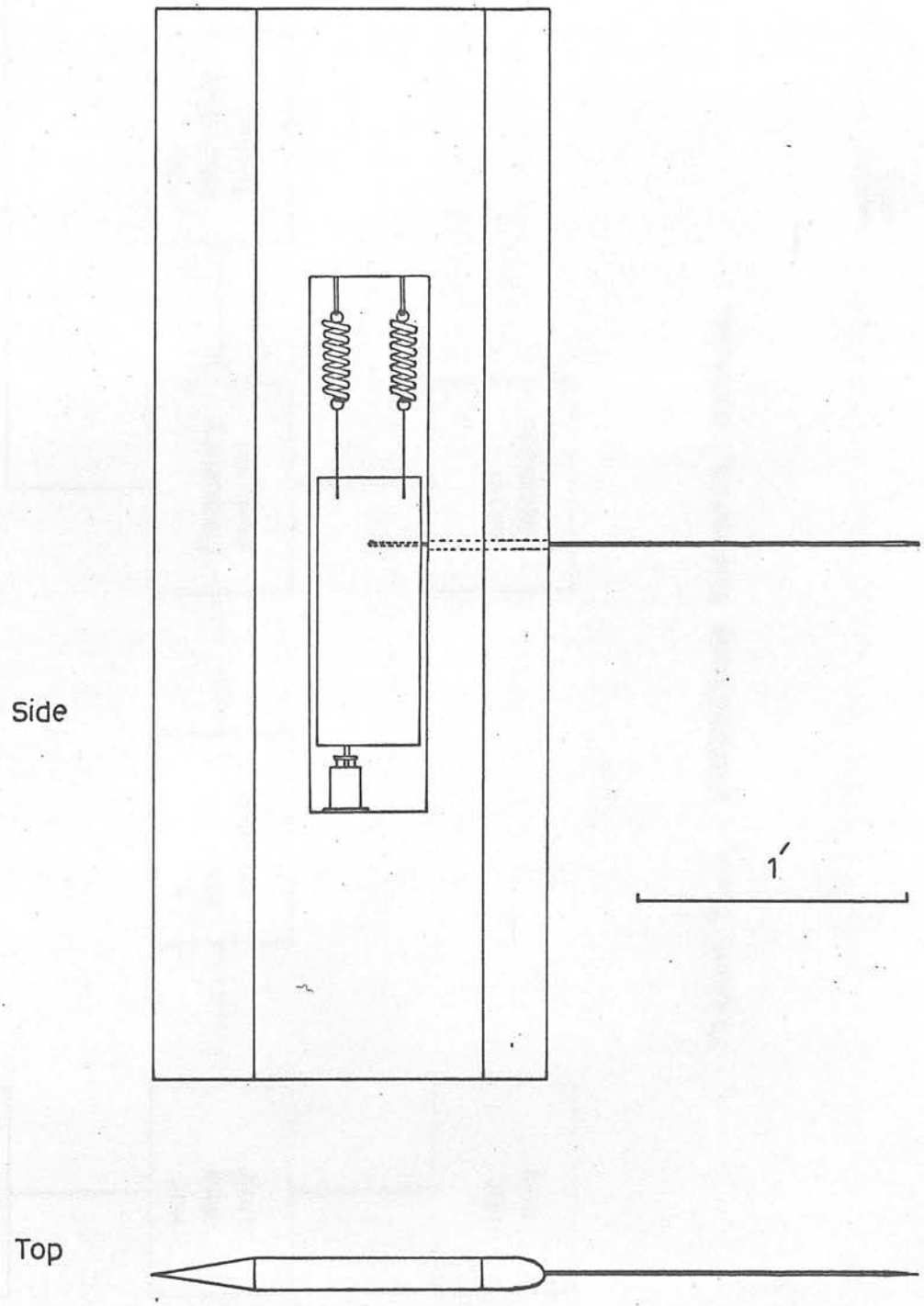

Figure VI.3 Support for the Final Investigation.

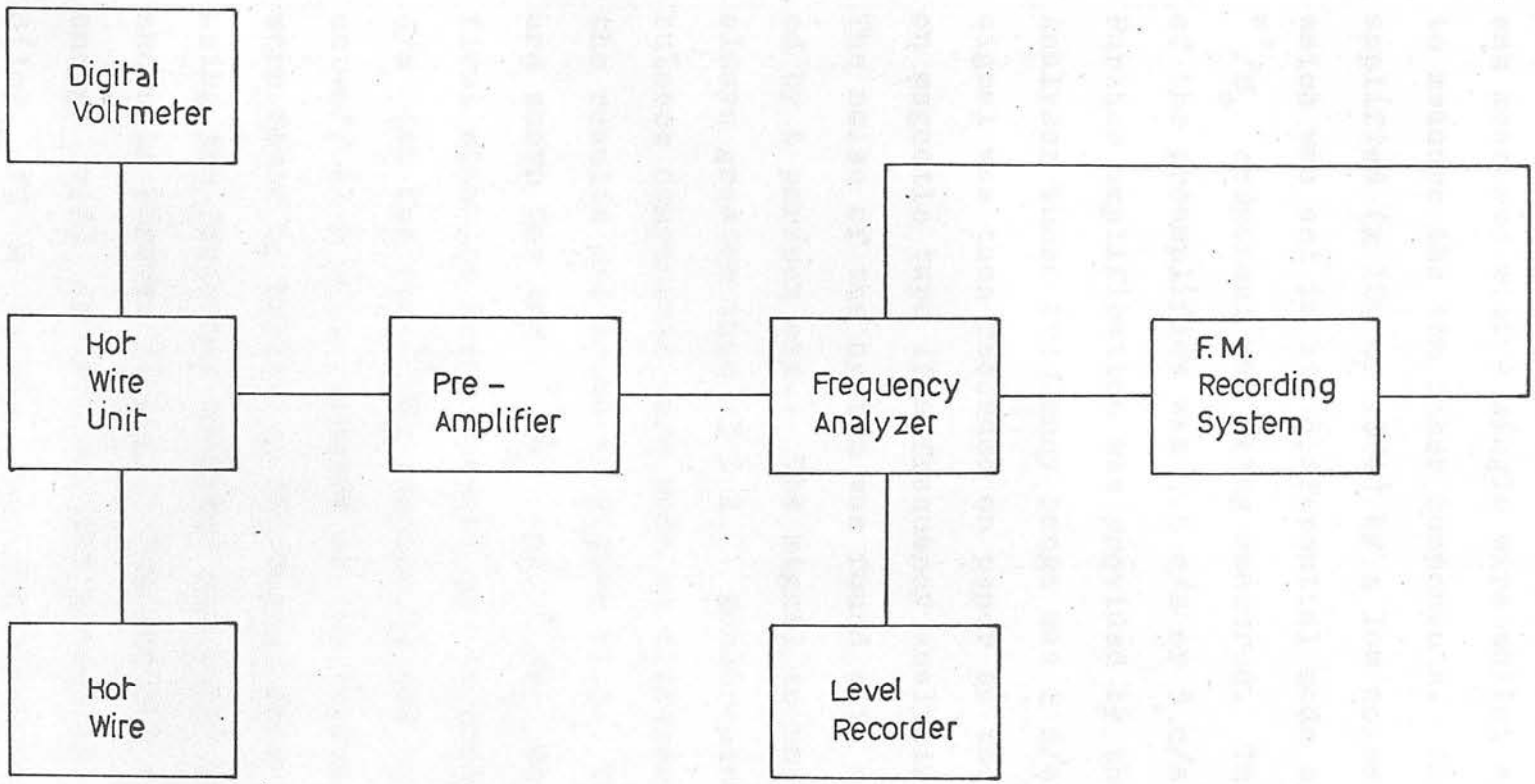

Figure VI.4 Turbulence Measuring System.

b) Measurement of the Turbulence Components

The u'/U_o component of the free stream turbulence was measured with a single wire whilst a V-wire was used to measure the two other components. The signal was amplified (x 100 or 1000) by a low noise preamplifier which was set in its differential mode when the v'/U_o or w'/U_o component was being measured. The frequency range of the preamplifier was 0.8 c/s or 8 c/s to 1 Kc/s. Further amplification was provided by the Frequency Analyser whose frequency range was 2 c/s to 40 Kc/s. The signal was then recorded on paper by the Level Recorder or on magnetic tape if a frequency analysis was required. The noise of the system was found with the hot-wire covered by a perspex cap. The signal to noise ratio was always greater than 3 : 1. Measurements of the turbulence components were made at different wind speeds and the results are shown in Figure VI.5. Two sets of results are shown for the v'/U_o and w'/U_o components, the first with the lower cut-off of the preamplifier at 0.8 c/s (as for the u'/U_o component) and the second with the cut-off at 8 c/s. Spectra of the turbulence components were found by analysing the signal from the magnetic tape using the frequency analyser and level recorder. They are shown in Figures VI.6-17. The decibel readings of the energy $e(f)$ in the constant percentage band width, $d(\log_{10} f) = 0.026$, were converted to linear values,

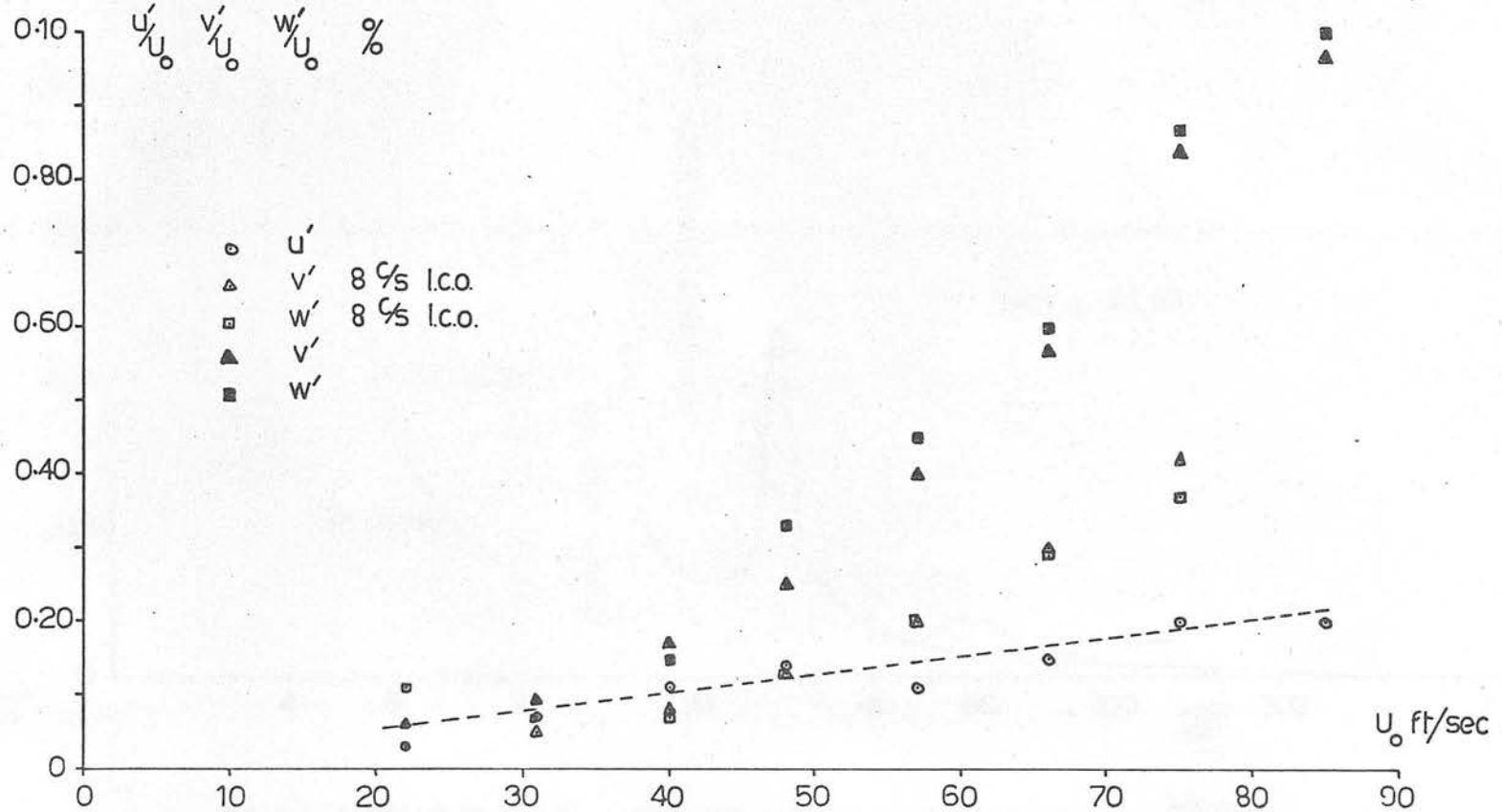

Figure VI.5 Final Results for the Turbulence Level.

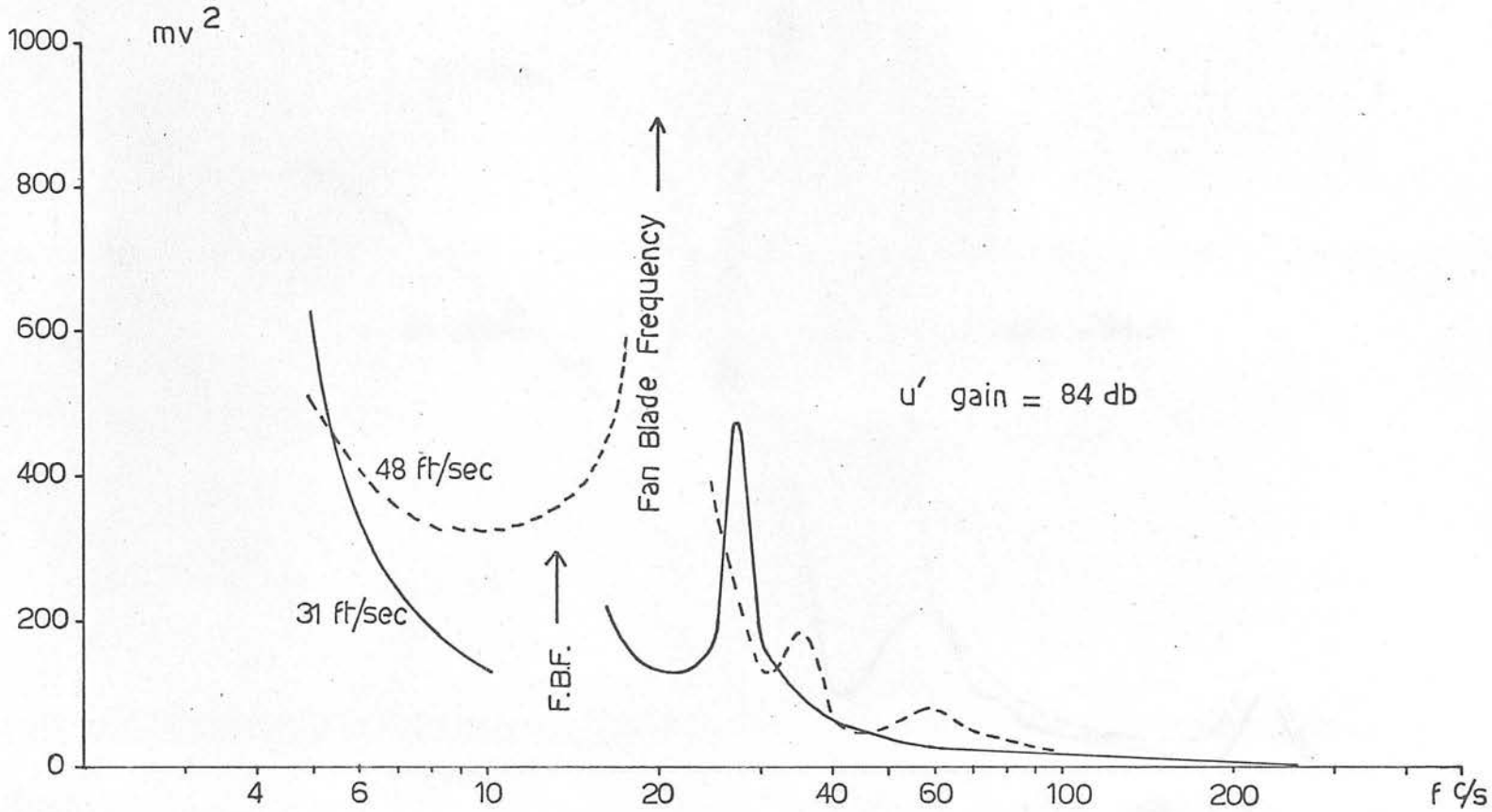

Figures VI.6-7 Spectra of the Turbulence Components.

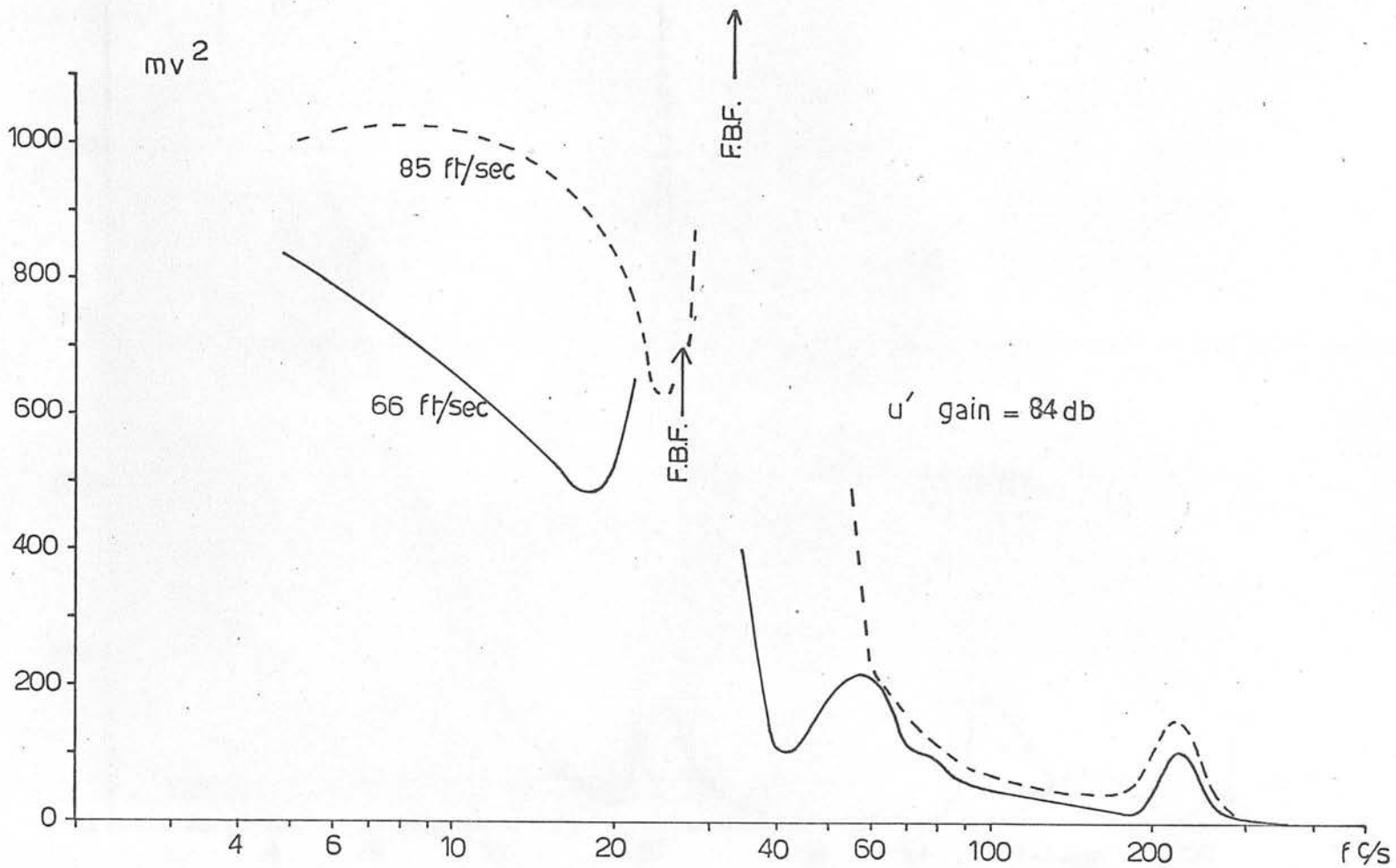

Figures VI.8-9 **Spectra of the Turbulence Components.**

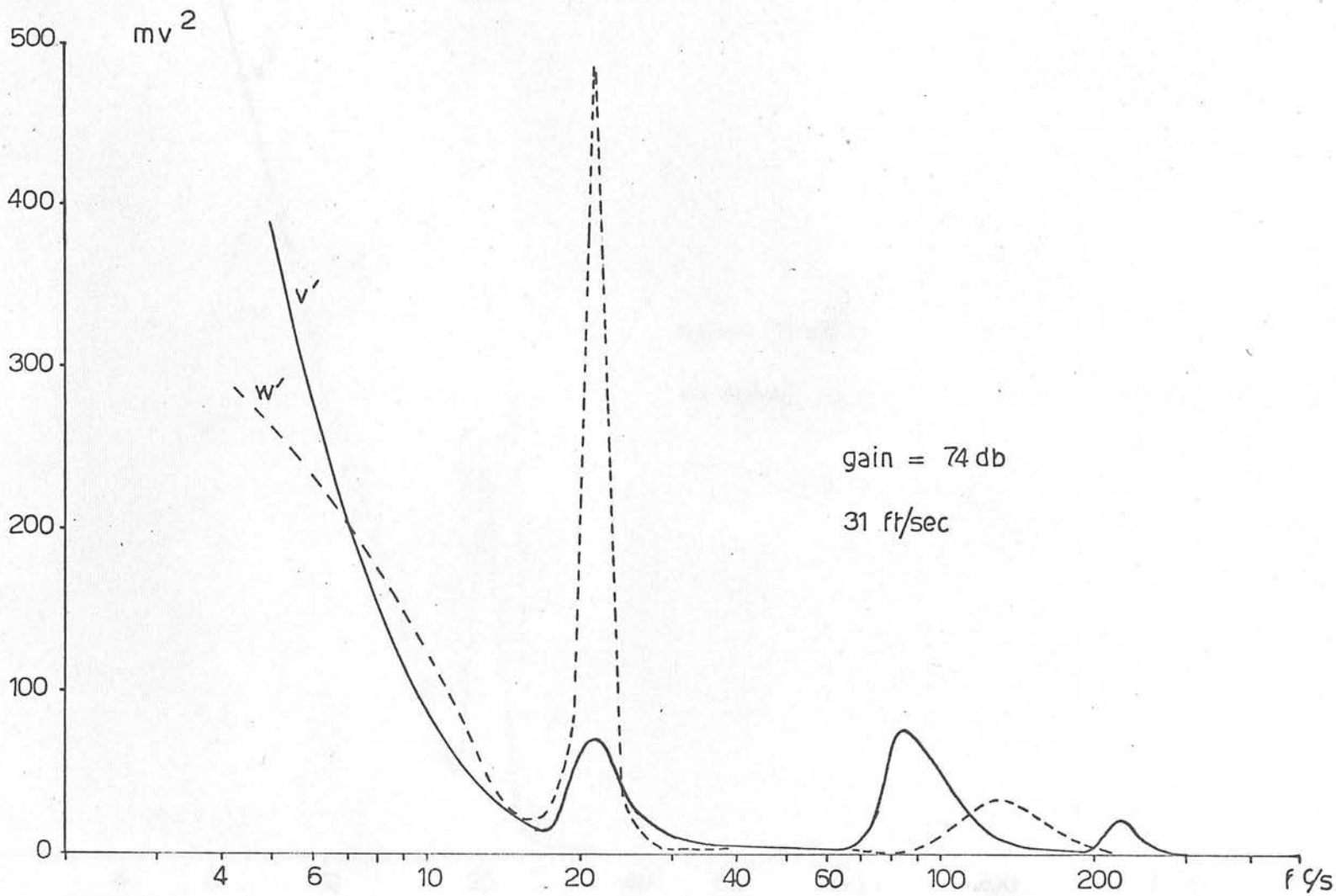

Figures VI.10-11 Spectra of the Turbulence Components.

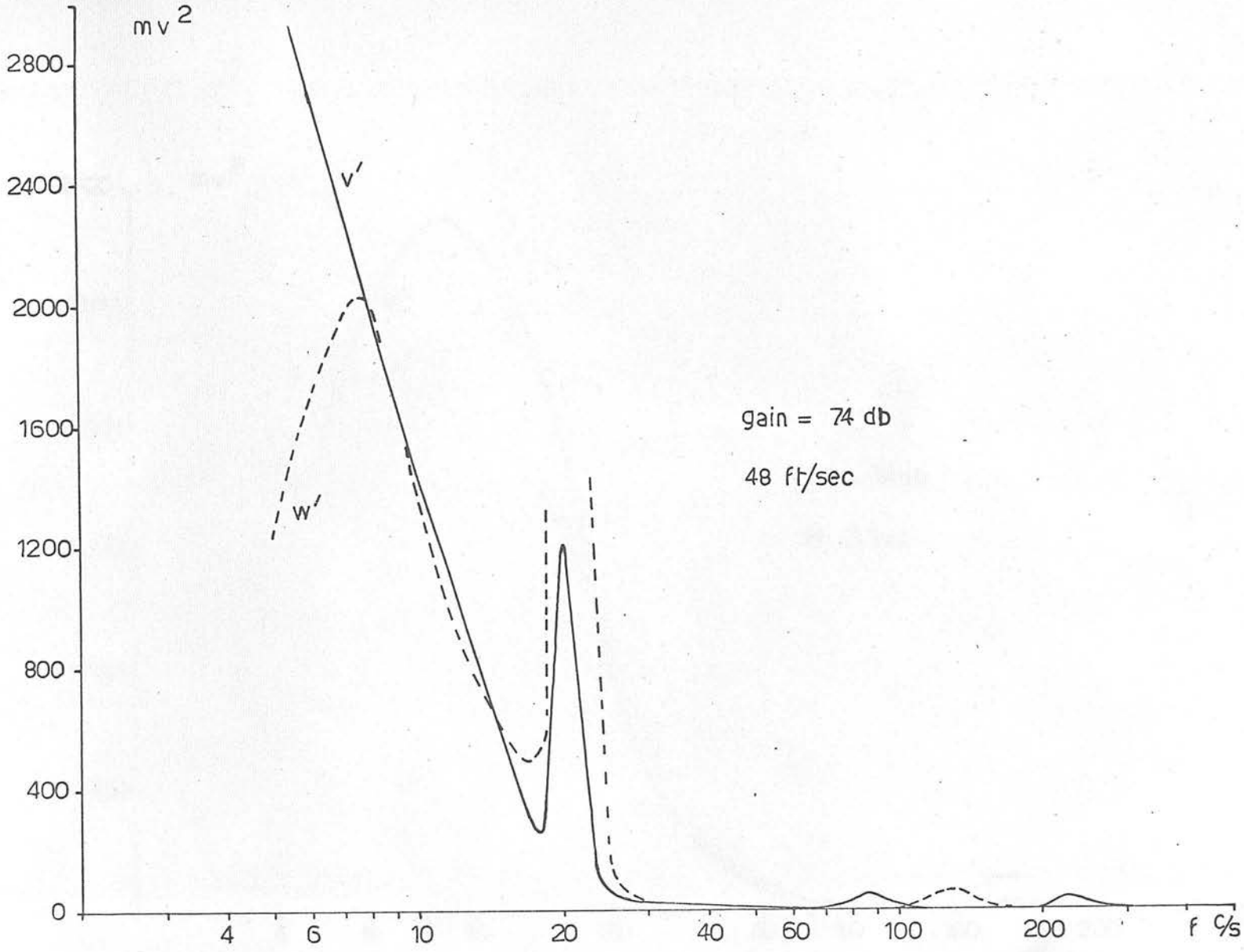

Figures VI.12-13 Spectra of the Turbulence Components.

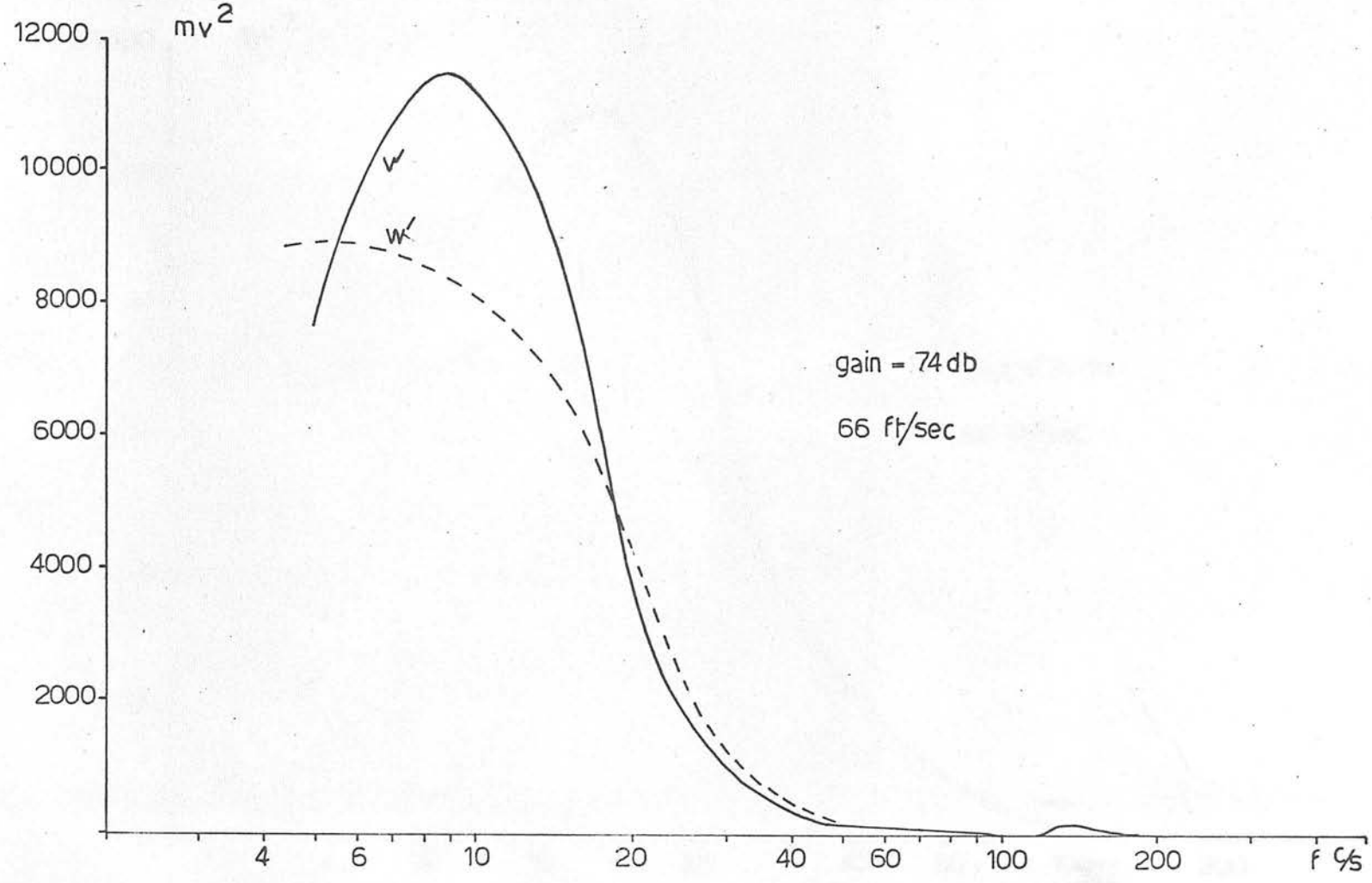

Figures VI.14-15 Spectra of the Turbulence Components.

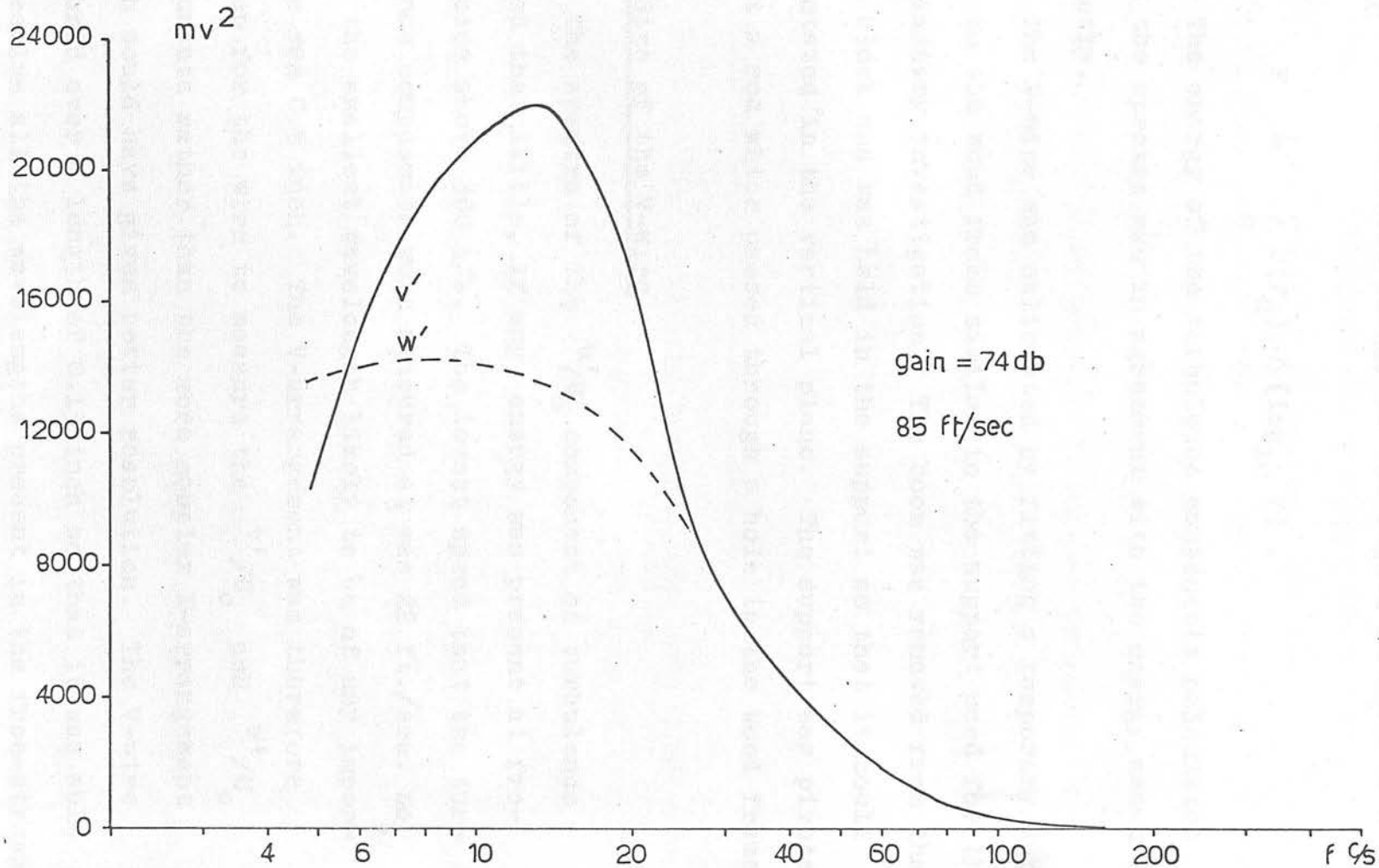

Figures VI.16-17 Spectra of the Turbulence Components.

corrected for instrumental noise and plotted against $\log_{10} f$. The total energy of the signal is then given by

$$E = \sum_n e(f_n) . \Delta(\log_{10} f) .$$

The energy of the turbulence components calculated from the spectra was in agreement with the energy measured directly.

The V-wire was calibrated by fitting a temporary support to the wood frame similar to the support used for the preliminary investigation. The boom was removed from the lead block and was held in the support so that it could be rotated in the vertical plane. The support was pivoted about a rod which passed through a hole in the wood frame.

c) Size of the V-wire

The spectra of the u'/U_o component of turbulence showed that little, if any, energy was present at frequencies above 300 c/s. The lowest speed that the turbulence components were measured at was 22 ft./sec. so that the smallest wavelength likely to be of any importance was 0.9 inch. The V-arrangement was therefore chosen for the wire to measure the v'/U_o and w'/U_o components rather than the more complex X-arrangement which would have given better resolution. The V-wire measured over a length of 0.13 inch so that it was able to resolve all the wavelengths present in the free-stream turbulence.

d) Frequency Compensation of the Wires

The time constant of the platinum wires varied between $5.5 \cdot 10^{-4}$ sec. at 30 ft./sec. and $3.5 \cdot 10^{-4}$ sec. at 85 ft./sec (see Schubauer and Klebanoff (1946)). The upper frequency cut off of the system was therefore determined by the wires and varied between 300 c/s and 450 c/s. It will be seen from the spectra of the turbulence components that little, if any, turbulence energy lay above 200 c/s. Frequency compensation of the wires was therefore not used.

4. Discussion of the Final Results

Figure VI.5 shows the level of the turbulence components plotted against wind speed. Two sets of results are given for the v'/U_o and w'/U_o components, the preamplifier lower cut-off being 0,8 c/s or 8 c/s. Below 40 ft./sec. the three components of turbulence are nearly equal in magnitude but above that wind speed the v'/U_o and w'/U_o components increase rapidly whilst the u'/U_o component only slowly increases. Similar results have been reported by Schuh (1953), Ferriss (1964) and Bradshaw and Hellens (1964). Lowering the preamplifier cut-off from 8 c/s to 0.8 c/s approximately doubles the v'/U_o and w'/U_o turbulence components. An examination of the spectra shows that such an increase is to be expected at the two lower wind speeds where the major part

of the energy is at frequencies < 10 c/s. However, it is likely that at the two higher speeds a large part of the increase is attributable to vibration of the boom at approximately 2 c/s. Facilities were not available to examine the spectra below 5 c/s, so the results for the v'/U_o and w'/U_o components with a preamplifier cut-off of 0.8 c/s have to remain in doubt.

The spectra of the u'/U_o component of turbulence, Figures VI.6-9, show two main features, a continuous spectrum and superimposed upon it a large peak at the fan blade frequency. Approximately $3/4$ of the total energy of the u'/U_o component lies in the band at the fan blade frequency. The ratios of the energies in that band are $1 : 4.5 : 4 : 7.1$ for the four spectra shown. The ratios of the total energies of the u'/U_o component for the same spectra are $1 : 3.2 : 3.7 : 6.6$. The small increase in energy of the u'/U_o component with wind speed can therefore be explained by the increase in energy in the fan frequency band.

The spectra of the v'/U_o and w'/U_o components show no evidence of the fan blade frequency except for the two spectra at a wind speed of 48 ft./sec. The w'/U_o spectrum at 31 ft./sec. shows a peak at a little over 20 c/s so it is likely that the peaks at 20 c/s in the v'/U_o and w'/U_o spectra at 48 ft./sec. are due to a resonance of part of the tunnel structure. The spectra of the two components of turbulence show a shift to higher frequencies

as the wind speed is increased and indicate that the turbulence is spatially distributed. The spectra frequencies were therefore reduced by dividing them by the wind speeds at which the spectra were found. The energies in a band of the reduced frequencies were found to vary as the fourth power of the wind speed and they were therefore reduced by that factor. The reduced spectra for the v'/U_o and w'/U_o components are plotted in Figures VI.18, 19, and show clearly that the turbulence is spacially dependent for the v'/U_o and w'/U_o components. The energy levels have an error of approximately $\pm$ 25°/o ($\pm$ 1 db from the spectra produced by the Level Recorder) so that the reduced energy levels are in reasonable agreement. The same analysis as described above was made on the spectra of the u'/U_o component but no clear conclusions could be drawn.

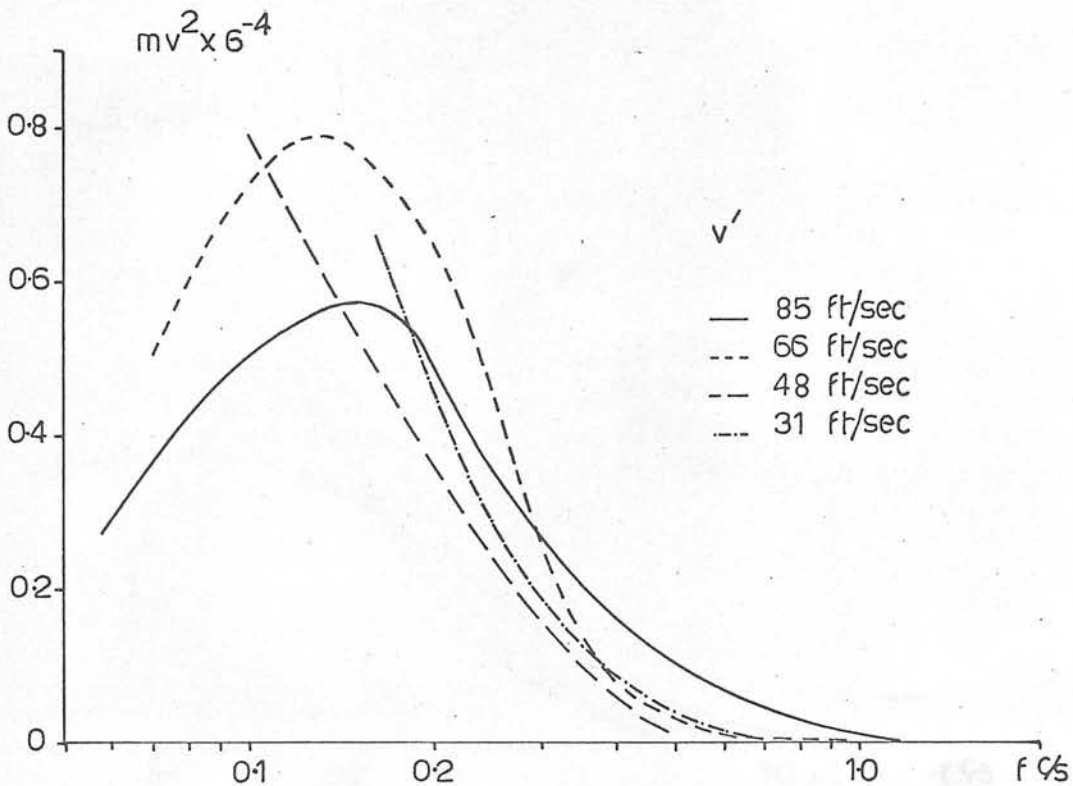

Figures VI.18 **Reduced Spectra.**

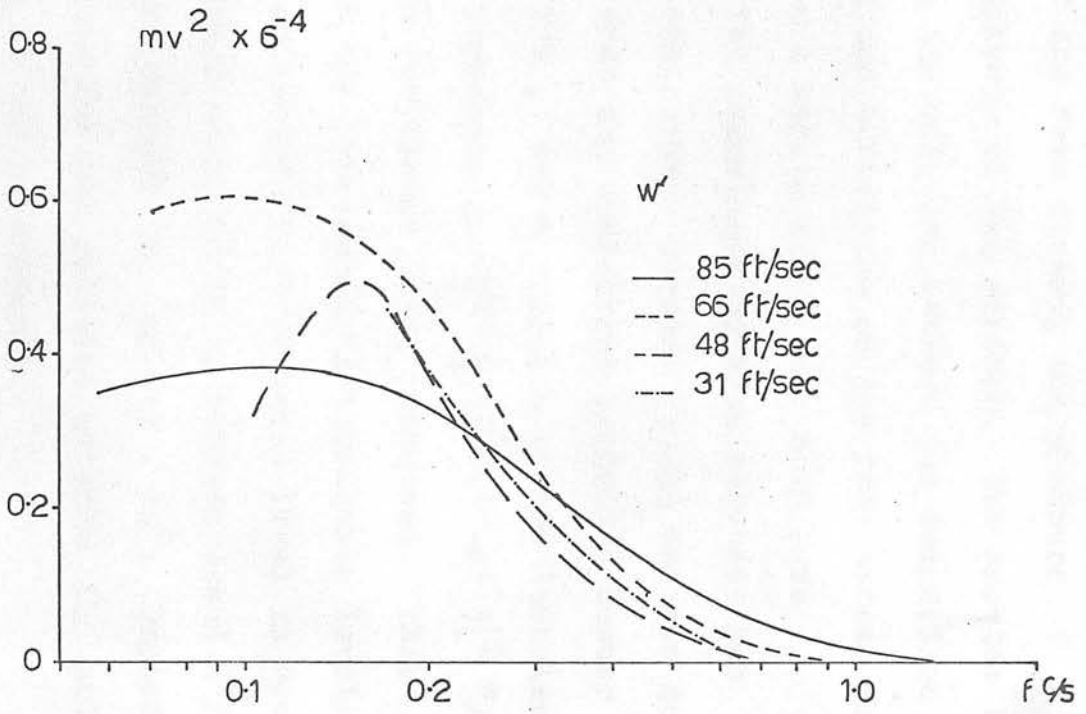

Figure VI.19 Reduced Spectra

CHAPTER VII

NATURAL TRANSITION OF THE BOUNDARY LAYER

VII.1 Introduction

The Reynold's Number for onset of transition to turbulence of the boundary layer on a flat plate is dependent on the turbulence of the free stream, the pressure gradient and the roughness of the surface. The problem to be discussed here is the relation between the transition Reynold's Number and the turbulence of the free stream for the boundary layer on a smooth flat plate with zero pressure gradient. The importance of this relation has been recognised for some time. Burgers (1924) and van der Hegge Zijnen showed that the transition Reynold's Number R_T, where $R_T = U_o x_T/\nu$, was a function of the turbulence of the free stream, expressed by $\frac{100}{U_o}\left[\frac{1}{3}(u'^2+v'^2+w'^2)\right]^{\frac{1}{2}}$ o/o, R_T decreasing as the turbulence level increased. They measured R_T but not the corresponding turbulence levels. Dryden (1936) later estimated the turbulence level in van der Hegge Zijnen's experiments as being between 1 and 2 o/o with the corresponding maximum R_T of $0.3 \cdot 10^6$. Dryden gave two sets of values for the relation between R_T and the turbulence level of the free stream.

$R_T \times 10^6$	Turbulence Level
1.1	0.5 o/o
0.1	3.0 o/o

The nature of the relationship between R_T and the free stream turbulence was, during the 1930's, open to argument. In Chapter 1 it was pointed out that there were two main views on the cause of turbulence in boundary layers. The theory due to Taylor gave a quantitative relationship between R_T and the turbulence level, whilst the Tollmein-Schlichting theory was unable to do this as it considered small disturbances only. Hall and Hislop (1938) made the first extensive study of the effect of free stream turbulence on R_T. They carried out their experiments in a low turbulence wind tunnel whose free stream turbulence was found to be non-isotropic. However Taylor's theory assumed isotropic turbulence. Hall and Hislop therefore created isotropic turbulence in the free stream by placing a square mesh screen upstream of the flat plate. By varying the dimensions of the screen they were able to vary the level of turbulence. Hall and Hislop came to the conclusion that a criterion for transition did exist and that it depended on the fluctuating pressure gradients in the turbulence of the free stream. It should be pointed out, however, that their results were for large levels of turbulence, that is, greater than $0.4^{o}/o$. When isotropic turbulence was not introduced into the free stream a maximum R_T of $2.35 \cdot 10^6$ was obtained (see Figure VII.1).

Schubauer and Skramstad (1947) investigated the relation between R_T and the free stream turbulence for low levels of turbulence in the range $0.02^{o}/o$ to $0.34^{o}/o$.

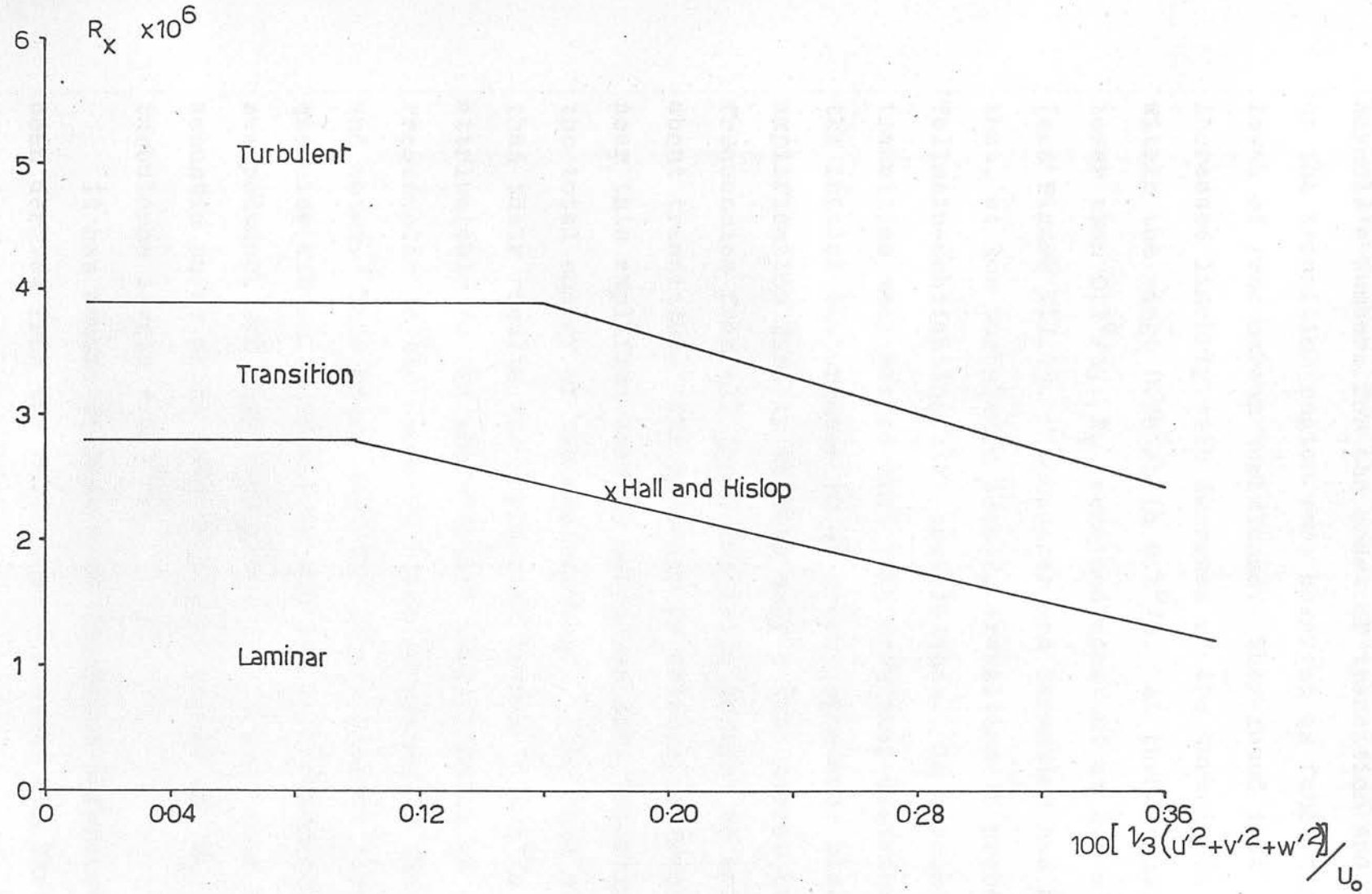

Figure VII.1 R_T as a function of the Turbulence Level (Schubauer and Skramstad)

Reynold's Numbers for the onset of transition and the end of the transition region were observed as functions of the level of free stream turbulence. They found that R_T increased linearly with decrease of the turbulence level within the range 0.34°/o to 0.1°/o. At turbulence levels lower than 0.1°/o, R_T remained constant at 2.8×10^6 (see Figure VII.1). Schubauer and Skramstad had shown that, at low turbulence levels, transition is preceded by Tollmein-Schlichting like oscillations. In discussing transition they stated that "the frequency distribution of the initial disturbance is of great importance since amplification finally selects only a very narrow band of frequencies from all those initially present to bring about transition. The presence or absence of frequencies near this amplified band is obviously more important than the total energy of the disturbance". They then suggested that their results for turbulence levels < 0.1°/o were attributable to the preferential amplification of certain frequencies in the acoustic noise generated by the fan and motor. They found that the intensities at these frequencies did not decrease as the total turbulence level was reduced, and they recognised that a reduction of acoustic noise might lead to higher values of R_T for turbulence levels < 0.1°/o.

It has become evident that incorrect inferences have been derived from the results of Schubauer and Skramstad. A number of authors have accepted the maximum R_T found

by Schubauer and Skramstad as a true maximum, implying that it was impossible to obtain higher values for R_T. Bradshaw and Pankhurst (1962), referring to Schubauer and Skramstad's graph of R_T against turbulence level, stated that "this graph has very frequently been used as an argument that 0.1°/o turbulence is "small enough", but it is difficult to see why transition Reymold's Numbers should not be increased indefinitely by reducing disturbances in the tunnel". They went on to say that "the most likely explanation of the National Bureau of Standards results is that lateral vibration of the test plate relative to the air stream determined the transition position when the tunnel turbulence was very low: either oscillations in the wake behind the test plate or mechanical vibration transmitted from the nearby fan could have been responsible". Bradshaw and Pankhurst have apparently rejected Schubauer and Skramstad's argument as to why a maximum R_T was found. Also their belief that R_T might be increased indefinitely is open to some doubt. Betchov and Szewczyk (1963) have suggested that there is a maximum upper limit for R_T, determined by the energy level of the Brownian motion of the fluid.

The present work is not concerned with a full investigation of the relation between R_T and the turbulence level. It was hoped that the results would give an indication of the tunnel's performance and also some information on the problems discussed above. The turbulence level was not altered, therefore, by varying the number of

smoothing screens or by introducing grids into the tunnel. Any variation in turbulence level was due to the different wind speeds at which R_T was found.

VII.2. Measurement of the Position of the Beginning of Natural Transition

The position of the beginning of natural transition of the boundary layer on a flat plate was found by traversing a surface pitot tube longitudinally down the centre line of the flat plate. The surface pitot tube was made of hypodermic tubing 0.028 inches outside diameter and 0.0165 inches inside diameter. The end of the tube was flattened so that the orifice was approximately oval shaped with axes 0.024 inches and 0.007 inches.

Traversing downstream, the pressure, which was measured using a sloping tube manometer, fell slowly due to boundary layer growth and then quickly rose due to the modification of the mean velocity profile of the boundary layer with the onset of transition to turbulence. The position of minimum pressure was taken as the point of onset of natural transition. It was found that transition could not be observed for wind speeds below 65 ft./sec., the 9 foot flat plate not being long enough. It was decided, therefore, to find the position of the beginning of natural transition for three wind speeds 65 ft./sec., 75 ft./sec. and 85 ft./sec.

The results are shown in Table VII,1, with the corresponding turbulence levels.

Table VII.1

Wind speed U_o ft./sec.	$R_T \times 10^6$	Total Turbulence Level Lower cut-off 8 c/s.
65	3.6 ± 0.1	$0.029 \pm 0.003\%$
75	3.5 ± 0.1	$0.037 \pm 0.004\%$
85	3.5 ± 0.1	$0.044 \pm 0.004\%$

VII.3. The Effect of Pressure Gradient

The three results for the position of onset of natural transition were found at wind speeds of 65 ft./sec., 75 ft./sec. and 85 ft./sec and x-positions of 8 feet 10 inches, 7 feet 5½ inches and 6 feet 7 inches respectively. From Figure IV.1 it will be seen that the third result was found at the end of the small stabilising pressure gradient. However, Figure VII.2 indicates that for large R and a Pohlhausen parameter of only + 0.8 the pressure gradient would have little, if any, effect on x_T. The second result was found at the end of a destabilising pressure gradient whose Pohlhausen parameter is approximately -4. The observed x_T is therefore probably too small. It is difficult to surmise the effect of the pressure gradient on the first result which was found with x_T in a strongly stabilising pressure gradient but immediately following a strongly destabilising gradient.

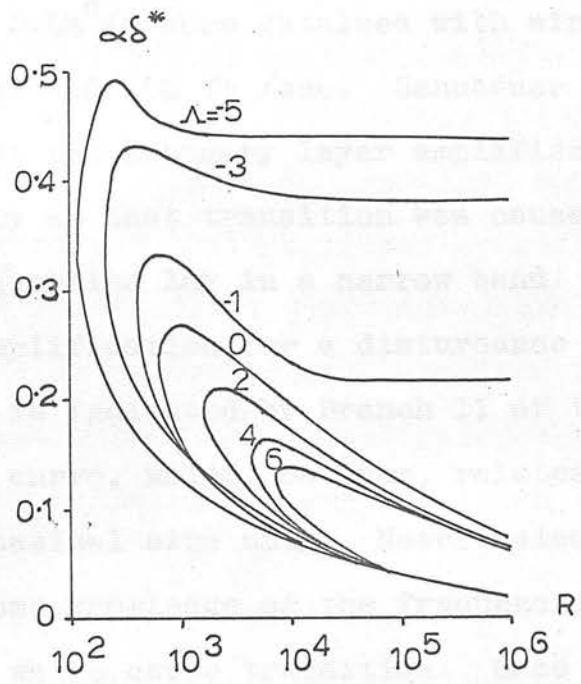

Figure VII.2 The effect of a Pressure Gradient on the Neutral Curve (Schlichting)

VII.4. Discussion of the Relationship between R_T and the Turbulence Level

The results of Schubauer and Skramstad for the relationship between R_T and the turbulence level have already been described in the Introduction. Figure VII.1 shows these results, with R_T remaining constant for turbulence levels $< 0.1^{o}/o$. The results for turbulence levels $< 0.04^{o}/o$ were obtained with wind speeds between 40 ft./sec. and 100 ft /sec. Schubauer and Skramstad showed that the boundary layer amplified the disturbances selectively so that transition was caused by disturbances whose frequencies lay in a narrow band. The position of maximum amplification for a disturbance of particular frequency is indicated by Branch II of the neutral stability curve, which, however, relates to disturbances of infinitesimal size only. Nevertheless it is possible to have some knowledge of the frequencies of the disturbances which cause transition. Once the disturbance has reached an amplitude which is no longer small according to linear theory, Klebanoff and Tidstrom (1958) have shown that the process to transition is rapid. It is assumed, therefore, that the position of onset of transition lies close to Branch II of the neutral stability curve. The frequencies of the disturbances which caused transition may then be calculated. The relevant frequencies for the results of Schubauer and Skramstad for turbulence levels $< 0.04^{o}/o$ lie between 50 c/s and 320

c/s for wind speeds between 40 ft./sec. and 100 ft./sec. respectively. Between these frequencies Schubauer and Skramstad found that a large part of the turbulence signal was attributable to acoustic noise and that the level of certain frequency bands was not reduced with decrease of the total turbulence level. They explained their results, therefore, by attributing the cause of transition to disturbances introduced by acoustic noise, when the turbulence level was $< 0.1\%$.

Bradshaw and Pankhurst have put forward another suggestion to explain why R_T remained constant for turbulence levels $< 0.1\%$. They suggested that transition was due to plate vibration caused by oscillations in the wake or by mechanical vibration from the nearby fan. Taneda (1958) has investigated the oscillations in the wake of a flat plate and has shown that

$$N\ell/U_o = \text{const} \left(U_o \ell / \nu \right)^{1/2}$$

for Reynold's Numbers up to $R = 10^5$. N is the frequency of the oscillations and ℓ is the length of the flat plate. If we assume that this relationship is valid beyond $R = 10^5$, then the oscillation frequencies in the wake behind the 12 foot long flat plate used by Schubauer and Skramstad were in the range 286 c/s. to 1,130 c/s. for the wind speed range of 40 ft./sec. to 100 ft./sec. Thus, for a given wind speed, the frequency of the plate vibration due to oscillations in the wake is very much greater than the frequency of the

disturbance thought to be causing transition. The mechanical vibration of a flat plate in the lateral direction is an extremely complex problem. The plate used by Schubauer and Skramstad was an aluminium sheet 12 feet long, 4½ feet wide and $^1/_4$ inch thick. The plate was bolted along its top and bottom edges to steel channels. Some estimate of the lower limit of the frequencies of the system is given by assuming it to be equal to the fundamental frequency of the transverse vibration. Assuming only transverse vibrations of the plate, it may be treated as a "Clamped - clamped" bar whose vibrational frequencies are $v_1 = 17.6$ c/s, $v_2 = 48.8$ c/s, $v_3 = 85.6$ c/s and so on (Morse (1948)). Thus, disturbances introduced by mechanical vibration of the flat plate very probably contributed to the disturbances which caused transition. It is interesting to point out that the disturbances introduced by the free stream turbulence and by the vibration of the plate do not necessarily reinforce each other. For disturbances of the same frequency, Wehrmann (1965) has shown that the lateral vibration of a flat plate can severely reduce the amplitude of a disturbance already present in the boundary layer.

The results presented here are for too small a range of turbulence level to reveal much of the nature of the relationship between R_T and the total turbulence level in the free stream. However, the importance of these results is that they show that transition Reynolds Numbers greater than $2.8 \cdot 10^6$ may be obtained. In fact,

the maximum R_T found by Schubauer and Skramstad is not an upper limit.

The frequency range of the disturbance causing transition in the present case is 130 c/s - 220 c/s for a wind speed range 65 ft./sec. to 85 ft./sec. The frequency range of the oscillations in the wake of the flat plate for the same wind speeds is 700 c/s - 1,000 c/s. Vibration of the plate due to these oscillations does not, therefore, affect transition of the boundary layer. The plate is 9 feet long, 4 feet wide and ½ inch thick and making the same analysis as previously the vibrational frequencies are $v_1 = 11.3$ c/s, $v_2 = 31.5$ c/s, $v_3 = 61.5$ c/s and so on. Vibration of the flat plate could contribute, therefore, to the disturbances causing transition. However, the results are over too small a range to give any evidence as to whether or not the values of R_T obtained are limited by this vibration.

Betchov and Szewczyk (1963) have suggested that there is a maximum upper limit for R_T, determined by the energy level of the Brownian motion of the fluid. Betchov (1964) has made some simplified calculations for a perfect gas, and has shown that the energy associated with the Brownian thermal motions is of the order 80 - 100 db below the level of turbulence. An estimate of the amount of amplification undergone by the disturbance, within the frequency range responsible for transition, can be made knowing R_T. Shen (1954) calculated the

amplification curves for small disturbances of different frequencies within the amplifying region of the neutral stability curve. The envelope of the system of curves was a straight line given by

$$\log (A/A_o)_{max} = 0.00327\ R - 1.75.$$

The amplification curves reported in Chapter VIII are in reasonable agreement with those predicted by Shen. It must be remembered that the amplification curves are valid for small disturbances only. The results of Chapter II indicate that the departure from linear theory occurs when u'/U_o is 1°/o and that the beginning of transition occurs approximately 8 inches downstream from departure. These results are in agreement with those of Klebanoff and Tidstrom (1959). For the present results, therefore, the estimated Reynolds Number at departure from linear theory is $3.3 \cdot 10^6$. The expected amplification is then $e^{8.06}$ from Shen's equation, that is, $3.2 \cdot 10^3$. Transition occurs when u'/U_o is approximately 10°/o so that the total amplification is $3.2 \cdot 10^4$, an energy gain of 90 dbs. The value of R_T obtained in this tunnel is therefore close to the suggested maximum possible R_T. It should be emphasised that the analysis is necessarily of an approximate nature.

VII.5. Conclusion

Results have been given which show a Reynolds Number, for natural transition of the boundary layer on a flat plate, 25°/o greater than the previous maximum transition Reynolds Number reported by Schubauer and Skramstad. It is estimated that this Reynolds Number lies close to the maximum permissible R_T suggested by Betchov and Szewczyk. It must be emphasised that the value of R_T depends on the frequency spectrum of the disturbances in the boundary layer. Although the relationship between the disturbances in the boundary layer and in the free stream is not known exactly, it has been assumed that a discussion of R_T as a function of the properties of the free stream turbulence is valid.

The early results of Chapter VI and the results of Chapter VII are contained in a paper reproduced in Appendix III.

CHAPTER VIII

THE NEUTRAL STABILITY CURVE AND THE GROWTH OF SMALL DISTURBANCES

1. Introduction

The development of the theory of small disturbances with especial reference to the stability of the boundary layer on a flat plate, has been described in Chapter I. An outline of the theory will now be given. The case to be considered is that of the two dimensional boundary layer on a flat plate which is subjected to a two dimensional disturbance. The disturbance is assumed to be small so that all quadratic terms in the fluctuating components may be neglected with respect to the linear terms. The mean velocities of the flow U and V are assumed to be a function of y only and zero respectively, and the pressure is assumed to be a function of x and y. The mean flow therefore has

$$U(y), \quad V = 0 \quad \text{and} \quad P(x,y) .$$

The two dimensional disturbance superimposed on the mean flow is a function of time as well as space and its velocity components and pressure are given by

$$u'(x,y,t), \quad v'(x,y,t), \quad p'(x,y,t) .$$

The resultant motion is therefore described by

$$u = U + u', \qquad v = v', \qquad p = P + p' \quad .$$

If both the resultant motion and the mean motion satisfy the Navier-Stokes equations we find that

$$\begin{aligned} \frac{\partial u'}{\partial t} + U \frac{\partial u'}{\partial x} + v' \frac{dU}{dy} + \frac{1}{\rho} \frac{\partial p'}{\partial x} &= \nabla^2 u' \\ \frac{\partial v'}{\partial t} + U \frac{\partial v'}{\partial x} + \frac{1}{\rho} \frac{\partial p'}{\partial y} &= \nabla^2 v' \end{aligned} \qquad (1)$$

The disturbance must satisfy the equation of continuity, so that

$$\frac{\partial u'}{\partial x} + \frac{\partial v'}{\partial y} = 0 \qquad (2)$$

The disturbance is assumed to be composed of a number of discrete partial fluctuations and as it is two dimensional it can be represented by a stream function $\psi(x,y,t)$. The stream function which represents a single oscillation of the disturbance is assumed to be of the form

$$\psi(x,y,t) = \phi(y)\, e^{i\alpha(x-ct)} \quad ,$$

where α is the wave number of the disturbance and c is complex, $c = c_r + ic_i$, where c_r is the phase velocity of the wave and c_i determines the degree of amplification, or damping with time. Making α real and c complex results in the wave amplifying with time and not distance. The components of the disturbance are

$$u' = \frac{\partial \psi}{\partial y} = \phi'(y) e^{i\alpha(x-ct)}$$
$$v' = \frac{\partial \psi}{\partial x} = -i\alpha\, \phi(y) e^{i\alpha(x-ct)} \qquad (3)$$

Substituting these values into equation (1) and eliminating the pressure terms gives

$$(U-c)(\phi'' - \alpha^2 \phi) - U''\, \phi = -\frac{i}{\alpha} (\phi'''' - 2\alpha^2 \phi'' + \alpha^4 \phi) \qquad (4)$$

By expressing lengths and velocities non-dimensionally in terms of ∂ and U_o equation (4) becomes

$$(U-c)(\phi'' - \alpha^2 \phi) - U''\, \phi = -\frac{i}{\alpha R} (\phi'''' - 2\alpha^2 \phi'' + \alpha^4 \phi) \qquad (5)$$

The boundary conditions are

$$y = 0 \;:\; u' = v' = 0 \;:\; \phi = 0, \quad \phi' = 0$$
$$y = \infty \;:\; u' = v' = 0 \;:\; \phi = 0, \quad \phi' = 0 \qquad (6)$$

Equation (5) with the boundary conditions (6) gives one eigenfunction $\phi(y)$ and one eigenvalue c for each pair of values α and R.

Tollmein (1929) solved equation (5) and defined the neutral stability curve where $c_i = 0$. Lin (1945) reproduced Tollmein's neutral curve and Shen (1954), following the same procedure used by Lin, calculated curves of constant amplification within the amplifying region of the neutral stability curve. Shen's neutral

curve is shown in Figure VIII.1 compared with the experimental results of Schubauer and Skramstad. Osborne has recalculated the neutral curve and the amplification curves and for the latter case he predicted the damping of a disturbance outside the neutral curve.

2. Amplification of a Small Disturbance

The amplification curves calculated by Shen and Osborne are expressed as curves of $\log (A/A_o)$ against R for periodic disturbances of constant $F = \beta_r \nu / U_o^2$ where β_r is the angular frequency of the disturbance, ν is the kinematic viscosity, U_o the wind speed in the free stream, A the amplitude of the disturbance and A_o the amplitude at Branch I of the neutral curve. Choosing both a wind speed and a frequency of the injected disturbance fixed the value of F. The variation of the amplitude of the disturbance with Reynolds Number was then found by tracking a hot-wire along the centre of the plate downstream from the ribbon. No measurements were taken within 3 inches of the ribbon. The wire was positioned in the boundary layer so that it measured the maximum disturbance amplitude, that is its position was close to $y/\delta = 0.2$. It was then moved downstream at a constant y/δ position; the wire resistance therefore remained constant. This mode of operation meant that A/A_o was equal to e/e_o where e was the r.m.s. output from the wire measured by the

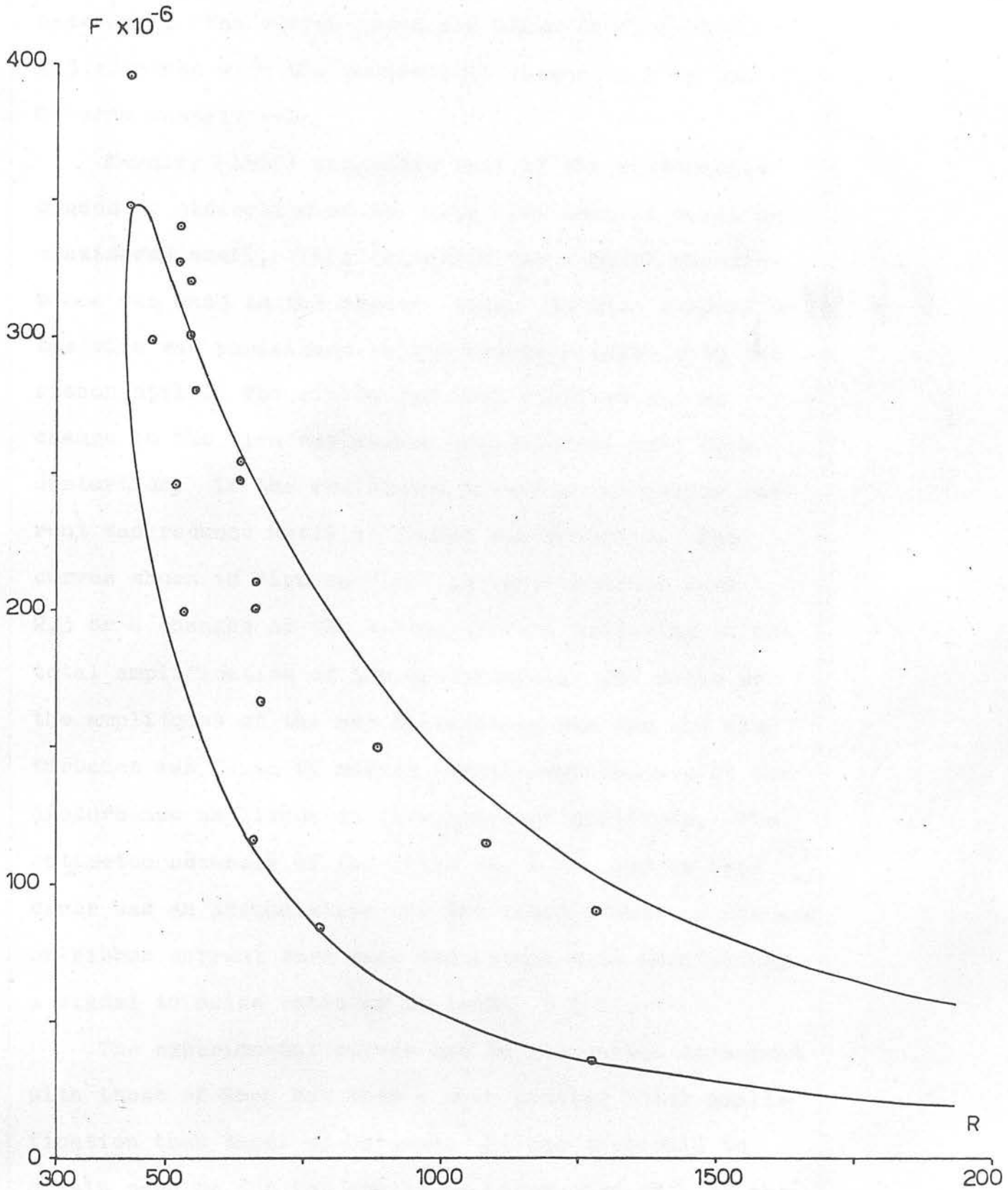

Figure VIII.1 Shen's Neutral Curve compared with the Results of Schubauer and Skramstad

frequency analyser, and calibration of the wire was unnecessary. The curves found are shown in Figures VII 2,3 compared with the theoretical curves of Shen and Osborne respectively.

Kersley (1965) suggested that if the disturbance caused no distortion of the mean flow then it could be considered small. This criterion for a small disturbance was used in the present case. At each x-position the wire was positioned in the boundary layer with the ribbon still. The ribbon was then vibrated and no change in the wire resistance indicated no mean flow distortion. If the resistance altered, the ribbon current was reduced until no change was detected. The curves shown in Figures VIII 2,3 were obtained with 2,3 or 4 changes of the ribbon current depending on the total amplification of the disturbance. The ratio of the amplitudes of the new disturbance and the old disturbance was found by making repeat measurements of the disturbance amplitude at five previous positions. The estimated accuracy of the ratio was $\pm$ 3% and as this error was an accumulative one the least number of changes of ribbon current were made consistent with maintaining a signal to noise ratio of at least 5 : 1 .

The experimental curves are in reasonable agreement with those of Shen but show a much greater total amplification than those of Osborne. It was difficult to obtain results for the amplitude before Branch I of the

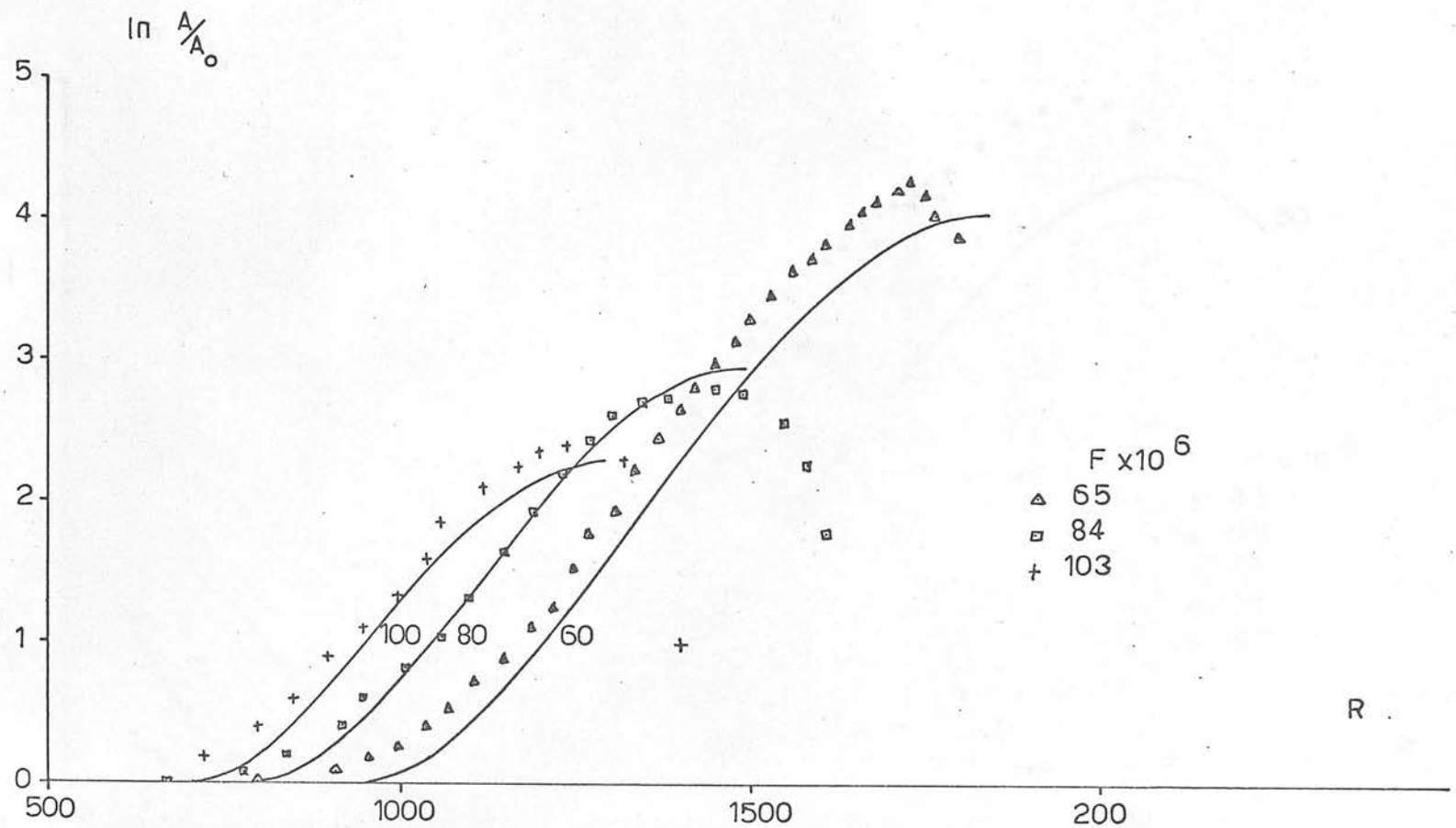

Figure VII.2 Growth Curves compared with Shen's Curves

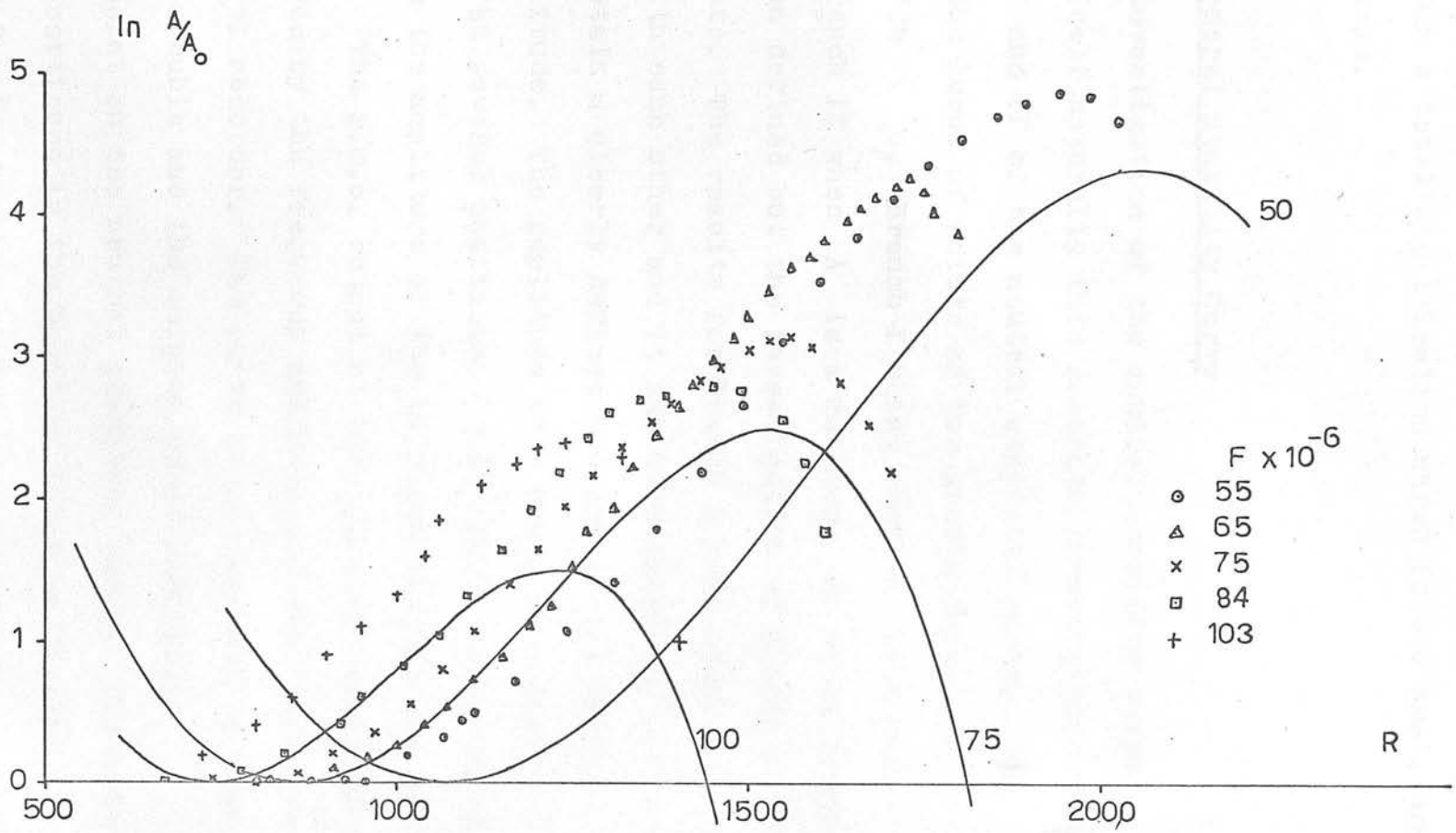

Figure VIII.3 Growth Curves compared with Osborne's Curves

neutral curve. However, any error in the definition of A_o will mean a total amplification which is too small and not too large.

3. The Neutral Stability Curve

The investigation of the neutral stability curve divided itself naturally into separate investigations of Branches I and II of the neutral stability curve. The curve is the locus of points on the growth curves for which $dA/dR = 0$, Branch I being when A is a minimum and Branch II when A is a maximum. To date, Branch II has been defined but the investigation of Branch I is not complete. The results for Branch I have been inconsistent with each other and it has been extremely difficult to obtain a clearly defined minimum in the disturbance amplitude. The amplitude of a small disturbance was found at several positions (≥ 6) about the neutral curve with the amplitude of the injected disturbance kept constant. The r.m.s. output at the injected frequency was measured by the frequency analyser and also recorded by the level recorder. The curve of e against x was fitted to a cubic and the turning point found, thus giving a point on the neutral stability curve. The hot-wire was positioned in the boundary layer as it was positioned for the work described in the previous section.

A new criterion for a small disturbance was used

for this work. Lin (1945) stated that "the disturbance is small in the sense that its behaviour is unaltered when its amplitude is (say) doubled or halved". The disturbance in the boundary layer was tested by attenuating the injected disturbance by ± 5db. using a set of attenuators in the ribbon circuit, see Chapter V. The r.m.s. output of the hot-wire was recorded with and without the attenuation of the injected disturbance by the level recorder. It was found that for a small disturbance the amplification in the boundary layer was independent of the amplitude of the disturbance to within about ± 3%.

The results for Branch II of the neutral stability curve are shown in Figures VIII 4,5 compared with the theoretical curves of Shen and Osborne and in Figure VIII 6 compared with the results of Schubauer and Skramstad. The error in the measurement of x has been discussed in Chapter III and was less than ± 0.3%. The error in e as measured from the recording produced by the level recorder was ± 2%. A cubic curve was therefore fitted to the values of e and x assuming no error in x. The turning point of the curve was found and hence a pair of values, F and R, for Branch II was determined. The error in the x-position of the maximum in e was estimated using the standard deviation of the fitted cubic curve and the error in R was then calculated. The error in F was also estimated and was found to

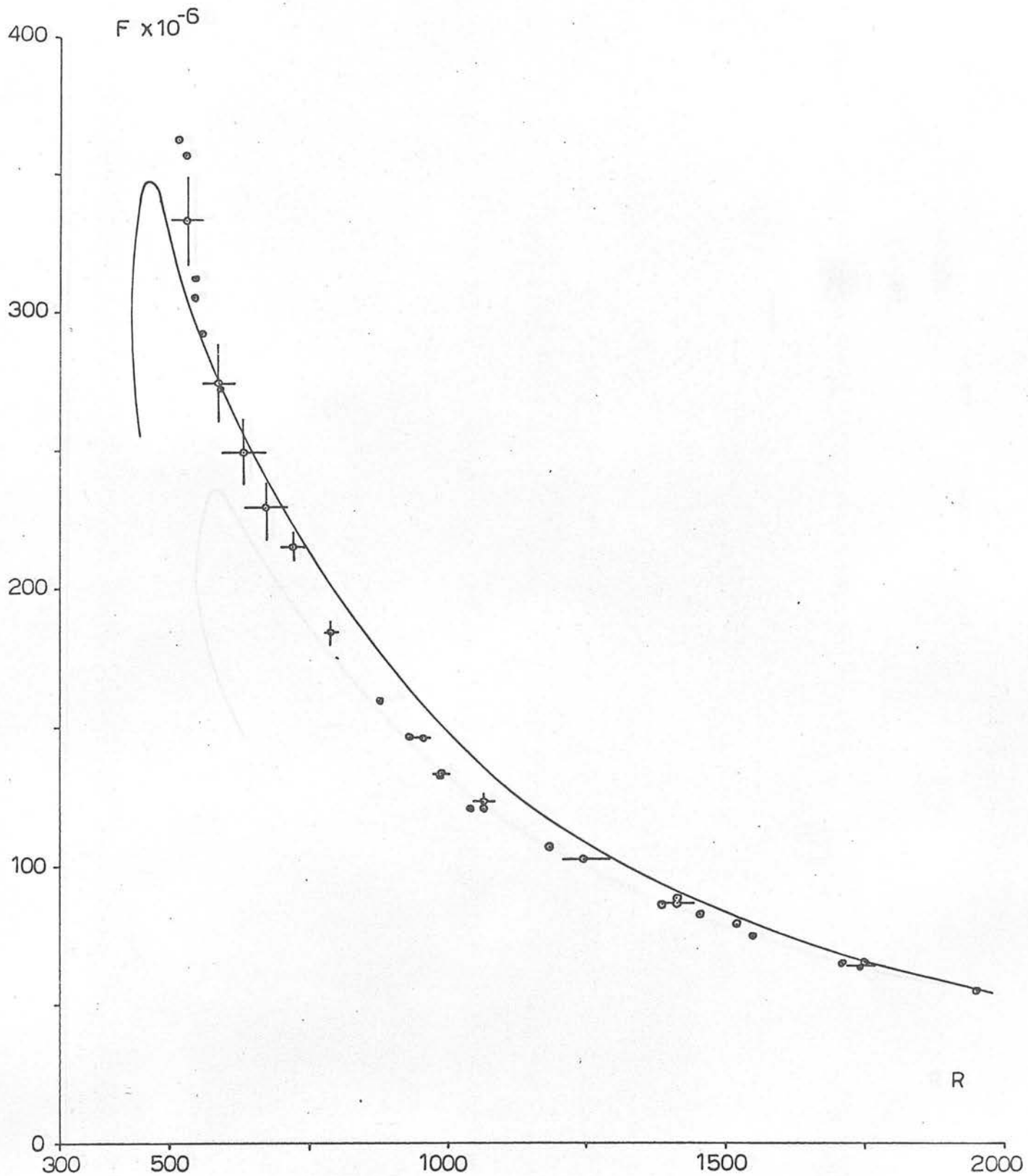

Figure VIII.4 Branch II compared with Shen's Result

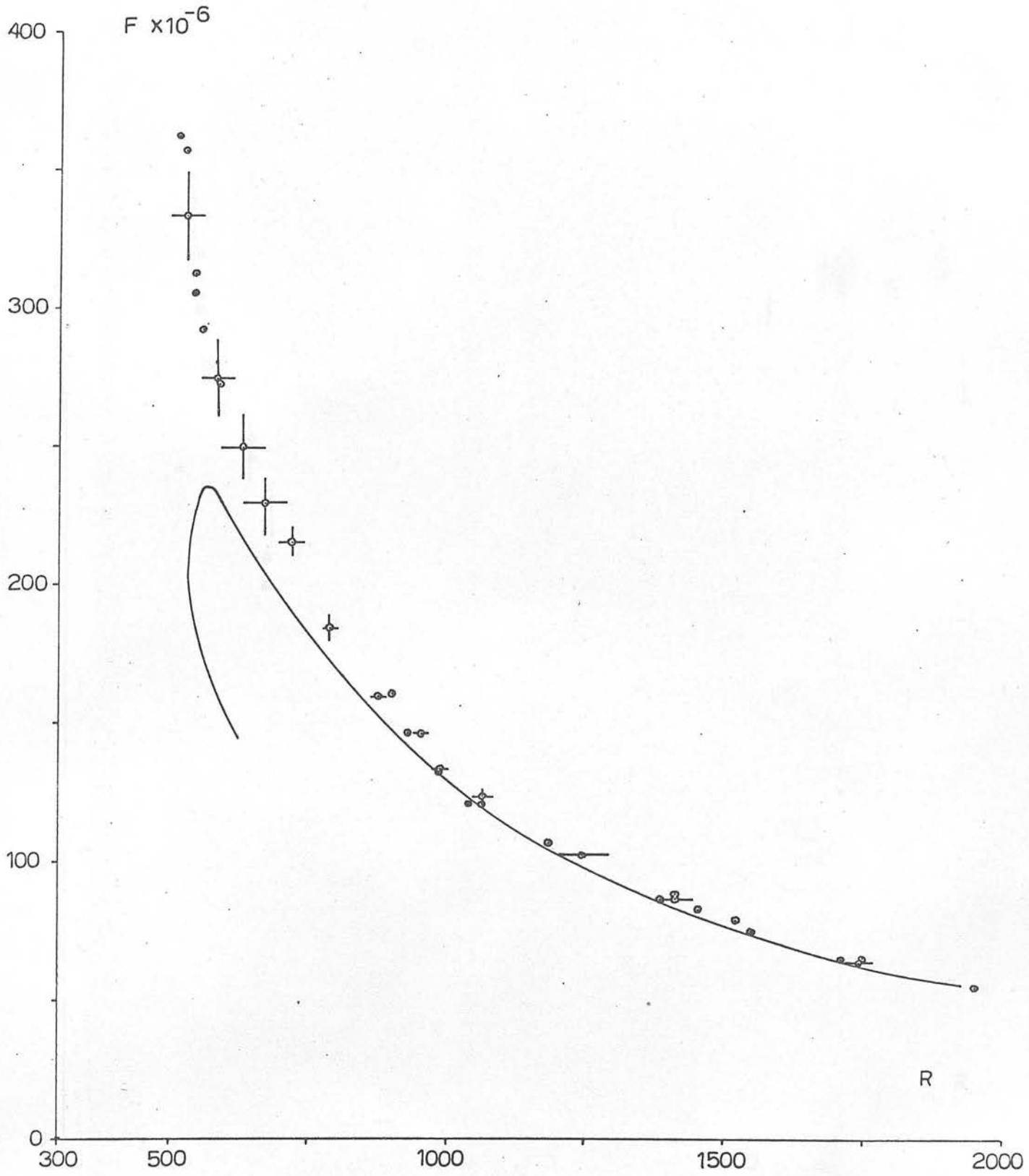

Figure VIII.5 Branch II compared with Osborne's Result

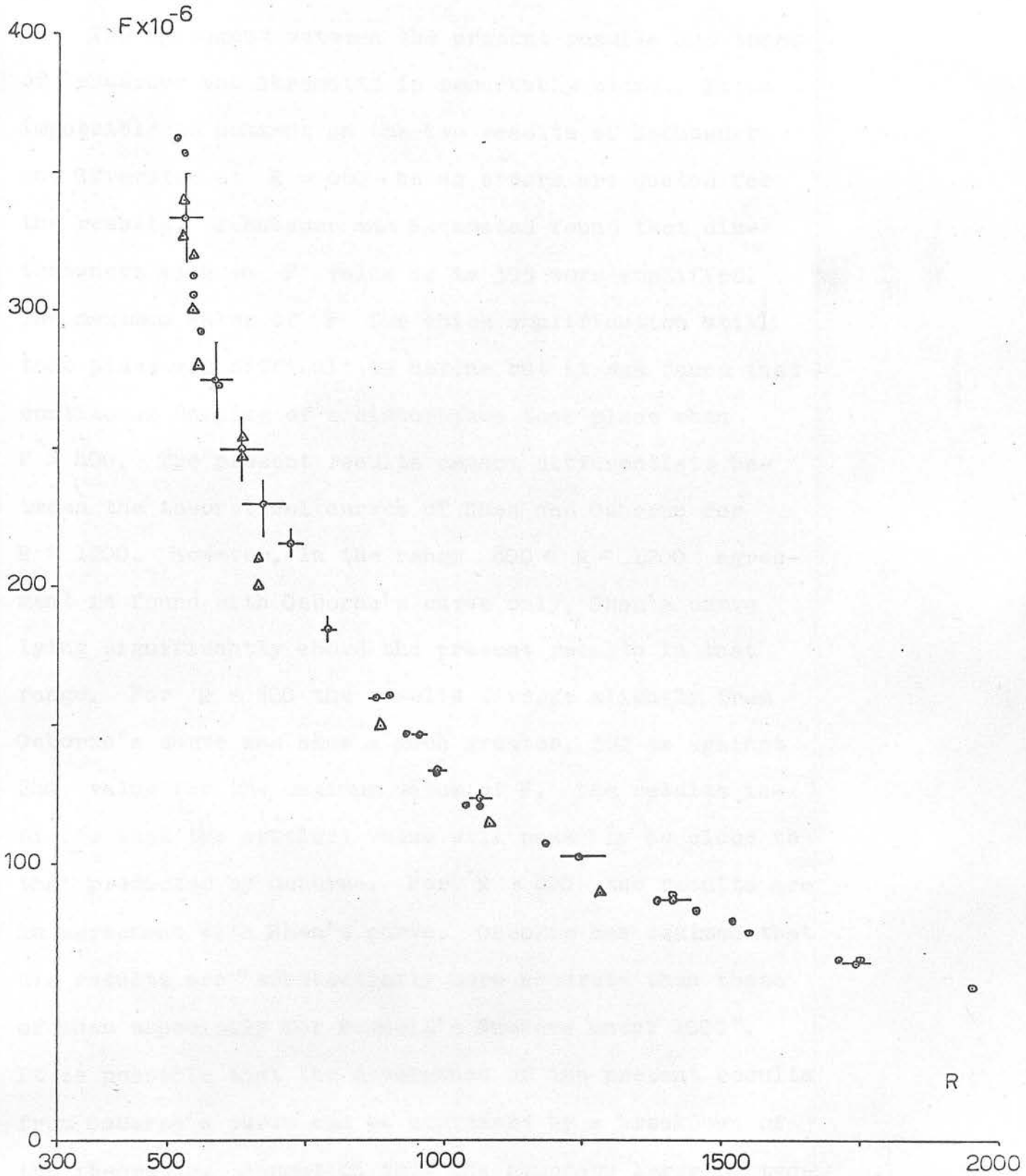

Figure VIII.6 Branch II, the present Results compared with those of Schubauer and Skramstad

be mainly due to the error in U_o particularly for low Reynold's Numbers.

The agreement between the present results and those of Schubauer and Skramstad is remarkably close. It is impossible to comment on the two results of Schubauer and Skramstad at $R = 660$ as no errors are quoted for the results. Schubauer and Skramstad found that disturbances with an F value up to 395 were amplified. The maximum value of F for which amplification still took place was difficult to define but it was found that continuous damping of a disturbance took place when $F > 400$. The present results cannot differentiate between the theoretical curves of Shen and Osborne for $R > 1200$. However, in the range $800 < R < 1200$ agreement is found with Osborne's curve only, Shen's curve lying significantly above the present results in that range. For $R < 800$ the results diverge slightly from Osborne's curve and show a much greater, 360 as against 240, value for the maximum value of F. The results indicate that the critical value will possibly be close to that predicted by Osborne. For $R < 800$ the results are in agreement with Shen's curve. Osborne has claimed that his results are "substantially more accurate than those of Shen especially for Reynold's Numbers under 1000". It is possible that the divergence of the present results from Osborne's curve can be explained by a breakdown of the theoretical assumption that the boundary layer is two-

dimensional. This objection to the theory was first raised by Taylor and it is probable that the assumption is not valid for low Reynold's Numbers.

A description has been given of the criteria used to define a small disturbance. Kersley (1965) concluded that with the ribbon system described in Chapter V the injected disturbance was two-dimensional over a two inch region about the centre of the vibrating span of the ribbon. An investigation of the mean flow at a constant distance from the plate was therefore made over that span at $x = 4$ feet 6 inches and with a wind speed of 60 ft./sec. It was found that at a mean position of $y/\delta = 0.44$ the variations in the mean flow were approximately $\pm 1\%$. None of the measurements described here were made beyond $x = 6$ feet. Three results for the neutral stability curve, at $F = 55.1$, 64.4 and 75.6, were obtained with the x-position of the maximum in the disturbance amplitude within the region of the small stabilising pressure gradient (see Chapter IV). All the other results for the neutral curve were obtained in the region where the pressure gradient was effectively zero. The experimental arrangement was therefore a good approximation to the theoretical model described in Section 1.

The locus of the points on Branch II of the neutral curve was evidently a smooth curve. It was convenient, to obtain a representation of the curve, to fit polynomials of various orders to the experimental points.

The process was taken to the fifth order polynomial which gave only a marginally better fit than the fourth order polynomial. The fifth order polynomial gave

$$F.10^{6} = 2,125 - 7,230.10^{-3}R + 10,803.10^{-6}R^{2} - 8,177.10^{-9}R^{3} + 3,067.10^{-12}R^{4} - 453.10^{-15}R^{5} .$$

It is realised that this polynomial was found assuming no error in R and also attaching equal weight to all the points.

The experimental results for Branch II of the neutral curve are given in the following table.

TABLE VIII.1

R	$F.10^{-6}$	R	$F.10^{-6}$
514	364	987	135
533	358	986	134
528	334	1065	124
543	313	1066	122
543	306	1038	121
559	293	1184	108
585	275	1245	103
589	274	1413	88
629	251	1413	87
667	231	1386	86
718	216	1451	83
788	185	1522	80
901	161	1549	76
876	160	1748	66
952	148	1711	65
928	147	1949	55

4. Suggestions for Further Work

Results for Branch I of the neutral curve would be of great interest when compared with the results described in Chapter VIII.

The effect of a disturbance in the free stream is, at the moment, a matter of conjecture. It is suggested that an experiment which showed how and when a disturbance was taken up by a boundary layer would help to explain how natural transition to turbulence of a boundary layer occurs.

Klebanoff, Tidstrom and Sargent have suggested that the boundary layer necessarily becomes three-dimensional before transition occurs. A complete investigation of the mean flow of the boundary layer in the present tunnel would give information on the above suggestion. For a nominally small disturbance, it is necessary to investigate its effect, if any, on the mean flow of a boundary layer. Small disturbance theory assumes no such effect. For a disturbance no longer small, a further investigation of the harmonic production of a disturbance would be of interest, especially if an attempt were made to explain the large growth of second harmonic at $y/\delta = 0.3$.

APPENDIX I

CONTROL AND MEASURING EQUIPMENT

A brief description is given here of the control and measuring equipment.

A.I.1. The Data Logger

Figure A.I.1. shows a block diagram of the data logger.

The basic ranges of the D.C. Digital Voltmeter are given in Table A.I.1.

Range	Input Resistance	Sensitivity
0-20 mv	50 M	10 μv
0-200 mv	500 M	100 μv
0-2 v	5000 M	1 mv
0-20 v	10 M	10 mv
0-200 v	10 M	100 mv

The voltmeter had an accuracy of $\pm$ 0.05°/o of range or $\pm$ 1 digit, and the sensitivity could be increased by multiplying the range by two or four. The input signals were sent to the Command Range Unit and the range and multiplication used was determined by the plugging arrangement of the system patchboard. The Scanner scanned up to twenty channels in a variety of modes and its speeds were 3, 2 and 1 channel/sec. and 1 channel every 2 seconds. Signals which indicated the channel number were generated by the system in coincidence with the channel scanning. The Punch encoder drove a Creed

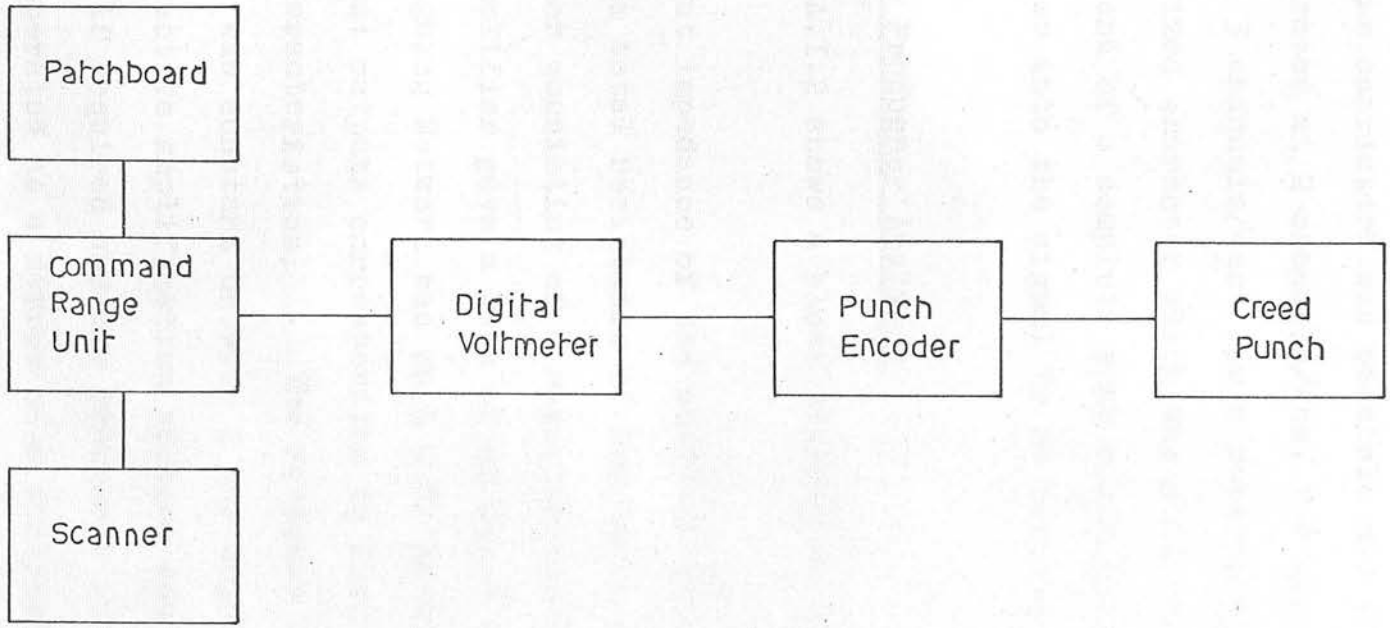

Figure AI.1 The Data Logger

Model 25 Paper Tape Punch Machine and received signals from the voltmeter which represented the channel identity, the signal reading (4 digits), and the voltmeter range, multiplication and polarity. A maximum word length of nine characters was possible and the scanner could be operated at 2 channels/sec. for the full word length or at 3 channels/sec. for a restricted word length. A fixed character which was able to change its form at the end of a complete scan could be introduced by the encoder into the signal to be punched.

A.I.2. The Frequency Analyser

Figure A.I.2 shows a block diagram of the frequency analyser.

The input impedance of the analyser was 2.22 M Ω which was the total resistance of the input attenuator, the attenuator consisting of 6 resistors and 4 capacitors. The input Amplifier gave a gain of 40 db. $\pm$ 2 db.

The Weighing Network was an L C.R. network and gave five different outputs corresponding to five different frequency characteristics. The response used in the present case was constant between 2 and 40,000 c/s.

The Selective Amplification section could be switched in if required and for frequency analysis the instrument operated as a narrow band analyser with a frequency range 20 - 20,000 c/s. A number of frequency characteristics were available, which were:

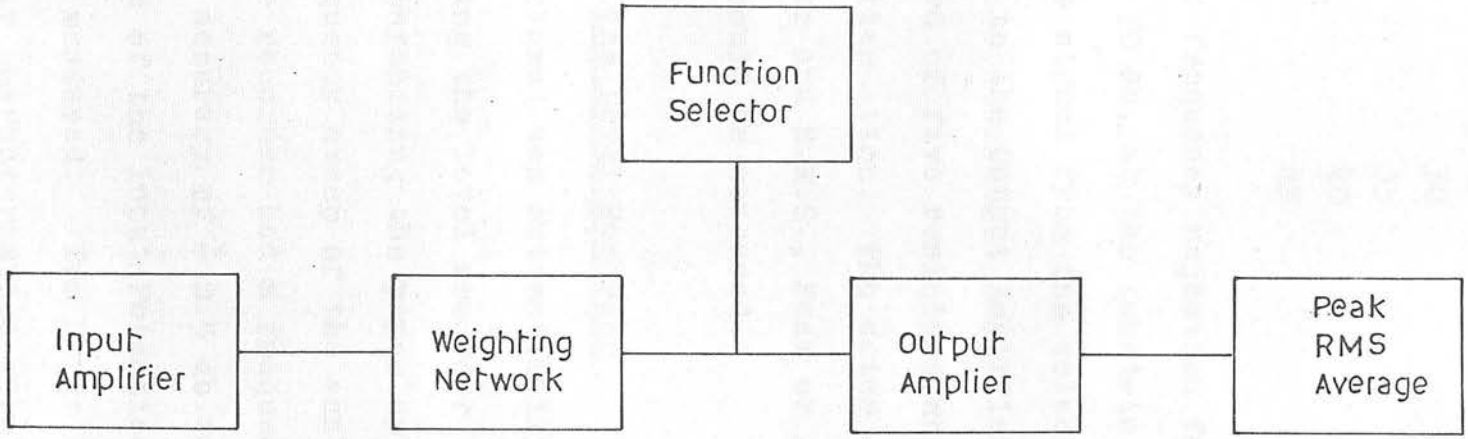

Figure AI.2 The Frequency Analyser

TABLE A.I.2

Octave Selectivity in db.	3 db Bandwidth °/o.
20	29
25	21
30	16
35	12
40	8.5
45	6

The frequency rejection facility allowed an attenuation of 70 db. at the tuned-in frequency.

The signal from the selective amplification section was fed to the Output Amplifier via an attenuator which consisted of five resistors which gave five steps of 10 db attenuation. The meter circuit followed the output amplifier and R.M.S., Peak or Arithmetic Average of the signal could be measured.

A.I.3 The Level Recorder

A signal was automatically frequency analysed by connecting the level recorder to the frequency analyser and synchronising the paper speed of the recorder with the frequency sweep of the analyser.

The recorder had a frequency range 2 - 200,000 c/s with an accuracy of $\pm$ 0.5 db to $\pm$ 1 db dependent on the position of the Input Potentiometer. D.C. levels could also be measured. Two Range Potentiometers were used and their characteristics were:

TABLE A.1.3

Range	Accuracy
10-110 mv Linear	± 0.1 db.
50 db Logarithmic	± 0.3 db

The input impedance was 16 - 18 kΩ dependent on the input potentiometer which had a continuously variable range of 0 - 12 db. The Input Attenuator had a range of 60 db. in 6 equal steps and was accurate to ± 0.25 db. RMS, Arithmetic Average or Peak of the signal could be recorded and the accuracy of the RMS level was ± 0.5 db. for crest factors up to 5. A number of writing speeds was available between 4 and 2000 mm/sec. The available paper speeds lay between 0.0003 and 100 mm/sec. and the lower limiting frequency could be selected to be 2, 10, 20, 50 and 200 c/s.

A.I.4. The Frequency Meter

The frequency meter measured the frequency and period of input signals up to 1.1 c/s and measured time intervals from 1 μsec. to 10^7 seconds. The accuracy of the frequency measurement was ± 1 count and the gating times were 0.1, 1.0 or 10.0 secs. The input impedance was 250 kΩ . For period measurement the accuracy was ± 1 μsec. and the gating period was from 1 to 10^7 cycles of the input frequency.

A.I.5. The Emidata System

The bandwidth of the system ($\pm$ 0.25 db) was d.c. - 1.5 Kc/s at 7½ in./sec. and d.c. - 6 Kc/s at 30 in/sec.

On the record side the signal was first amplified (approximately × 5) and then passed to the modulator. The modulator was essentially a multivibrator whose frequency of oscillation varied linearly with the input voltage. The frequency of the multivibrator at zero voltage input was 1 Kc/s per in./sec. tape speed. The modulator was followed by a circuit suitable for driving a magnetic recording head. The maximum frequency band was $\pm 33\frac{1}{3}$ °/o of the carrier frequency and the dynamic range was 40 db.

On the replay side the signal from the replay head was amplified and then demodulated. A filter removed the carrier frequency.

The harmonic distortion of the system was less than 1°/o.

APPENDIX II

THE PROGRAM

The program used for the reduction of the hot-wire results was a data directed program developed by Dr. Burns. The program used the following dictionary and routines

ROUTINES

eta : evaluates ν [T,p]

U_o : evaluates U_o [T,p, manometer]

readname

printname

polyfit

check devn. : inspects to see if deviation of a point is $\geq$ 2 (say) standard deviations

reduce traverse data : alternative modes of operation

reduce delta data

calibrate : calibrate hot wire

read data

graph : graph of output

locate turn

MAP : contour map of output

DICTIONARY

TRAV DELTA FREE BDRY CALB CON LAYER WIRE END TOTAL SIGNAL 1st HARM 2nd 3rd GRAPH DATA TEMP PRES CHAT BETZ MAP XCAL YCAL ZCAL.

An example showing how the program works is given in the flow diagram Figure AII.1.

TYPICAL FLOW CHART OF DATA REDUCING PROGRAM.

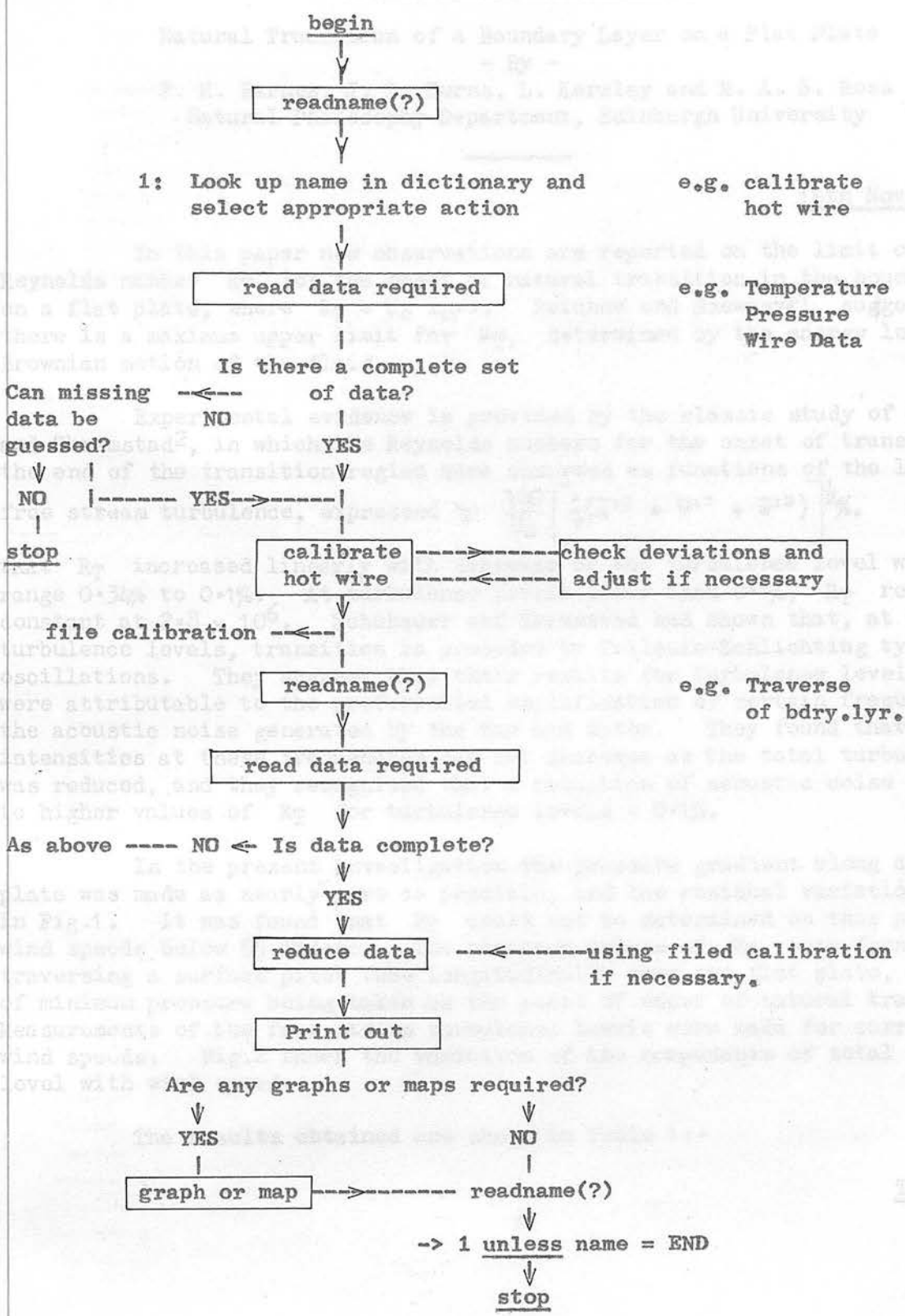

Figure A.II.1 The Program.

APPENDIX III

A.R.C.27 445 AERONAUTICAL RESEARCH COUNCIL A.R.C.27 445

F.M.3662 FLUID MOTION SUB-COMMITTEE F.M.3662

Natural Transition of a Boundary Layer on a Flat Plate

- By -

F. H. Barnes, J. G. Burns, L. Kersley and M. A. S. Ross

Natural Philosophy Department, Edinburgh University

15th November, 1965

In this paper new observations are reported on the limit of Reynolds number R_T for the onset of natural transition in the boundary layer on a flat plate, where $R_T = U_o x_T/\nu$. Betchov and Szewczyk[1], suggest that there is a maximum upper limit for R_T, determined by the energy level of the Brownian motion of the fluid.

Experimental evidence is provided by the classic study of Schubauer and Skramstad[2], in which the Reynolds numbers for the onset of transition and the end of the transition region were observed as functions of the level of free stream turbulence, expressed by $\frac{100}{U_o}\left[\frac{1}{3}(\overline{u}'^2 + \overline{v}'^2 + \overline{w}'^2)\right]^{\frac{1}{2}}\%$. They found that R_T increased linearly with decrease of the turbulence level within the range 0·34% to 0·1%. At turbulence levels lower than 0·1%, R_T remained constant at $2{\cdot}8 \times 10^6$. Schubauer and Skramstad had shown that, at low turbulence levels, transition is preceded by Tollmein-Schlichting type oscillations. They suggest that their results for turbulence levels < 0·1% were attributable to the preferential amplification of certain frequencies in the acoustic noise generated by the fan and motor. They found that the intensities at these frequencies did not decrease as the total turbulence level was reduced, and they recognised that a reduction of acoustic noise might lead to higher values of R_T for turbulence levels < 0·1%.

In the present investigation the pressure gradient along a 9 ft flat plate was made as nearly zero as possible, and the residual variations are shown in Fig.1. It was found that R_T could not be determined on this plate for wind speeds below 65 ft/sec. The observed values of R_T were found by traversing a surface pitot tube longitudinally down the flat plate, the position of minimum pressure being taken as the point of onset of natural transition. Measurements of the free stream turbulence levels were made for corresponding wind speeds. Fig.2 shows the variation of the components of total turbulence level with wind speed.

The results obtained are shown in Table 1:-

Table 1/

Table 1

Wind Speed U_o (ft/sec)	$R_T \times 10^6$	Total Turbulence Level $\frac{100}{U_o}\left[\frac{1}{3}(\overline{u'^2}+\overline{v'^2}+\overline{w'^2})\right]^{\frac{1}{2}}\%$
65	3·6 ± 0·1	0·027 ± 0·003%
75	3·5 ± 0·1	0·035 ± 0·004%
85	3·5 ± 0·1	0·042 ± 0·004%

These values of R_T are about 25% greater than those found by Schubauer and Skramstad.

In view of the discussion by Schubauer and Skramstad of the part played by acoustic noise, an analysis of this noise was made. It was found that the total noise level, 80 db in the bandwidth 2 c/sec to 20 Kc/sec, was only about 7% of the total turbulence level, but, when the spectrum of the noise was examined it was found that, in the frequency range which Tollmein-Schlichting theory suggests is most amplified at $R \simeq 3{\cdot}0 \times 10^6$, the acoustic and turbulence amplitudes were comparable.

We conclude that if a value of R_T approximating more closely to the Brownian motion limit is to be obtained, close attention must be paid to the acoustic perturbations which are subject to selective amplification.

This work was carried out in the 4 ft low-turbulence wind tunnel at Edinburgh University. The tunnel and its flow characteristics are described in a paper by Burns et al.[3]

References

No.	Author(s)	Title, etc.
1	R. Betchov and A. Szewczyk	Phys. Fluids 6 (10), 1391 (1963).
2	G. B. Schubauer and H. K. Skramstad	J. Res. Nat. Bur. Stand. 38, 251 (1947).
3	J. G. Burns and M. A. S. Ross	To be published.

DH

Fig 1 27 445

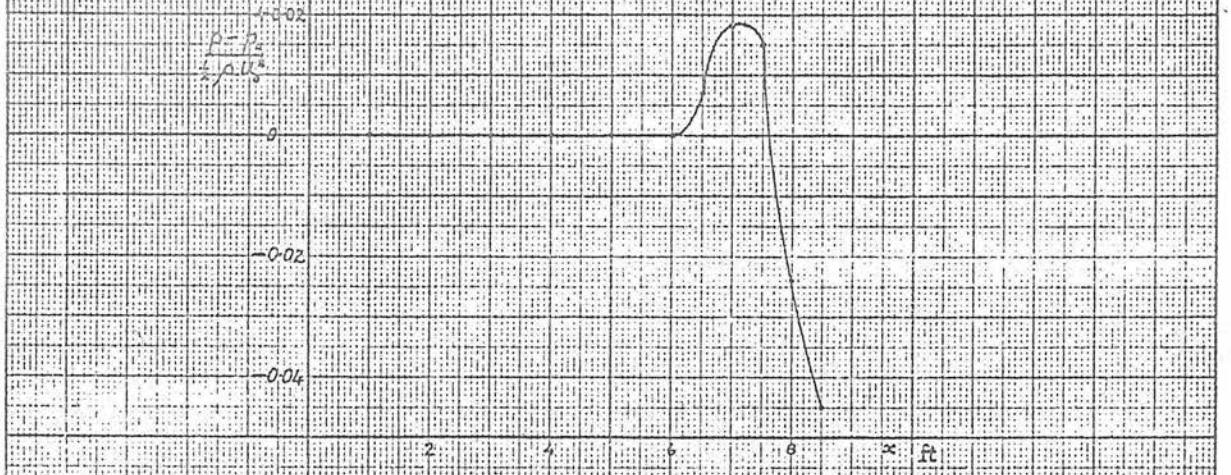

Fig 2

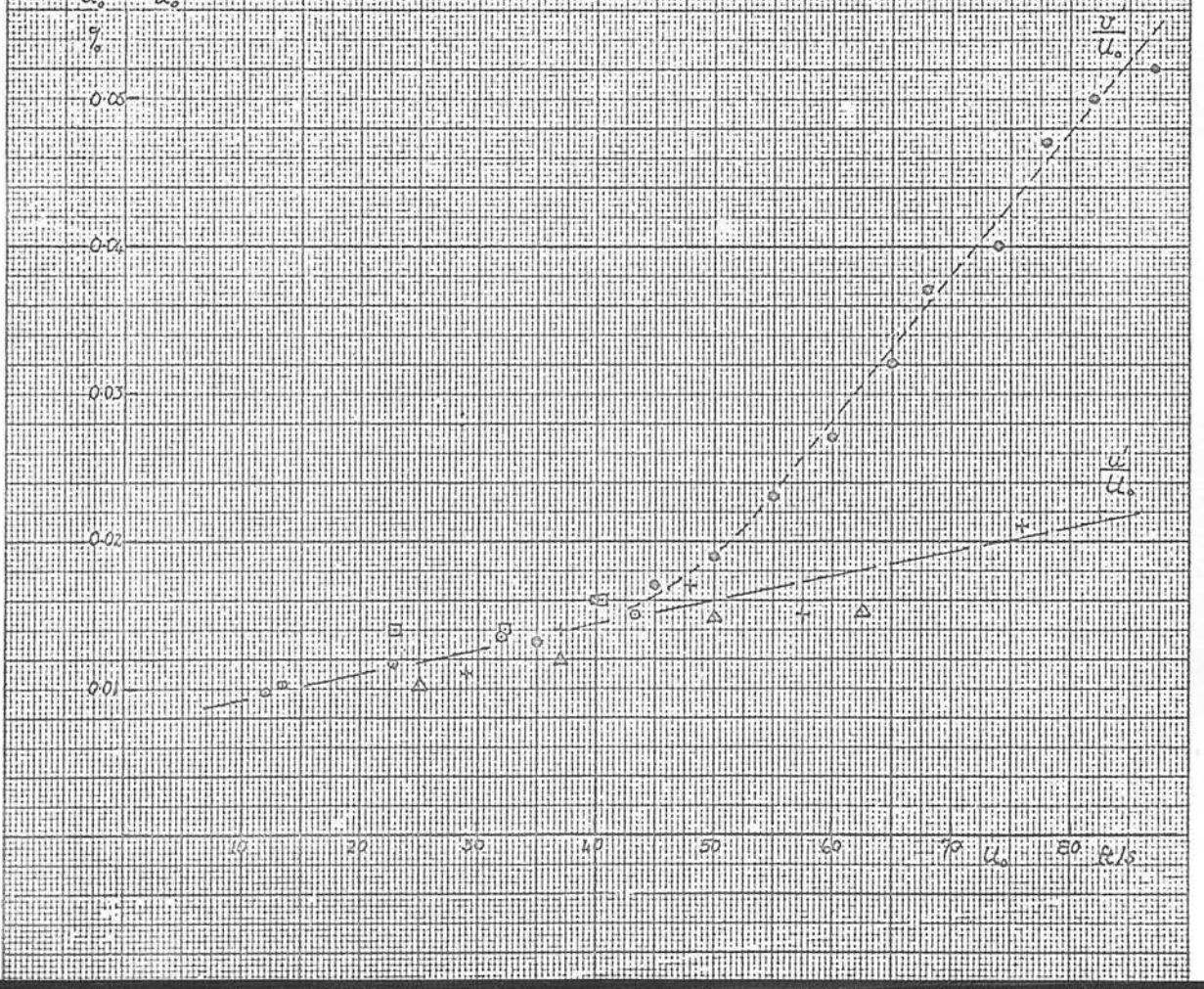

REFERENCES

Bennett, H.W. 1953 Kimberley-Clark Corporation Report, Neenah, Wisconsin.

Benney, D.J. 1961 J. Fluid Mech. 10, 209.
1964 Phys. Fluids, 7, 319.

Benney, D.J. and Lin C.C.
1960 Phys. Fluids, 3, 656.

Betchov, R. 1964 Phys. Fluids, 7, 1160.

Betchov and Szewczyk, A.
1963 Phys. Fluids, 6, 1391.

Blasius, H. 1908 Z. Math. u Physik, 56, 1.

Bloomer, N.T. 1957 Aero. Quart. 8

Bradshaw, P. 1964 J. Roy. Aero. Soc. 68, No. 639, 198.

Bradshaw, P. and Hellens, G.E.
1964 N.P.L. Aero Report 1119.

Bradshaw, P. and Pankhurst, R.C.
1962 N.P.L. Aero Report 1039.

Bradshaw, P., Stuart, J.T. and Watson, J.
1960 AGARD Report No. 264.

Burgers, J.M. 1924 Proc. 1st Internat. Cong. Appl. Mech., Delft, 113.

Burns, J.G. 1958 Ph.D. Thesis, Edinburgh.

Charters, A.C. 1943 N.A.C.A., T.N. 891.

Collis, D.C. and Williams, M.J.
1959 J. Fluid Mech. 6, 357.

Cooper, R.D. and Tulin, M.P.
1955 AGARD ograph, N.A.T.O., Paris.

Couette, M. 1890 Ann. chim. phys. 21, 433.

De Santo, D.F. and Keller, H.B.
1962 J. Soc. Ind. App. Math. 10, (4), 569.

Dhawan, S. and Narashimha, R.
1958 J. Fluid Mech. 3, 418.

Dryden, H.L. 1936 N.A.C.A. T.M. 562.

REFERENCES (Contd.)

Dryden, H.L. 1955 Proc. Conf. High-Speed Aeronautics, Brooklyn, 41.

Elder, J.W. 1960a J. Fluid Mech. 9, 133.
1960b J. Fluid Mech. 9, 235.

Emmons, H.W. 1951 J. Aero. Sci. 18, 490.

Fage, A. 1942 A.R.C. R. and M. No. 1896.

Fales, E.N. 1955 J. Franklin Inst. 259, 491.

Ferriss, D.H. 1964 A.R.C. C.P. No. 719.

Goldstein, S. 1930 Proc. Camb. Phil. Soc. 26, 1.

Gortler, H. and Witting, H.
1958 Proc. Symp. Boundary Layer Res. (Ed. Gortler). I.U.T.A.M. Freiburg (1957), 110.

Hall, A.A. and Hislop, G.S.
1938 A.R.C. R. and M. No. 1843.

Hama, F.R. 1960 Proc. 1960 Heat Transfer and Fluid Mech. Inst. (Eds. Mason Reynolds and Vincenti), 92.
1962 a, Phys. Fluids 5, 644.
b, Phys. Fluids 5, 1156.
1963 Phys. Fluids 6, 526.

Hama, F.R., Long, J.D. and Hegarty, J.C.
1957 J. Appl. Phys. 28, 388.

Heisenberg, W. 1924 Ann. Phys. Lpz. (4), 74, 577 see N.A.C.A. T.M. 1291.

Howarth, L. 1938 Proc. Roy. Soc. A 164, 547.

Lord Kelvin 1880 Math. Phys. Pap. 4, 152.

Kersley, L. 1965 Ph.D. Thesis, Edinburgh.

King, L.V. 1914 Phil. Trans. Roy. Soc. A 214, 373.

Klebanoff, P.S. and Tidstrom, K.D.
1959 N.A.S.A. T.N. D-195.

Klebanoff, P.S., Tidstrom, K.D. and Sargent, L.M.
1962 J. Fluid Mech. 12, 1.

Kovasznay, L.S.G. 1953 N.A.C.A. T.N. 2893.

REFERENCES (Contd.)

Kovasznay, L.S.G. 1960 Proc. Durand Cent. Conf., Stanford. Aeronautics and Astronautics (Eds. Hoff and Vincenti), Pergamon, London 1960.

Kuethe, A.M. 1956 J. Aero. Sci. 23, 444.

Landau, L.D. 1944 C.R. (Doklady) Acad. Sci. U.S.S.R. 44, 311.

Lin. C.C. 1945 Quart. Appl. Math. 3, 117, 218, 277.
1955 'Theory of Hydrodynamic Stability', C.U.P.
1958 Proc. Sym. Boundary Layer Res. (Gortler) I.U.T.A.M. Freiburg (1957), 144.

Lorentz, H.A. 1898 Collected Papers, 4, 15. Martinus Nyhoff, The Hague (1937).

Meksyn, D. 1964 Z. fur Phys. 178, 159.

Meksyn, D. and Stuart, J.T. 1951 Proc. Roy. Soc. A 208, 517.

Mitchner, M. 1954 J. Aero. Sci. 21.

Morse, P.M. 1948 Vibration and Sound, McGraw-Hill.

Nikuradse, J. 1933 Z. a.Math. Mech. 13, 174.
1942 Monograph, Zentiale f. wiss. Berichtaresen, Berlin.

Noether, F. 1921 Z. a. Math. Mech. 1, 125.

Orr, W.M.F. 1907 Proc. R. Irish Acad. A, 27, 9 and 69.

Osborne Private communication.

Pankhurst, R.C. and Holder, D.W. 1952 'Wind-Tunnel Technique', Pitman & Sons, London.

Prandtl 1904 Proc. 3rd Internat. Math. Cong., Heidelberg, see N.A.C.A. T.M. 452.
1914 Nacht. Geo. Wiss., Gottingen Math. - Phys. Kl. 177.

REFERENCES (Contd.)

Prandtl	1921	Z. a. Math. Mech. 1, 431.
	1935	'Aerodynamic Theory' III, (Ed. Durand), Berlin, 34.
Lord Rayleigh	1880	Scientific Papers, C.U.P. I, 474.
	1887	Do. III, 17.
	1892	Do. III, 575.
	1895	Do. IV, 203.
	1913	Do. VI, 917.
	1914	Do. VI, 266.
	1915	Do. VI, 341.
Reynolds, O.	1883	Phil. Trans. 174, 935.
	1895	Scientific Papers, C.U.P., II, 535.
Rosenhead, L. (Ed.)	1963	'Laminar Boundary Layers', O.U.P.
Schlichting, H.	1960	Paper prepared for A.G.A.R.D. Wind Tunnel Panel Meeting on Boundary-Layer Research, London, April, 1960.
Schubauer, G.B. and Klebanoff, P.S.	1946	N.A.C.A. A.C.R. 5K-27.
	1955	Proc. Symp. Boundary-Layer Effects Aerodyn., N.P.L. Also N.A.C.A. Report 1289.
Schubauer, G.B. and Skramstad, H.K.	1947	J. Res. Nat. Bur. Stand. 38, 251.
Schuh, H.	1953	R.A.E. Report Aero 2494.
Shen, S.F.	1954	J. Aero. Sci. 21, 62.
Squire, H.B.	1933	Proc. Roy. Soc. A 142, 321.
Stokes	1851	Trans. Camb. Phil. Soc. 9, II, 8.
Stuart, J.T.	1958	J. Fluid Mech. 4, 1.
	1960	a. Proc. 2nd Internat. Cong. Aeronaut. Sci., Zurich, 1960. see Advances in the Aeronautical Sciences, vol. 3, 143.
	1960	b. Proc. Xth Internat. Cong. Appl. Mech., Stresa, 63.
	1960	c. J. Fluid Mech. 9, 353.
Synge, J.L.	1936	J. Math. Phys. 15, 205, 210.
Taneda, S.	1958	J. Phys. Soc. Japan, 13, 418.

REFERENCES (Contd.)

Tani, I. 1960 Proc. 2nd Internat. Cong. Aeronaut, Sci., Zurich, 1960. See Advances in the Aeronautical Sciences, vol. 3, 143.

Tani, I. and Komoda, H. 1962 J. Aerosp. Sci. 440.

Taylor, G.I. 1936 Proc. Roy. Soc. A 156, 307.

Tietjens, O.G. 1925 Z. a. Math, Mech. 5, 200.

Tollmein, W. 1929 Nach. Ges. Wiss., Gottingen. 21. see N.A.C.A. T.M. 603 (1931).
1935 N.A.C.A. T.M. 792 (1936).

Townsend, A.A. 1958 Proc. Symp. Boundary Layer Res. (Ed. Gortler) I.U.T.A.M. Freiburg (1957), 1.

Watson 1960 J. Fluid Mech. 9, 371.

Wehrmann 1965 Phys. Fluids, 8,

Zaat, J.A. 1958 Proc. Symp. Boundary-Layer Res. (Ed. Gortler) I.U.T.A.M. Freiburg (1957), 127.

ACKNOWLEDGMENTS

I should like to thank Dr. M.A.S. Ross for suggesting the topic of this thesis and for her help and encouragement during the work, Professor W.H.J. Childs for providing laboratory accommodation in the Heriot Watt University and Professor N. Feather, F.R.S. for the use of facilities in the Department of Natural Philosophy, University of Edinburgh. My thanks go also to the S.R.C. for a maintenance grant during part of this work.

I am indebted to Dr. J.G. Burns for many helpful discussions and suggestions and to my wife for all her help.
